JOURNAL OF APPLIED PHYSICS

Vol. 11, No. 5 MAY, 1940

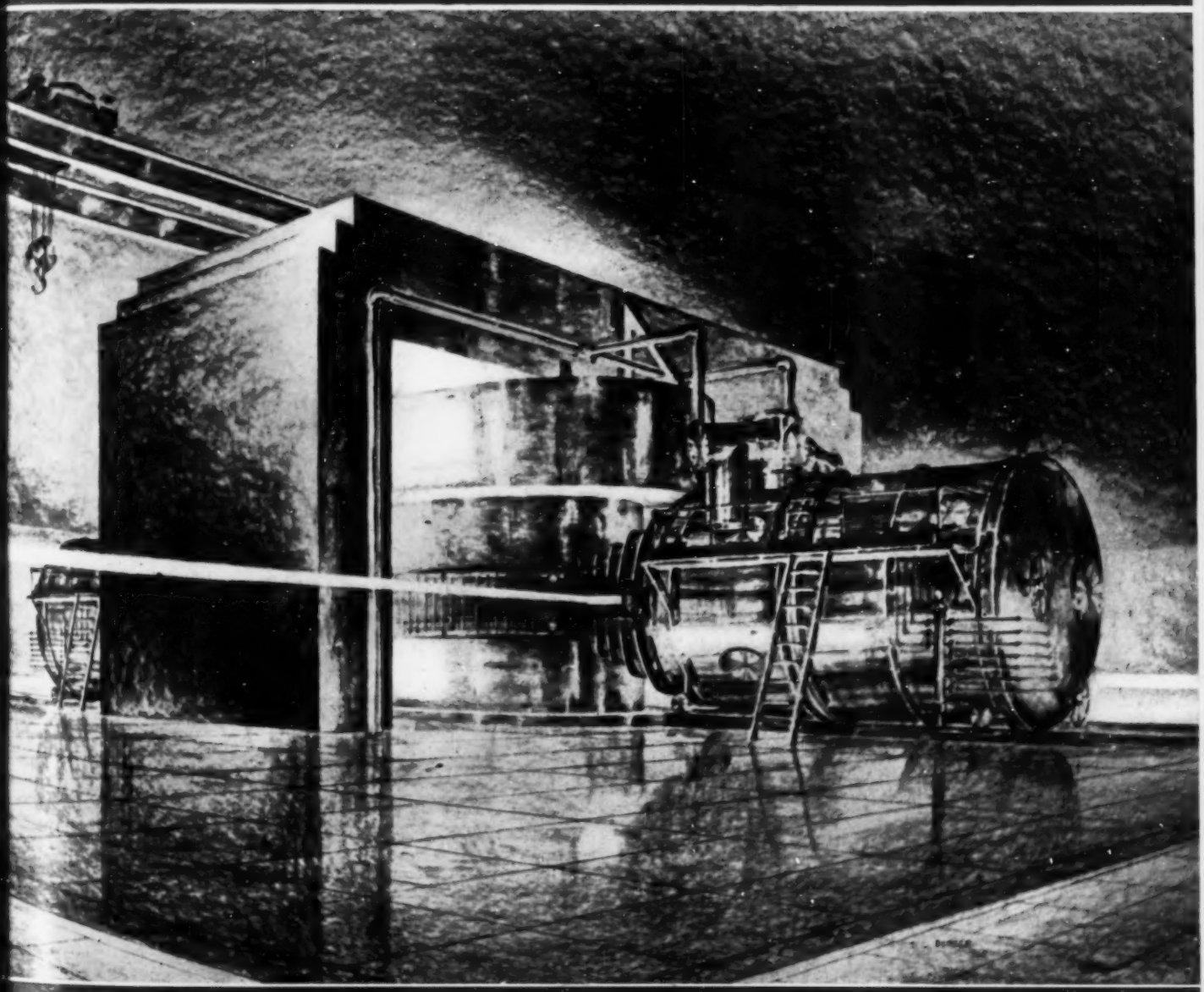

Artist's Drawing of California's Proposed Giant Cyclotron
Rockefeller Foundation provides funds for it

JOURNAL OF APPLIED

PHYSICS

MAY, 1940 Vol. 11, No. 5

In This Issue

Page

The Analytical Physicist 301

Trends in Design of Fractionating Pumps
KENNETH C. D. HICKMAN 303

Pendulum Analysis in the Scale Industry
GLENN R. CARLEY 314

Development of Water-Cooled Quartz Mercury Lamps
EDWARD B. NOEL 325

Resumés of Recent Research 337

Contributed Original Research

Note on Heaviside's Expansion Theorem F. H. MILLER 343

Recorder for Electrical Potentials. The Damping of Piezoelectric Systems FRANKLIN OFFNER 347

Computation of Some Physical Properties of Lubricating Oils at High Pressures. I. Density
R. B. DOW AND C. E. FINK 353

X-Ray Method of Determining Rates of Diffusion in the Solid State JESSE DUMOND AND J. PAUL YOUTZ 357

Use of Radioactive Phosphorus in Soil Studies
STANLEY S. BALLARD AND L. A. DEAN 366

In Every Issue

Here and There 339

Contributors to This Issue 342

Innovations in Instruments vi

Index to Advertisers x

BOARD OF EDITORS

ELMER HUTCHISSON,
Editor

Associate Editors

F. BITTER
W. E. FORSYTHE
L. A. JONES
B. E. WARREN
J. B. WHITEHEAD

Publication of the
American Institute of Physics

ADMINISTRATIVE STAFF

HENRY A. BARTON,
Director

MADELINE M. MITCHELL,
Publications Manager

JOHN T. TATE,
Adviser on Publications

GOVERNING BOARD

PAUL E. KLOPSTEG,
Chairman
GEORGE B. PEGRAM,
Secretary
KARL T. COMPTON
WHEELER P. DAVEY
FLOYD A. FIRESTONE
HARVEY FLETCHER
R. C. GIBBS
ARTHUR C. HARDY
GEORGE R. HARRISON
A. STUART HUNTER
H. R. LILLIE
FREDERIC PALMER, JR.
GEORGE B. PEGRAM
W. B. RAYTON
JOHN T. TATE
WALLACE WATERFALL

THE JOURNAL OF APPLIED PHYSICS, published monthly at Prince and Lemon Sts., Lancaster, Pa., is devoted to physics in its role as the science basic to other natural sciences and to the arts and industries. Previous to 1937 this publication was known as PHYSICS. It aims to be of service not only in physical laboratories, but also in the laboratories of industrial, chemical, geological, geophysical, meteorological, radio, and similar concerns. THE JOURNAL OF APPLIED PHYSICS publishes editorials, news of physicists and reviews, as well as technical papers of applied physics.

Manuscripts should be submitted to Elmer Hutchisson, Editor, University of Pittsburgh, Pittsburgh, Pennsylvania.

SUBSCRIPTION PRICE

	U. S., POSS. AND CANADA	FOREIGN
To members of scientific societies	$5.00	$5.70
To all others	7.00	7.70

Single copies are $.70 each.

Changes of address and proofs should be addressed to the Publications Manager.

Subscriptions and orders for back numbers should be addressed to Prince and Lemon Streets, Lancaster, Pa. or to the American Institute of Physics, 175 Fifth Avenue, New York, N. Y.

Advertising rates supplied on request. Orders, advertising copy and cuts should be sent to the American Institute of Physics.

Entered as second class matter at the Post Office at Lancaster, Pennsylvania, under the Act of March 3, 1897. Accepted for mailing at the special rate of postage provided for in the Act of February 28, 1925, authorized May 2, 1932.

Copyright 1940, by the American Institute of Physics.

A-C RESISTANCE BOXES

Low Inductance — Low Capacitance

Low "Zero" Resistance — High Accuracy

Negligible inductance and capacitance effects account for the wide use of these boxes in highly precise a-c measurements. With no measurable difference between a-c and d-c resistance, they are used at carrier as well as lower frequencies.

Illustrated at the right are a few of the constructional features of the 4764. The other boxes have many of the same features.

In the higher decades of the 4764, the resistance webbing (upper right) is wrapped around a ceramic cylinder and mounted in the rotating drum shown below it. Inductance and capacitance are minimized. Because the stationary brushes form the connections between decades, and because the active coils are always in the same position, the configuration of the circuit within the box remains constant . . . inductance and capacitance change is negligible.

An ingenious arrangement of brushes practically eliminates all wiring except between the two decades at one end and to the terminals at the other. These are stiff wire . . . there are no flexibles.

Strongly constructed to assure long usefulness, these boxes are priced from $50.00 to $300.00 . . . include the most accurate a-c resistance boxes we make.

Write for Catalog E-53

LEEDS & NORTHRUP COMPANY, 4978 STENTON AVE., PHILA., PA.

LEEDS & NORTHRUP

Measuring Instruments : Telemeters : Automatic Controls : Heat-Treating Furnaces

Jrl Ad EB25(2)

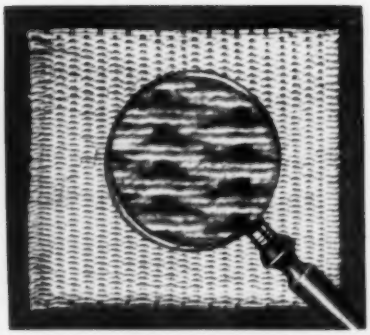

Inductive and capacitive effects are minimized in woven resistors. Enlarged area is about five times actual size.

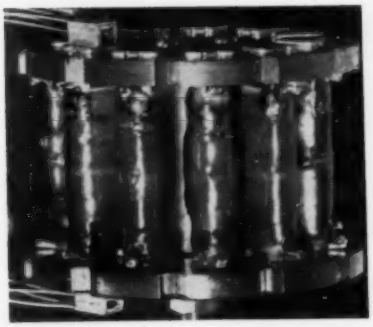

The decade drum, rotating between stationary brushes, introduces a single, separate resistor for each step.

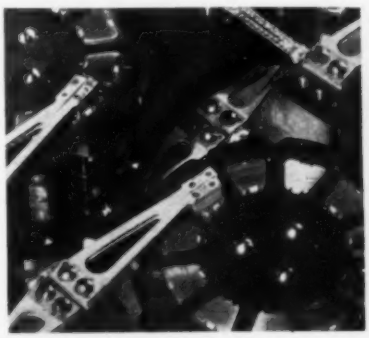

Slanted brush ends give a wiping contact. Multiple-blade brushes and short, heavy conductors reduce series resistance.

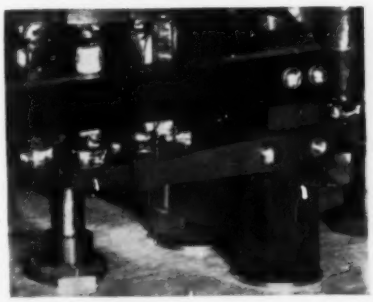

Rigid mechanical parts assure continued high accuracy. Materials are selected for excellence of mechanical and dielectric properties.

New! TWO LENS QUARTZ

SPECTROGRAPH

Range 1850Å to 12000Å

One Plate **covers the region 2100Å-3300Å most used in analytical work.**

One Control **sets wave range, focuses, and tilts plate holder, *automatically*.**

Any Spectrum Line **can be brought to center of plate.**

Projection **of wavelength setting, and of range covered, on large translucent screen. Numbers 1 inch high, always visible.**

Littrow Weaknesses Avoided. **No stray light. No tilting of lenses necessary. No right angle reflecting prisms. Illuminating bench aligned with slit.**

The GAERTNER SCIENTIFIC CORPORATION

1212 Wrightwood Ave. ▲ Chicago ▲ U. S. A.

JOURNAL OF SCIENTIFIC INSTRUMENTS

A MONTHLY PUBLICATION DEALING WITH
THEIR PRINCIPLES, CONSTRUCTION AND USE
AND THE APPLICATION OF PHYSICS IN INDUSTRY

Produced by the Institute of Physics with the Co-operation of the National Physical Laboratory

CONTENTS

Special Articles dealing with the Trend of Development of various classes of Instruments, Working Processes, and with Matters of General Interest to Manufacturers.
By Recognised Authorities.

Contributed Papers on New Methods and Apparatus.
By Workers in every Branch of Science and Manufacture.

New Instruments Section: the scope includes
Physics and Chemistry
Optics and Surveying
Meteorology and Metrology
Electrical and Mechanical Engineering
Physiology and Medicine.

Laboratory and Workshop Notes, Correspondence, New Books, Catalogues, Notes and Comments, and Institute Notes are also included.

The subscription rate for a yearly volume is £ 1.10.0 net (post free) payable in advance. Separate parts 2s.8d. (post free). Subscriptions should be sent to the publishers.

THE INSTITUTE OF PHYSICS
THE UNIVERSITY, READING, BERKS ENGLAND

New notes on research in a forward-looking laboratory—

PRECIPITRON*

developed by Westinghouse

MODERN RESEARCH MAKES POSSIBLE SAFE, EFFICIENT REMOVAL OF AIR BORNE PARTICLES

The work of modern research is doing much to speed the advance of scientific progress. An outstanding example is the development of the PRECIPITRON, the new electrostatic air cleaner.

Previous electrostatic cleaners used in industrial processing generated unhealthy quantities of Ozone and were large, cumbersome and expensive to maintain.

After five years of research and experimentation, Westinghouse research laboratories developed the PRECIPITRON, which depends upon electrostatic principles for its operation, yet differs from previous electrostatic cleaners in that it requires a small amount of power, relatively small duct area, and generates a negligible amount of Ozone so that it can be safely used in the home, office or industrial plant. This new achievement, credited to the perseverance and high ability of modern scientists in research, not only makes possible more healthful living and working conditions for millions of Americans, but effects tremendous savings in reducing cleaning and redecorating costs and supplying positively cleaned air for delicate operating machinery and processes.

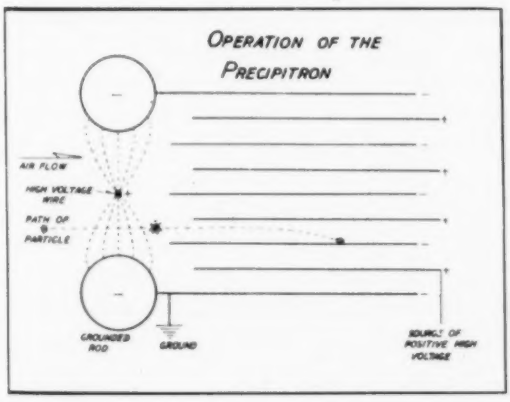

The adjoining figure illustrates the operation of the PRECIPITRON. A positive potential of approximately 12,000 volts is applied to the high voltage wire. This causes a high intensity electrostatic field to form between the wire and the rods (dotted lines in the figure). The plates marked with a positive sign are charged at 5,000 volts positive. As a result of this voltage, a high intensity electrostatic field of uniform gradient exists between the plates. As a particle passes through the field between the wire and the rod, positive ions attach themselves to the particle as a surface charge. Then the charged particle passes on through the plate assembly where the force action from the electrostatic field between the plates causes the particles to be precipitated on the plates.

FOR FURTHER DETAILS WRITE LIGHTING DIVISION, WESTINGHOUSE ELECTRIC AND MANUFACTURING COMPANY, CLEVELAND, OHIO

*Trade-mark registered in U. S. A.

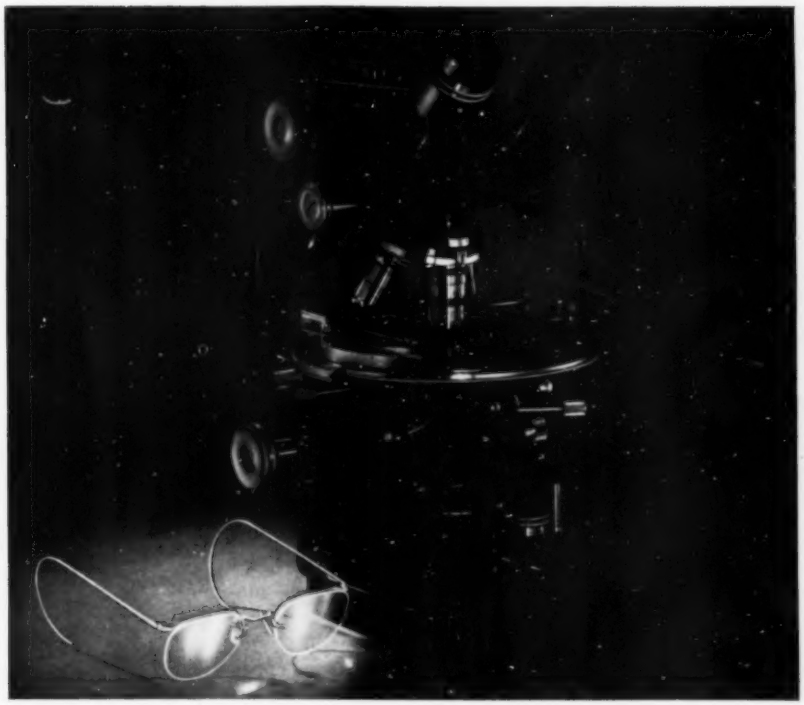

You'll want

BAUSCH & LOMB EYEWEAR, TOO

ACCURACY—and then more accuracy!

That is the demand which Science, Education and Industry for years have placed upon optical instruments. In answering that demand, Bausch & Lomb has formed the *habit of accuracy*—a habit which is largely responsible for the excellence of every B&L product.

Millions of eyeglass lenses a year, used to multiply the seeing power of mankind, are manufactured by the organization responsible for B&L instruments.

Such products as Orthogon corrected lenses, Panoptik Bifocals, Loxit Mountings, Nokrome Glass, and a wide variety of Ophthalmic Instruments are Bausch & Lomb contributions to better eyesight. That is why you should insist on Orthogon Lenses and B&L Frames and Mountings in your eyeglasses. Bausch & Lomb Optical Co., 670 St. Paul Street, Rochester, N. Y.

BAUSCH & LOMB

FOR YOUR EYES, INSIST ON BAUSCH & LOMB EYEWEAR, MADE FROM BAUSCH & LOMB GLASS TO BAUSCH & LOMB HIGH STANDARDS OF PRECISION

Please mention this journal when writing to advertisers

HARVARD COLLEGE
MAY 14 1940
LIBRARY

Journal of Applied

Physics

Volume 11 May, 1940 Number 5

The Analytical Physicist

THE role which the physicist plays as an analyst in industry seldom receives the attention it deserves. Even a very brief consideration of the analytical possibilities of such physical tools as the spectrograph, x-ray and electron diffraction cameras, mass spectrograph, and the Geiger counter gives evidence of the need for men trained in these particular techniques. A new profession, that of an analytical physicist, seems to be in the making.

In emission spectroscopy, for instance, the physicist provides rapid quantitative analyses for the metallurgist, ceramist and even the chemist. In absorption spectroscopy he has been able to identify components of organic compounds and thus determine the condition of paint vehicles, to study properties and changes in rubber and in plastic materials, and to measure impurities in air such as carbon monoxide that may be present to only one part in a million.

In the field of x-ray diffraction the physicist analyzes alloys and determines the atomic arrangements which are present. He determines the way in which organic molecules combine in aspirin and other drugs. Also with electron diffraction the presence of impurities in thin films may be detected or the structure of a tarnished or corroded surface identified.

The mass spectrograph is another analytical tool of the physicist which is taking its place in industry. It may be used to determine the composition of flue gases or the nature of a molecule produced in the cracking of crude oil. It is an almost necessary adjunct to the study of reactions by means of stable isotopes used as tracers.

One of the most recent analytical tasks presented to the physicist is in the field of radioactivity. By the addition to a melt of a small quantity of a radioactive isotope of an element for which an analysis is to be made, one can tell at all times how much the element has evaporated and can by a very simple test tell the exact quantity which is left in the finished product. For such work someone is needed who is familiar with electroscopes, Geiger counters, electronic amplifiers and all their related equipment.

With the rise of this new profession educators face two responsibilities. The first is to train students in techniques of spectroscopy, x-rays, electronics, etc. Since many of these students will probably not be called upon to carry on fundamental research, a splendid opportunity is provided for the student who is interested in physics and yet is unable to continue his studies in the graduate school. The second responsibility is to inform industrial executives that specialists in the analytical techniques of physics exist so that the executive is not disappointed by the failure of these techniques as a result of insufficient knowledge or inexpert handling.

June Meeting in Applied Physics

A special session is being provided at the Summer Meeting of the American Physical Society in Pittsburgh, June 20–22, for contributed papers in applied physics. This, together with planned tours of industrial laboratories and outstanding recreational possibilities, will, it is hoped, attract many industrial physicists to this meeting. Members who are interested in applied physics are invited to contribute to the special session.

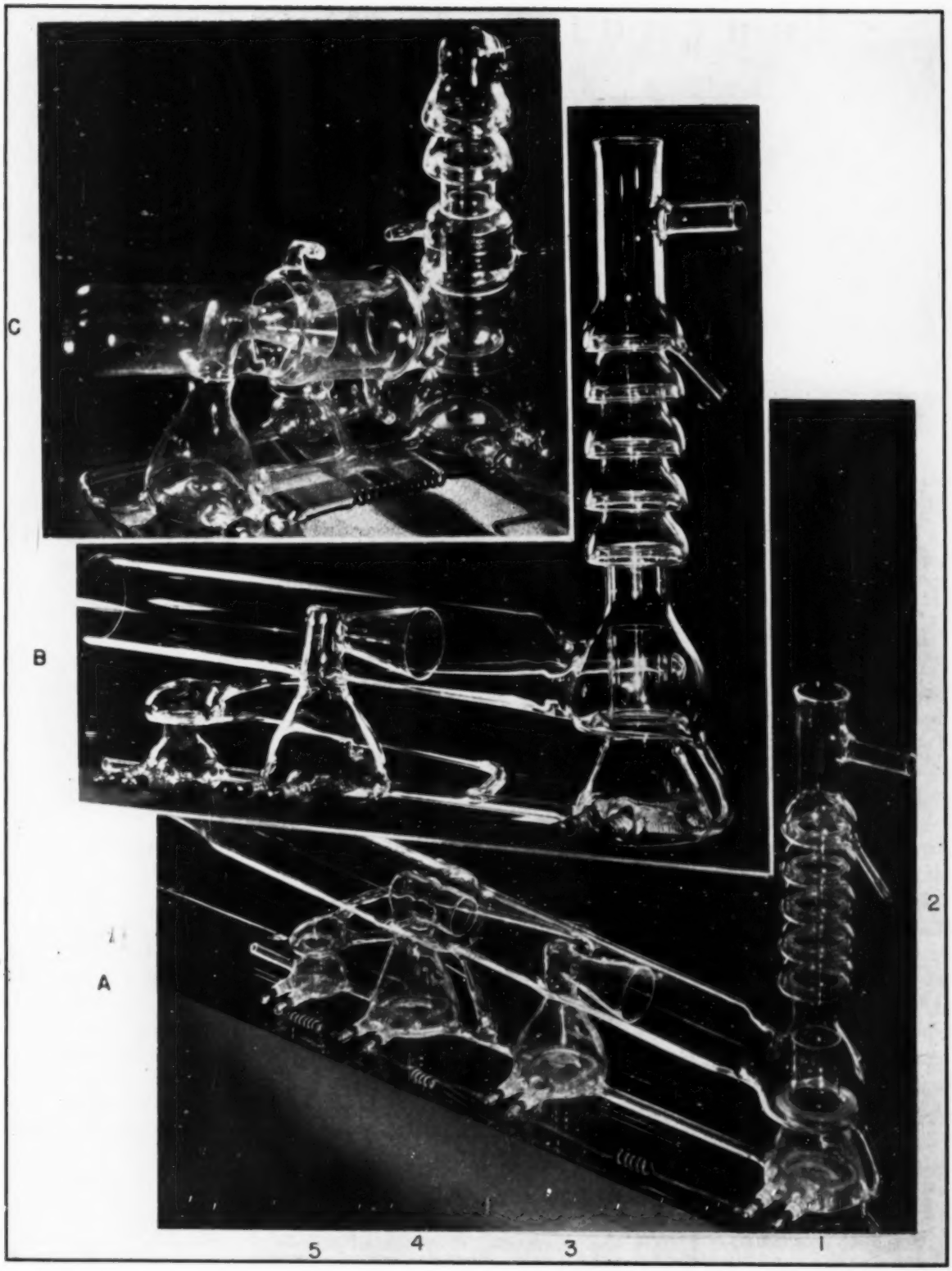

An assortment of oil diffusion pumps of recent design: (a) three-jet, (b) two-jet, (c) two-jet, water-cooled.

Trends in Design of Fractionating Pumps*

BY KENNETH C. D. HICKMAN

Distillation Products, Inc., Rochester, New York

AT the time when the fractionating diffusion pump was described,[1,2] the need for a rectifier on an oil condensation pump was becoming recognized in various quarters. Pilon[3] had emphasized Burch's original contention[4] that the fore-vacuum should be kept hot, and McCowen and Fawcett[5] were considering a pump with external fractionator. The efficacy of fractionation for producing higher vacua was soon confirmed, but a fractionating pump constructed entirely of metal had yet to be described.

The writer early became preoccupied with a horizontal type of pump. It remained for Lockenvitz,[6] Malter and Marcuvitz,[7] and Sykes and Bancroft[8] to realize the simplicity and constructional advantages of vertical patterns in which the evaporating zones are arranged in concentric circles. Lockenvitz's pump is reproduced in Fig. 1, Malter's in Fig. 2, and Sykes' in Fig. 3. The obvious merit of these designs is that they employ inexpensive commercial tubing that can be cut and machined in the lathe to ensure absolute parallelism of the parts. They fulfill their functions admirably. Nevertheless we list a number of factors which at the outset appeared to us to be limitations:

(a) Fundamental:† The low vacuum jets, nearest to the fore-vacuum which require the smallest projective area for the vapor stream, are the greatest in diameter. This necessitates fine clearances and careful construction.

(b) The boundaries of the concentric boilers are long compared with their areas. This encourages mixing of the contents and favors thermal leakage.

(c) The areas of the boilers are determined by the dimensions of the jets. The areas cannot be increased unless the tubes are expanded at the base. This would banish much of the constructional simplicity.

We have continued the evolution of the horizontal design for the following reasons:

(1) The boiler area is independent of the jet diameter.

(2) The heat input to each boiler division can be regulated with precision.

(3) A horizontal pump with the boiler on the underside has two free ends. The high vacuum end can be made large, the fore-vacuum end small in diameter.

(4) Most operations are done *horizontally* on the world's surface. It is generally more convenient to house mechanical pumps, condensation pumps, and vacuum chambers side by side than above one another. The horizontal construction allows the fractionating unit to serve as the straight pipe between the mechanical pump and the side of the vacuum vessel.

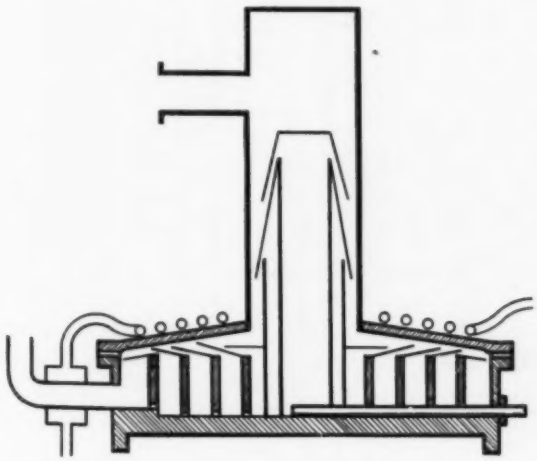

FIG. 1. Lockenvitz pump.

Glass Pumps

The first practical fractionating pumps from this laboratory were of glass, two- or three-jet models (figure on p. 302(a) and (b)). In these, 1 designates the high pressure jet working into the fore-vacuum, 2 comprises the lobes which prevent the major volatile contaminants falling back into the pump, 3 the intermediate, and 4 the high vacuum jets; 5 is the *sink* for nonvolatiles, tars, and polymerized products. The heaters consist of bare resistance wire immersed directly in the operating liquid. The boilers may be run unlagged or covered, preferably with padded felt jackets. It is probable that these pumps use the heat input more economically than any which

* Communication No. 13 from the Laboratories of Distillation Products, Inc., Rochester, New York.

† Unless the pump is turned inside out. This involves difficulties in construction.

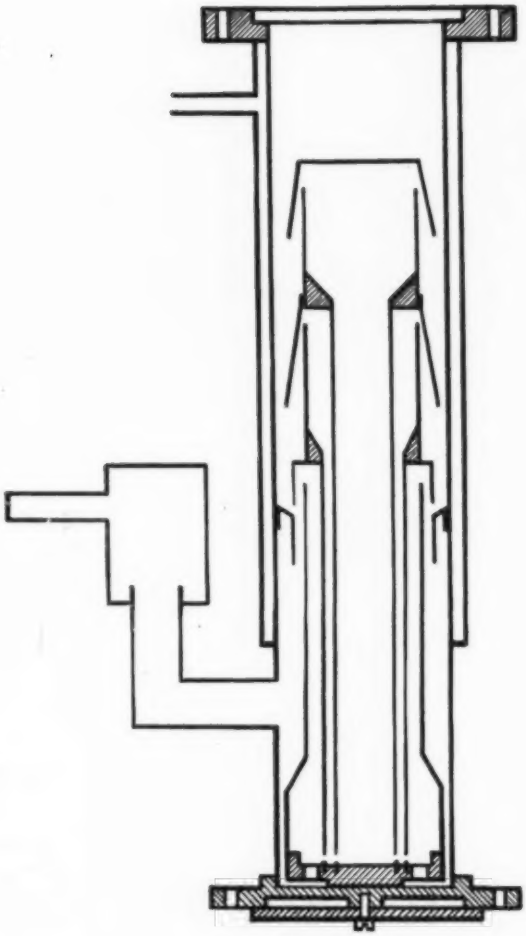

FIG. 2. Malter's pump.

have been built. Water cooling may be employed as on p. 302(c), which shows a model now in successful operation for the exhaustion of electronic devices. Cooling may be done by jets of air or by water, although air has certain advantages which will be considered presently. The lowest pressures which have been recorded against blank-off at 25°C, without the use of a cooled or absorbent trap, are shown in Table I. The ionization gauge, calibrated against air, was used for the measurements.

Vapor Phase vs. Liquid Phase Fractionation

Becker and Jaycox[9] early showed an arrangement of oil vapor pumps in tandem for which they claimed exceedingly low pressures. Studying p. 302 (a), it is evident that *all* the condensate from both pumps passes into the first pump's boiler, but by a minor alteration the condensate from each pump can be made to pass into its own boiler. In the latter case, traces of volatiles from the high vacuum jet would remain uncondensed and mingle with the vapor from the next jet and pass into the lower vacuum boiler; volatiles from the latter pass into the fore-vacuum and are carried away by the mechanical pump.† In the first scheme it is imperative that the

TABLE I. *Lowest pressures from pump fluids at 25°C.*

CHEMICAL NAME	TRIVIAL NAME	TYPE OF PUMP	MAXIMUM BACKING PRESSURE AT NORMAL WATTAGE	OPTIMUM VACUUM, TRAP AT 25°C*
Butyl sebacate		single boiler multi-boiler	0.1 .15	2.5×10^{-5} 10^{-5}
Amyl sebacate	Amoil-S	single boiler multi-boiler	.1 .17	10^{-5} 2×10^{-6}
2-ethyl hexyl phthalate	Octoil	single boiler multi-boiler	.1 .25	5×10^{-6} 2.5×10^{-7}
2-ethyl hexyl sebacate	Octoil-S	single boiler multi-boiler	.1 .2	10^{-6} 5×10^{-6}
Butyl phthalate		single boiler high pressure booster	.1 1.0	2.5×10^{-3} 10^{-3}

* The pressures recorded in this column will not agree accurately with our vapor pressure data published elsewhere. These are the practical pressures obtained with the oils from production manufacture.

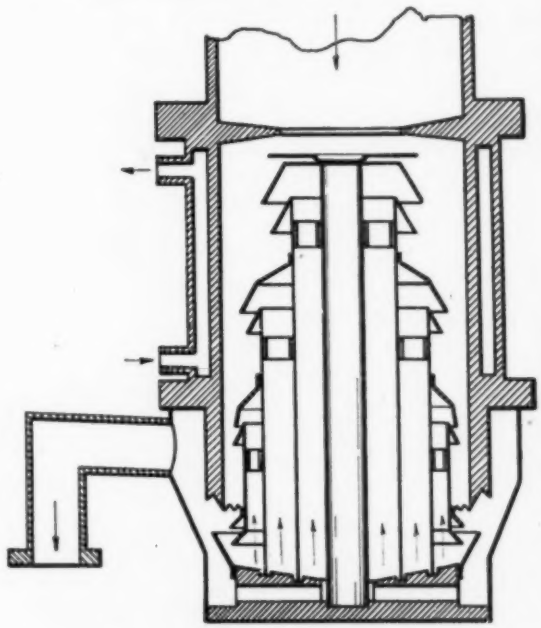

FIG. 3. Sykes and Bancroft pump.

† Metal condensation pumps set up in tandem with relatively long connecting pipes are not an equivalent of the arrangements on p. 302 because the volatiles are not readily transferred from pump to pump.

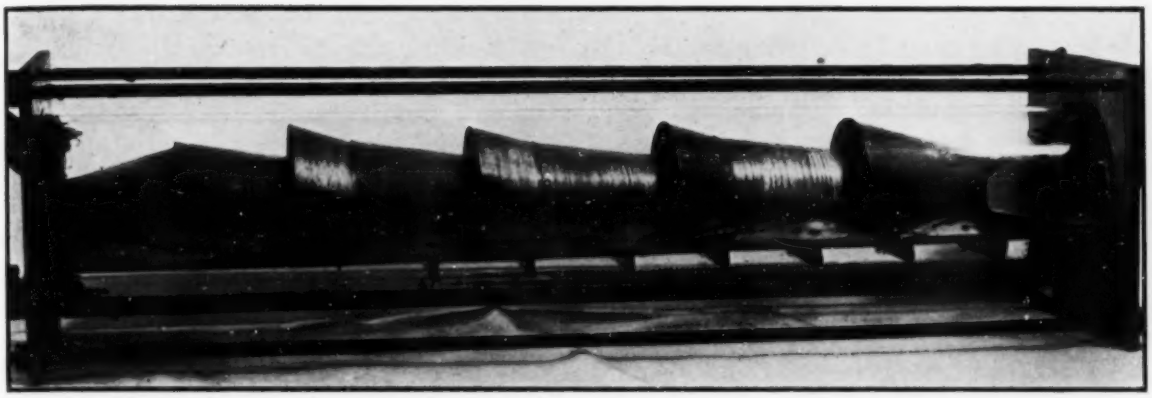

FIG. 4. First tubular fractionation pump.

boilers communicate below the liquid surface, in the second it is desirable: otherwise the rear boiler becomes empty. It is these return tubes, combined with short vapor paths, that convert the dual pump of Becker and Jaycox into continuously fractionating pumps.

There remains the question whether it is better to fractionate in the vapor phase only (scheme 1) or in both vapor and liquid phases (scheme 2). The answer must depend on the purpose. When the highest vacua are to be generated in a clean, dry, physical system, vapor fractionating between the last two boilers appears best, as on p. 302 (b). When large throughputs of semi-volatile contaminants must be cleaned from a relatively dirty *chemical* system, complete liquid phase fractionation is superior. The contaminant is then carried mechanically to the fore-end of the pump and the operating fluid becomes purged as it wanders back through points of duty.

Metal Horizontal Pump

The simplest horizontal pump is, perhaps, a tube containing baffles and partly filled with operating fluid. A pump similar to Fig. 4 was built and found to furnish a pressure of 10^{-7} mm, but it required a very good fore-vacuum (>0.05 mm). The tube was of glass, 4 inches in diameter, 20 inches long, and was heated underneath, cooled by air blasts above. It required much fluid to fill and was unsuitable for construction in metal because of thermal leakage due to the nearness of the hot and cold portions.

The first metal pump had a cross section and elevation, shown in Fig. 5. The boiler was a V-shaped annex running lengthwise underneath. The pump could be taken apart at the flanges near the fore-vacuum end, permitting insertion or removal of the jet manifold. The jets were formed of narrow skirts fastened over rows of perforations in the manifold. The jets resembled Mohammedan $\frac{3}{4}$ moons, with corners terminating at the boiler annex. The manifold was partitioned vertically so that each jet should be

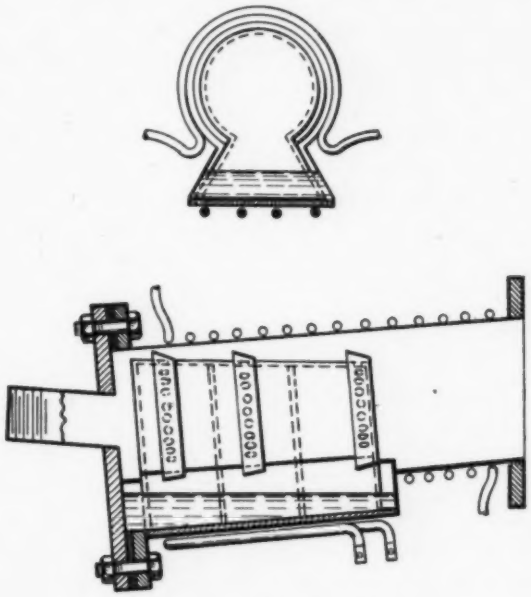

FIG. 5. First metal fractionation pump.

fed with a separate kind of vapor. Since the jets at the low vacuum end are required to operate into a denser fore-vacuum than those at the higher, the pressure of the operating vapor is

generally greater. Thus, while the fluid in the cold pump lies strictly level, during operation it runs uphill towards the high vacuum end. To prevent an accumulation of liquid where least is needed (the less the liquid present, the less the evolution of decomposition products), the

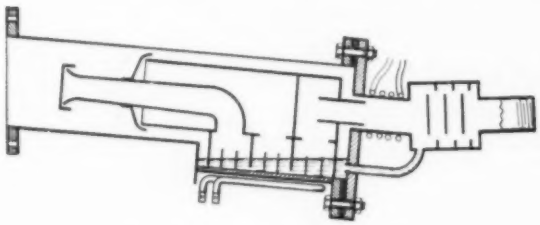

FIG. 6. 8-inch pump elevation.

pump is raised 5–10° towards the high vacuum end. This also ensures that the condensate from backstreaming returns to the body of the pump.

Pumps of this design have served excellently, but they suffer from minor defects, as follows:

1. The highest permissible fore-vacuum is about 0.1 mm.
2. The jets operate efficiently over not more than a semicircle. For a given cross section the pumps have only half the possible throughout.
3. Pump fluid evaporates from the junction of the manifold and the pump casing at the high vacuum end, hindering the ingress of gas.

These drawbacks have been remedied in the construction shown in Figs. 6, 7, and 8, which has been applied to 4-inch, 8-inch, and 21-inch pumps constructed by Distillation Products, Inc. It will be seen that the front compartment of the vapor manifold feeds vapor into a short tubular jet of small diameter which plays into a water-cooled receiving jet connecting with a fractionating manifold which is joined, in turn, to the primary vacuum pump. The next vapor compartment feeds the high speed, Embree jet, described below. The vapors to the Embree jet are kept warm by jacketing with the intermediate vapor supply, as in the Malter pump. Finally, there is a small, open compartment which serves to collect the tarry nonvolatiles. Some of the many variations of boilers and jet manifolds have been dealt with elsewhere.[2]

Because these pumps have only three jets in series, it might be assumed that their fractionation capacity would be three-plates or less. This is not necessarily so. The boilers are provided with a maze of baffles so that the liquid has to travel by a tortuous path to the high vacuum end. It is vaporizing so rapidly that although each element of liquid surface is in equilibrium with the vapor directly above, neighboring elements are not contaminated with one another's vapor. The liquid entering the last compartment has received far more than two stages of purification. The maze of barriers serves the secondary but important purpose of preventing surging from one compartment to another—induced by the dynamic balance of different levels, temperatures, and vapor pressures existing under the working load. In this respect the glass pumps, or metal pumps with completely separated boilers connected by relatively long, narrow tubes, are superior.

Jet Design

The original Langmuir inverted pump has been shown in the literature with a variety of mushroom- and umbrella-[10] or reflector-shaped[12]

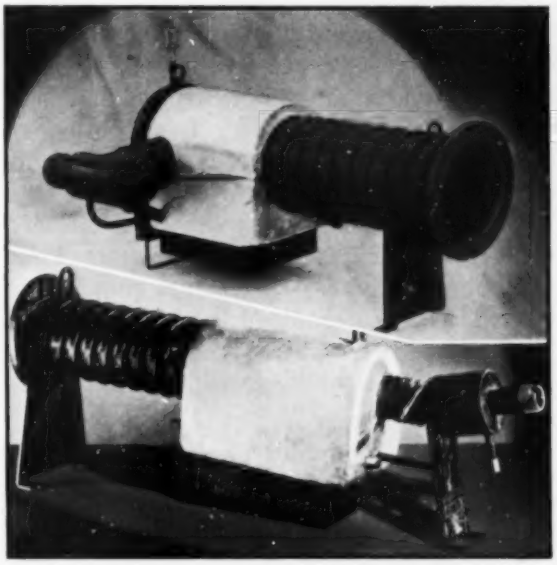

FIG. 7. 4 and 8-inch pump.

jets. We have had occasion to question three leading designers concerning the origin of their jets only to learn in each case that they were drawn freehand from "established geometric principles," as "the sort of shape that ought to work." Our own early efforts with the 4-inch glass-metal pump came from similar inspiration.

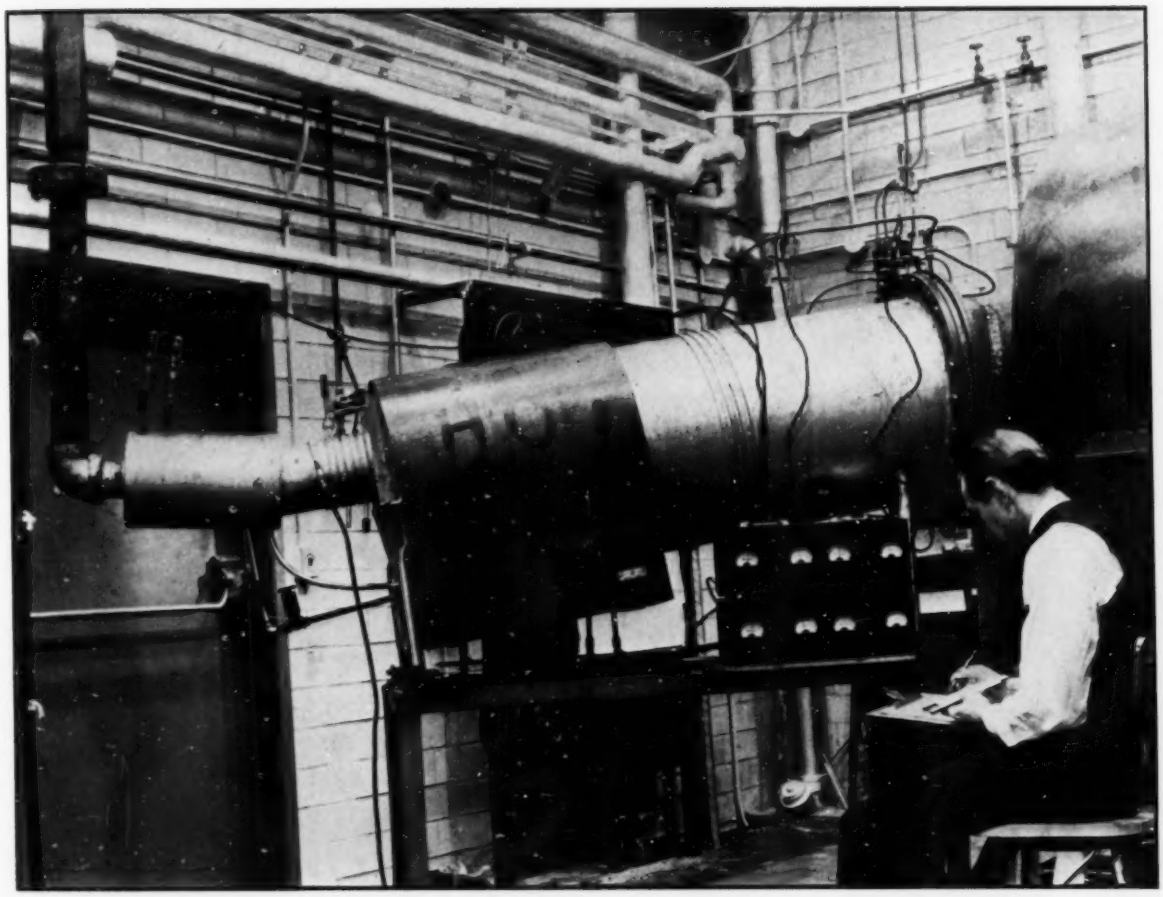

FIG. 8. 21-inch pump, with testing gauge.

Advance in design was stimulated in three ways: the necessity of making faster pumps for commercial molecular distillation; study of the transparent glass-metal pump; and learning how to spin complicated jet-shapes out of sheet aluminum on the laboratory lathe.

We had long noted that the hottest region in an air-cooled pump is not situated at the projection of the median of the jet, Fig. 10 (a) at x but is always displaced away from the fore-vacuum and may actually occur above the edge of the jet as at y. We had agreed with Ho[13] that the admission coefficient, that is to say, the actual quantity of gas that passes into the jet area compared with the quantity that would pass into an annulus of similar area communicating with an infinite source of perfect vacuum—is regrettably low, generally about 2–10 percent. We had also noted that in pumps with wide jet clearances employing organic vapors, the speed is not independent of the fore-vacuum. This is contrary to Langmuir's original experience.[14] Also we continued to observe, in contradiction to statements in the literature[7] that moderately cooled pumps were sometimes faster than well cooled pumps; that poorly conducting air-cooled glass bodies were occasionally superior to water-cooled metal bodies.

The reasons for the low admittance, the dependence on fore-vacuum, and the advantage of moderate cooling can be understood, perhaps, from Figs. 9 and 10, and the following argument. In Fig. 10, a conventional mushroom jet is shown with a wide clearance from the pump wall. The operating vapors are depicted as streamers headed with plain arrows. Air molecules are shown as crosses when relatively stationary, cross-headed arrows when moving.

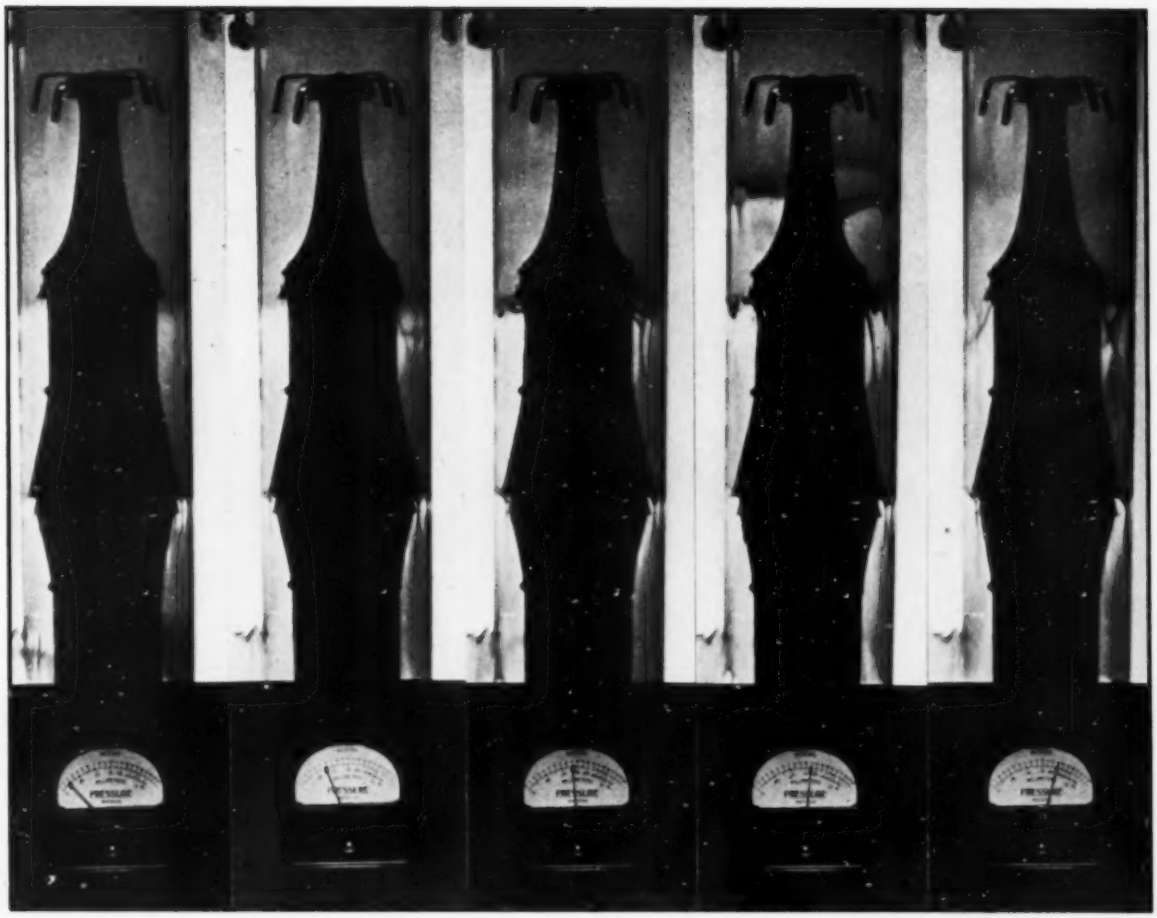

FIG. 9. Glass-metal pump working with low and high fore-vacuums (back lighting).

Since the pressures in the fine-vacuum, fore-vacuum, and boiler may be about 0.001 mm, 0.1 mm, and 1 mm, or less, respectively, the vapor stream expands laterally, as it passes downwards. This results, through collision, in a *curved* stream, the curvature and general direction depending upon circumstances. When the stream presents chiefly a downward component (however slight) to the incoming gas, the Ho coefficient is large. When, as shown to the right, the component is chiefly upwards, the admittance is poor or even zero. The expansion, and hence the upward component, is favored by increase of the pressure of working vapor, which accounts for the well-known fact that a pump's speed may fall off if the optimum heat input is exceeded. The curvature is aggravated by increase in fore-vacuum—the back-pressure pushes the vapors upwards. The effect is shown in the five photographs of Fig. 9 which were made with a 4-inch glass-metal pump filled with Octoil-S containing a few parts per thousand of the pilot dye dimethylaminoanthraquinone. Generating a transparent vapor, the condensate was colored a deep blue and could thus be photographed. The light portions in the figures show the vapor stream forcing the condensed dye away from the glass. The darker portions show the quieter regions of the pump. The meter of a Pirani gauge indicating the fore-vacuum was placed in front of the pump and photographed simultaneously, and no adjustment or rearrangement of the photographs has since been made. The numerals on the gauge are not legible, but the range is between 0 and 1 mm. Gauges from left to right give readings of approximately 0.02; 0.08; 0.13; 0.17; and 0.25 mm of

Hg, respectively. At the lowest fore-pressure, shown in the left-hand photograph, all the jets are streaming smoothly and the condensed fluid is being thrust downwards without breaking into streaks. In the next photograph the high pressure jet is showing signs of strain. The intermediate jet is feeling the poor performance of the lower jet but is, nevertheless, producing a sufficiently good vacuum for the upper jet to continue working under optimum conditions. In the center photograph the bottom jet has broken down, the intermediate jet is on the verge of breaking and is failing to produce an optimum vacuum for the top jet, which shows a ring of condensate forming just above the region where most of the vapors have been forced to condense. Note that in the previous photographs the vapors from the top jet travel undeflected right to the gap between the intermediate jet and casing. In the fourth photograph, the lower jets have broken down but are still producing a sufficient reduction of pressure for the vapors from the top jet to be able to struggle to the wall in a series of explosive bursts. In the last picture to the right, all three jets have broken down and the fine vacuum is now so dense that the vapors from the top jet are unable to reach the walls in their original formation. It is a matter of regret that we did not include above each photograph a meter recording the fine vacuum, but the experiment was too tedious to warrant a repetition after this thought had occurred. The probable high vacuum readings from left to right are as follows: 5×10^{-6}; 5×10^{-6}; 5×10^{-5}; $5\times10^{-3}-5\times10^{-2}$, fluctuating; 0.2 mm.

Langmuir[10] has shown that the air handled by the pump collects as a layer against the walls before being driven down to the exit and expelled. Now it is apparent in Fig. 10 (a) that air which is entrained near the jet may be rejected again laterally where the operating vapors curve upward. The high concentration of air which has been left by vapors condensed at the wall is in especially favorable position to pass back. The passing back is favored by high fore-pressures which bend the operating stream backwards. It is also favored by too thorough condensation of the operating fluid. The molecules of this fluid, although exhibiting random motion, have a forward impressed velocity which we observe is *not* entirely lost on collision with condensate if this is maintained at a sufficiently high temperature. Incomplete condensation is needed to provide dilution and entrainment of the gas concentrated near the walls and also to preserve the downward passage of the gas stream. Where a water-cooled metal pump casing of high conductivity is employed, the jets must be redesigned to supply more vapor. The region that *does* need to be kept cold is just above

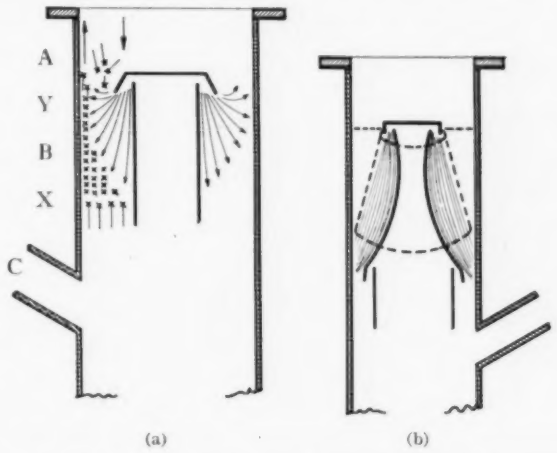

FIG. 10. (a) Diagram of conditions round high vacuum jet. (b) Diagrammatic representation of Embree jet, U. S. Patent 2,150,676.

the jet, at *A* in the figure. Region *B* should be kept warm, and *C* relatively hot. This is all achieved with air cooling or cooling by a spiral of tubing supplied at the top with a slow stream of cold water.

We have repeatedly confirmed the advantage of matching the cooling to the design of jet. We may define speed as the net profit of passage forward over passage back, and ultimate vacuum as the position of equilibrium between pumping speed and rate of contamination or leakage. Both speed and ultimate vacuum may benefit from moderate cooling. Thus a three-jet glass fractionating pump, filled with Octoil, gave an ultimate vacuum 1.6×10^{-7} when air-cooled; 2.1×10^{-7} water-cooled. A glass-metal pump of capacity 220 l.p.s. had a speed of 120 l.p.s. when the glass envelope was replaced by water-cooled metal. This observation was confirmed independently by Mead of British Drug Houses and Burrows of Metropolitan-Vickers.* When,

* Private communications.

however, the jets were redesigned for service in the metal casing of the horizontal 4-inch fractionating pump, a speed of 250 l.p.s. was obtained; at the expense, however, of increased heat input.

The Ho coefficient and the permissible width of annulus between jet and walls are increased by lowering the fore-vacuum and improving the design of jet. Perhaps the most convenient way to obtain a low fore-pressure for any given jet is to place another jet in advance. Two jets in tandem have long been in use, but only recently has the advantage of a third or even fourth jet been appreciated. Thus when the fore-pressure for the high vacuum jet has been reduced to 10^{-3} mm or less, the mean free path of the gas in random or sideways motion below the jet is more than an inch and clearances of 1–3 inches can be used without diminishing the admission coefficient. Expansion of the vapors after the manner of Crawford[15] should be used to the extent that the operating fluid will boil under compression without cracking. But most important of all, the jet should be directed straight downward with provision for expansion of the vapors toward the *center* of the pump. Inward expansion has been provided for by Gaede[16] and others[8] with jets similar to those in Fig. 3, but to the best of our knowledge the vertical downward, inwardly expanding jet has not hitherto been described. It was evolved by Dr. Norris Embree, working with Mr. Percy Coomber who acquired some skill in spinning cups of various types out of sheet aluminum on the laboratory lathe. Embree has measured the speeds for a large number of jets of different designs and placed in the three positions of a glass-metal pump. The final jet assembly with the high speed jet at the top is shown in Figs. 9 and 10 (b). The 4-inch pump has a theoretical admittance of 730 liters per second and an actual speed of 250 liters. A Ho coefficient of over 30 percent has thus been obtained. This may be contrasted with efficiencies of 2–20 percent mentioned in Ho's paper. It is evident that the high Ho coefficient of the present pump is more apparent than real. The collecting zone with the Embree jet is not measured by the area of the annulus between the jet gap and the walls but by the area of the cone indicated by the dotted lines in Fig. 10 (b). The speed of the pump is thus the summation of the mechanical admittance to the jet region and the diffusive admittance through the cone of actuating vapors themselves. A further study of visible vapor streams in transparent apparatus should lead to further improvements in design. The present glass-metal pumps, which consume only 220 watts on normal load operated against a starting back-pressure of 0.2 mm are useful where the ultimate vacuum of 5×10^{-6} mm provided by a nonfractionating pump is sufficient. They may be found on cyclotrons and vacuum spectrographs, but their special value appears to be on vacuum vessels for the production of mirrors by evaporation of metals.

Testing and Speed Measurements

The Embree jet has been applied to the horizontal fractionating pump, as shown in Figs. 6 and 7. The testing of a large pump, with the conflicting interplay of jets and boilers, is somewhat of a task. The set-up of gauges and subsidiary apparatus for testing and adjusting the 21-inch pump is shown in Fig. 8. The speed at 10^{-6} is about 7000 liters per second. Part of a molecular still appears to the right in the photograph.

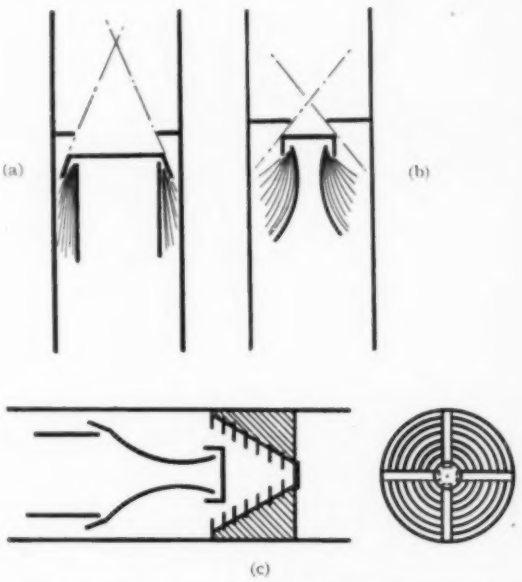

FIG. 11. (a) and (b), conventional baffle. (c), conical baffle.

Much has been written,[10, 11, 13, 17] concerning speed measurements, the units and nomenclature

for which are well established. The speed is defined as the volume of gas handled per second measured on the high vacuum or working side of the pump. The speed usually remains constant over wide ranges of working pressure. As a consequence, the *mass* of gas handled diminishes proportionally with the decrease of pressure. Our fractionating pumps have approximately constant and optimum speeds between 10^{-4} and 10^{-6} mm, above and below which the speeds diminish. Speeds at pressures outside the steady range must be the subject of special inquiry and measurement. We prefer to determine speeds by the use of an external adjustable leak, graduated pipette, and pneumatic oil trough, rather than trusting to a calibrated orifice in a closed circulatory system. With the external leak, the conservative and useful speed is measured. In a closed system, semivolatile constituents may cruise round and round, causing an additional difference of pressure which is not indicative of useful performance. Applying a refrigerant which will not afterwards be employed in practice introduces errors.

Each region in a multi-jet pump, proceeding towards the fore-vacuum, handles gas at a higher pressure and smaller volume than the next, yet the mass to be handled by each is the same. In a terminology, due we believe to Sykes of Metropolitan-Vickers, the jets all handle the same liter-microns or liter-μ. Each jet in series, consequently, should have slightly greater liter-μ capacity.

The jets in the 4, 8, and 21-inch pumps have been adjusted to the necessary relative liter-μ capacities, and as a result each pump has an admittance at the high vacuum inlet of 20 liters per second per square inch of area at the mouth, giving a Ho efficiency of a little over 50 percent. If we feel prone to congratulate ourselves on the "colossal" speed of the largest pump—7000 liters per second—we may refrain by reflecting that the volume at 10^{-5} mm becomes a small fraction of a cubic centimeter of free air at atmospheric pressure after passage through the mechanical fore-pump. Since many kilowatts are required to heat the fractionator and drive the fore-pump, the mechanical efficiency is appallingly low—less than one in a billion. The volume of tenuous gas cleared by the pump is equal to that swept aside by a car traveling at moderate speed. Yet if the car were moving in a vacuum of 10^{-5}, it would be considered to suffer absolutely no opposition, and thus do no work in sweeping aside this residual gas. Though the pump handles two thousand gallons per second, it would take seven years to clear one cubic mile of interlunar space at a cost, with electricity at a penny a kilowatt-hour, of $5000–$10,000. Clearly, the means of producing an empty cabinet neatly and economically still eludes the engineering physicist.

Baffles and Traps

Even in the most carefully exhausted vessel there remains a vaporous atmosphere. At 10^{-6} mm, for instance, there are approximately 10^{10} particles of oil vapor per cm^3. The atmosphere, being in contact with condensed pump fluid, may be saturated or unsaturated, humid or dry, in exact analogy with terrestrial weather. There is indeed a "weather" in a vacuum system and the humidity may be aggravated by backstreaming, analogous to rain. Backstreaming may be cured by a mechanical baffle, but the humidity can be decreased only by lowering the temperature of the pump intake below that of the evacuated chamber or by placing an actual absorbent of the vapor in the connecting pipe—hence the well-known charcoal trap.

Mechanical baffles to cure backstreaming in high speed pumps with wide jet clearances cannot usefully follow accepted design because of their geometry. This is at once apparent from Fig. 11 (a) and (b). If the baffles are made to cover the projection of the jet, the admittance is decreased until all advantage of the high speed jet is lost. We prefer to employ the stepped conical baffle, shown in Fig. 11 (c) applied to a horizontal pump. The baffle is made of thin aluminum rings held in stout jaws which conduct heat away to the walls of the intake. The baffle decreases the intake of the pump approximately 30 percent but stops backstreaming effectively.

To lower the internal humidity, the baffle should be cooled below room temperature. Where only moderate lowering is available, as from city water supply in late summer, two baffles may be employed in series. The second baffle catches the vapor evaporated from the back of the wet,

slightly warm rings of the first baffle. Generally a lowering of 10–15°C is all that is required, which can be secured with city water. This gives an internal humidity of about 25 percent, which is sufficiently low to prevent condensation of

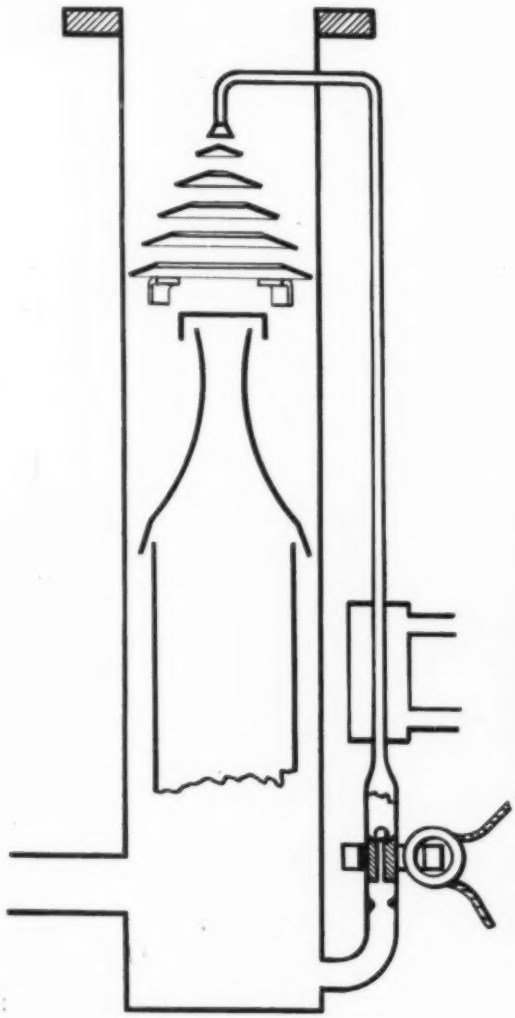

FIG. 12. Conical baffle with fluid circulation.

pump fluid on mirrors, gratings, and metal parts. Where absolute exclusion of pump fluid vapor is demanded by unusual circumstances, mechanical refrigeration or dry ice are indicated.

The charcoal trap, useful as it has proved in relatively small physical systems, in our opinion finds no place in the present day high speed pump system. The charcoal retards gas flow and consumes valuable time in conditioning before vacuum can be established. Nearly every vacuum requirement is available by choice of the appropriate pump, fluid, and simple cooling device.

A method of reducing internal humidity, which we have tested but have not had occasion to practice, is to circulate over the conical baffle a nonvolatile component specially added to the pump fluid. This becomes segregated and purged in the last compartment of the pump from which it is ready, when cooled, to dry almost completely the residual pump fluid atmosphere. The device is drawn in Fig. 12.

In the broadest sense a trap is not only an adjunct to a pump but has inherent pumping capacity. Old-fashioned traps, cooled with liquid air, not only removed mercury vapor from the pump, but they condensed volatiles from the evacuated chamber and thus accelerated the establishment of vacuum. Traps may, therefore, be classified as static or dynamic according as

FIG. 13. Glass booster.

to whether they merely prevent backstreaming and diffusion or actually accelerate pumping. Adsorption devices[18] and electrical means for decomposing or accelerating the incoming vapors show promise for future development. These

aspects of the trap problem are being dealt with elsewhere.[19]

Pump Fluids

Since 1936 the phlegmatic phthalates have been augmented by the still less volatile sebacates. Table I copied from our commercial literature gives their operating characteristics. Octoil-S has, so far, given the highest vacua, pressures of 10^{-9} mm at room temperature having been recorded. Butyl sebacate and Amoil-S provide moderate vacua under extremely heavy duty. Certain chlorinated hydrocarbons not listed, are showing promise as booster fluids which can operate against high fore-pressures because of their density. A glass booster pump capable of operating against 0.6 mm with butyl phthalate and 1.0 mm with chlorinated fluid is shown in Fig. 13. It has a speed of 4 liters per second at 10^{-2} mm and will provide about 10^{-3} mm on reduced wattage after vacuum has been established at higher wattage.

Conclusion

Although little that is new in principle has been described in this paper, design is shown to have advanced so that pumps now handle as many liters per second as they formerly handled in cubic centimeters. Our first pump of 1930, speed 1000 cc per second, is contrasted with the present 21-inch pump, speed 7000 liters per second.

In closing, the author wishes to thank his colleagues for their assistance and ingenuity; thanks to Dr. Embree for permitting the description of his high speed jet; to Mr. R. S. Morse for bringing many of the pumps to final industrial usefulness, and to Dr. J. G. Baxter and Mr. R. L. Edwards for producing the sebacate fluids in quantity.

Bibliography

1. K. C. D. Hickman, J. Frank. Inst. (1936).
2. K. C. D. Hickman, U. S. Patent 2,080,421—applied for June 21, 1935, granted May 18, 1937; U. S. Patent 2,153,189—applied for May 18, 1937, granted April 4, 1939; U. S. Patent 2,150,685—applied for March 11, 1937, granted March 14, 1939.
3. Campagnie General de Radiologie and H. Pilon, Brit. Pat. 404,190—applied for May 3, 1923, granted January 11, 1934. See p. 2, lines 35–40.
4. C. R. Burch and F. E. Bancroft, Brit. Pat. 346,293—applied for January 6, 1930 granted April 7, 1931.
5. Brit. Pat. 466,514—applied for November 29, 1935, granted November 27, 1936.
6. A. E. Lockenvitz, Rev. Sci. Inst. **8**, 322 (1937).
7. L. Malter and N. Marcuvitz, Rev. Sci. Inst. **9**, 92 (1938).
8. Brit. Pat. 477,013—applied for June 20, 1936, granted December 20, 1937.
9. J. A. Becker and E. K. Jaycox, Rev. Sci. Inst. **2**, 774 (1931).
10. I. Langmuir, Gen. Elec. Rev. 1060 (1916); J. Frank. Inst. **182**, 719 (1916).
11. Lyman C. Parratt, Am. Phys. Teacher **7**, 207 (1939).
12. H. W. Edwards, U. S. Patent 2,063,665—filed March 21, 1934, granted December 8, 1936.
13. T. L. Ho, Physics **2**, 387 (1932).
14. I. Langmuir, Phys. Rev. **8**, 48 (1916).
15. Crawford, U. S. Patent 1,367,865—granted July 5, 1924.
16. Gaede, Zeits. f. tech. Physik **4**, 337 (see p. 366), (1923).
17. K. C. D. Hickman and Sanford, Rev. Sci. Inst. **1**, 155 (1930).
18. K. C. D. Hickman, Pat. applied. U. S. Serial No. 147,514.
19. R. S. Morse, to be published.

Pendulum Analysis in the Scale Industry

By Glenn R. Carley

Toledo Scale Company, Toledo, Ohio

Forces created when loads are applied to the platforms of automatic weighing mechanisms are frequently balanced by the rotation of pendulums. In certain types of pendulum-controlled scales it is desired that the relationship between the load applied and the angle turned by the pendulums be essentially linear. Even though the cams used for pendulum rotation are sectors of circles, it has been found experimentally that by the proper adjustment of various pendulum parameters, linear performance can be approximated to within less than 0.025 percent of scale capacity. An analysis of the forces involved in such systems leads to a mathematical statement of pendulum performance. Furthermore, experimental results confirm quantitatively the operation predicted by analysis. A method of selecting parameters for optimum performance is presented.

Introduction

THE art of weighing goods by balancing them against certain accepted standards of mass is very old and one of the first adventures of man into applied science. Archimedes observed the principles that govern a simple lever shortly after the Golden Age in Greece, yet the Babylonians, the Egyptians and many an ancient people had been using the most rudimentary forms of balances centuries, even, before his day.

Old though this practice is, neither the outward forms nor the principles of operation of these early balances were varied appreciably until quite recently. Only within the last two hundred years has it been discovered that, by connecting two or more levers together in a tandem arrangement, considerably larger loads could be weighed. With this innovation a more modern approach to scale design began—a movement, starting slowly enough, but which has been accelerating at an increasing rate in the past few years. As more exacting demands have been placed on weighing equipment by a materially expanding civilization, progressive scale engineering has developed new designs, new materials and a highly versatile response to our contemporary emphasis on automatism.

A major advance in design introduced the familiar beam type of scale which consists essentially of a system of levers in which a beam is attached to the final lever. The beam carries a poise which can be placed at any position along the beam to counter-balance the force transferred through the system when a particular load is placed on the platform. Thus, the system of levers always returns to a central position when equilibrium is reached while the magnitude of the platform load is a linear function of the poise position.

Fig. 1. A simple balance used in Egypt during the rule of the Pharaohs. Weighing by comparing masses has long been fundamental. Print taken from the paper, "On Ancient Desemers or Steelyards," by Herman Sokeland, published in the 1900 Report of the Smithsonian Institution.

This type of manipulated indication has prevailed for many years due to its simplicity and great accuracy. However, the increasing demand by commerce and industry for speed has led to the pendulum type of scale in which the platform

load is indicated automatically as a function of the pendulum rotation required for equilibrium.

Thus weighing mechanisms have emerged from such ancient and primitive forms as shown in Fig. 1, to a type shown in Fig. 2, which is a photograph of the pendulums and indicating mechanism used today in an industrial scale. Two beams are also shown in this figure—one for increasing the capacity of the scale, the other for counter-balancing the weight of any container of material being weighed. The platform, though not shown, is of familiar design.

A more detailed view of the pendulums is given in Fig. 3. Each pendulum consists of one large and two small sectors, a pendulum stem and a pendulum weight. The pendulum weight can be locked at any point along the stem. The sectors are turned and ground very accurately to

FIG. 2. The head mechanism in a typical industrial scale.

particular radii. Flexible steel ribbons, secured at one end to the lower terminal of the two small sectors, pass around these sectors, follow up the sector guide—the solid framework between the two pendulums—and have their other ends fastened to the upper portion of this sector guide. Similar steel ribbons secured to the upper terminals of the large sectors, which are called the power sectors, pass around these and are fastened to the lower ribbon connection as shown.

When mounted in this manner each pendulum has its fulcrum at the points of tangency of small

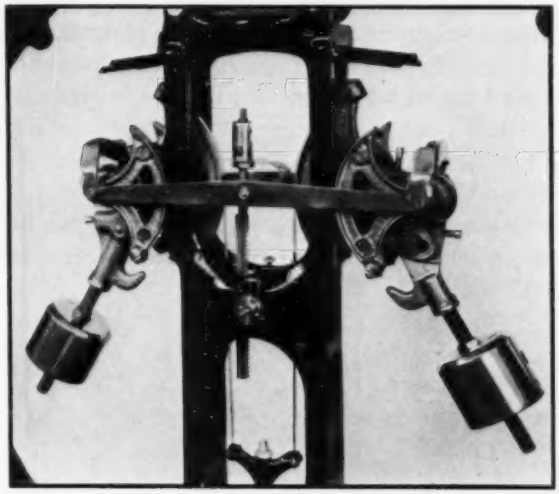

FIG. 3. A set of pendulums. For clarity, the indicator has been removed from the pinion shaft.

sectors and ribbons. Thus vertical displacement accompanies the rotation of the pendulums as force is applied to the lower ribbon connection. With this combination of motions each point of a pendulum sweeps out a small section of a cycloid. The indicating mechanism is linked directly with the vertical movement of the pendulums by means of a rack and pinion. This connection is such that a 60° rotation of the pendulums rotates the indicator through a chart of 345°. Indicator rotation is therefore a linear function of pendulum rotation.

The system of levers in a scale serves to transform the large force exerted on a loaded platform into a much smaller force which, in turn, is balanced by a rotation of the pendulums. Although the wide variety of installations for industrial scales demands an unusual number of platform capacities, these differing capacities can generally be reduced, by means of various lever multiplications, to a relatively narrow range of maximum forces at the pendulums. By selecting appropriate weights for the pendulum stems, the combined capacity of a set of pendulums can be

adjusted to accommodate a particular maximum force. In this way, a balance is attained between the capacity of the scale, the total multiplication of the levers and the capacity selected for the pendulums. The capacity of an individual pendulum can be varied from 5 to 15 pounds according to the weight selected for the pendulum stem.

With this assemblage of levers and pendulums, indicator rotation will not result, in general, in a chart having uniformly spaced graduations. For pendulums in which the sectors are concentric, the distribution of graduations would follow, approximately, an inverse sine function of the load on the scale. Since it is highly desirable that chart graduations be spaced uniformly, pendulums must be designed to rotate linearly with the load.

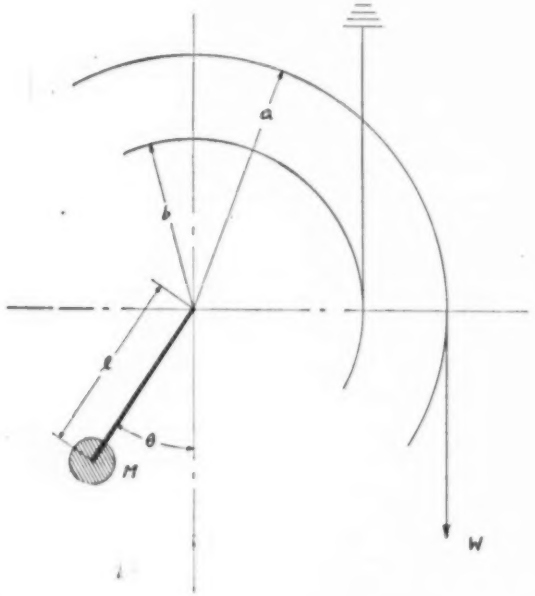

FIG. 4. Vertical pull on a concentric sector pendulum.

Several years ago scale engineers found, by placing the power sector slightly eccentric with respect to the small sector axis, that a close approximation to linear performance was possible. After considerable experimenting it was found that a delicate balance of the variables permitted pendulum performance with maximum deviations from linearity of less than 1 part in 4000. Using this technique engineers became very adept at developing pendulums when new applications were required. However, the labor involved in such developments seemed to be excessive, and it was thought that assistance might be rendered by attacking the problem of design from the theoretical point of view. Analyses show that the necessary characteristics of a pendulum can be calculated.

Although partial analyses have been made in the past, literature on this application of pendulums is negligible. For this reason the approach to a complete analysis will be presented in some detail. A derivation of the equations for both a vertical pull concentric pendulum and a vertical pull eccentric pendulum will be followed by a graphical description of the factors influencing performance of the eccentric pendulum. Then, corrections for pulling nonvertically on the power sector will be given for the eccentric pendulum. Finally, a method will be developed for obtaining the optimum performance conditions for a pendulum applicable to a counting scale.

A Concentric Sector Pendulum

Let the power sector in the pendulum sketched in Fig. 4 be concentric with respect to the small sector axis. Imagine this pendulum suspended from ribbons similar to the mounting already described. As force is applied to the power sector, the pendulum is free to roll in a vertical plane. Let: a = radius of the power sector, b = radius of the small sectors, M = weight of the entire pendulum, considered as concentrated at the center of mass of the pendulum, l = distance of this center of mass from the axis of the sectors, W = the vertical component of the force applied to the power sector ribbon, and θ = angle made by two lines drawn through the sector axis—one, vertical and the other, through the center of mass. θ is negative when measured counterclockwise from the vertical. Equating moments about the fulcrum—the points of tangency of ribbons and small sectors—for pendulum equilibrium,

$$W(a-b) = M(b+l\sin\theta) \tag{1}$$

or

$$W = \frac{M}{a-b}(b+l\sin\theta). \tag{2}$$

W is a function of $\sin\theta$ while for a chart with uniformly spaced graduations, the equation for

the pendulum should closely approximate a linear function of θ, i.e.,

$$W_L = K + J\theta. \tag{3}$$

An expression for the deviations from linearity, $(W_L - W)$, can be written. If (θ_1, W_1) and (θ_2, W_2) are the initial and the final coordinates of the pendulum equation, (2), and the straight line, (3), is passed through these points, K and J in (3) become,

$$K = (W_1\theta_2 - W_2\theta_1)/(\theta_2 - \theta_1),$$
$$J = (W_2 - W_1)/(\theta_2 - \theta_1), \tag{4}$$

so that

$$W_L - W = \frac{\theta_2 - \theta}{\theta_2 - \theta_1} W_1 + \frac{\theta - \theta_1}{\theta_2 - \theta_1} W_2 - W. \tag{5}$$

For a chart with uniformly spaced graduations, (5) gives the amount, in pounds, that scale indication would be in error. However, it is not this absolute deviation which is important, but rather the deviations with respect to pendulum capacity, i.e.,

$$(W_L - W)/(W_2 - W_1),$$

for this is the error which is finally observable when reading the scale. If this is multiplied by 100, an expression for the percentage error or the percent deviation from linearity with respect to

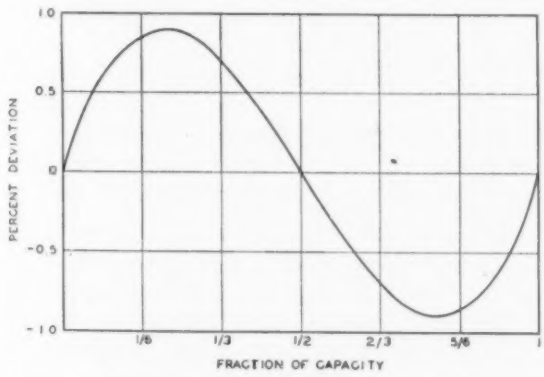

FIG. 5. Deviation from linear performance for the pendulum of Fig. 4.

pendulum capacity is obtained. Thus (5) becomes

$$\frac{W_L - W}{W_2 - W_1} 100 = \%\ \text{Dev.}$$
$$= \frac{100}{W_2 - W_1}\left[\frac{\theta_2 - \theta}{\theta_2 - \theta_1} W_1 + \frac{\theta - \theta_1}{\theta_2 - \theta_1} W_2 - W\right], \tag{6}$$

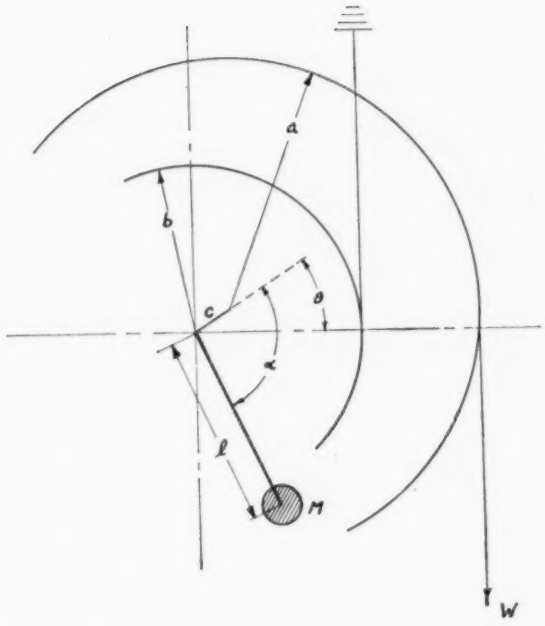

FIG. 6. An eccentric sector pendulum with vertical pull on the power sector.

which gives the percent deviations as a function of θ. Eq. (6) is general and will be used several times as the characteristic equations for different pendulums are derived.

Using (2) and (6), a group of deviations were calculated for this pendulum which, when plotted, gave the performance curve shown in Fig. 5. θ ranged from $\theta_1 = -30°$ to $\theta_2 = 30°$. The percent deviations with respect to capacity are independent of the dimensions of the pendulum. However, the maximum deviation from linearity is nearly 1 percent which is considerably greater than the limit of error of 0.025 percent usually required for pendulum performance.

An Eccentric Sector Pendulum

If in place of a concentric mounting, the power sector is mounted eccentrically with respect to the small sector axis, an extraordinary improvement is obtained in pendulum performance. Fig. 6 represents such a pendulum with an eccentric power sector. Let the center of the power sector be placed at a distance c from the axis of the small sectors. a, b, l and M have the same significance as before. W is again the vertical component of the force on the power sector. α is the angle between the two directions

defined by c and l. θ is the coordinate of pendulum position. In this notation it is considered a positive angle when measured counterclockwise from the horizontal through the small sector axis. Taking moments about the fulcrum, the characteristic equation defining equilibrium follows:

$$W = M[b - l\cos(\alpha - \theta)]/(a - b + c\cos\theta). \quad (7)$$

If (7) is substituted in (6), percent deviations from linearity are again given as a function of θ.

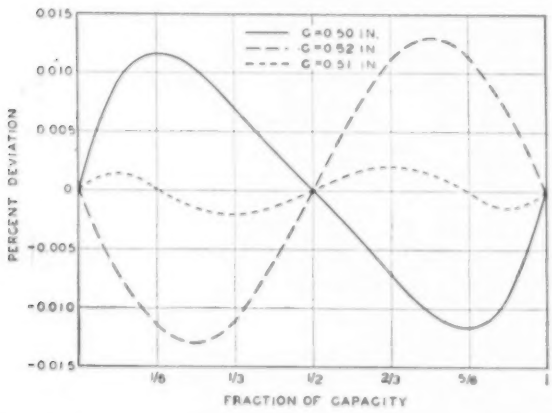

FIG. 7. Performance variations with respect to changes in eccentricity, c, for the pendulum of Fig. 6.

To demonstrate the operation of this eccentric sector pendulum, quite arbitrary values may be selected for a, b, l and θ_1. M may be neglected, for in Eq. (6), a constant factor in the pendulum equation occurs in both numerator and denominator. A 60° range for θ is again chosen. α is a parameter and, as such, is adjustable, both in theory and in practice, to permit maximum linear performance. (The two screws used for adjusting α as well as the screw used for locking the final position of the power sector are clearly visible in the right-hand pendulum of Fig. 3.) Just as α is adjusted in practice to give zero deviation at the one-half capacity position of the pendulum travel, so let it be adjusted, mathematically, to insure zero deviation for this same position. In terms of θ, the one-half capacity position is given by,

$$\theta = \theta_3 = (\theta_1 + \theta_2)/2. \quad (8)$$

Substituting (7) and (8) in (6) and equating to zero gives the equation defining α. After expansion and recollection of terms, this equation becomes

$$l(r\cos\alpha + s\sin\alpha) = t, \quad (9)$$

where r, s and t are the constants,

$$r = \left[\frac{\cos\theta_1}{a-b+c\cos\theta_1} + \frac{\cos\theta_2}{a-b+c\cos\theta_2} - \frac{2\cos\theta_3}{a-b+c\cos\theta_3}\right],$$

$$s = \left[\frac{\sin\theta_1}{a-b+c\cos\theta_1} + \frac{\sin\theta_2}{a-b+c\cos\theta_2} - \frac{2\sin\theta_3}{a-b+c\cos\theta_3}\right], \quad (10)$$

$$t = \left[\frac{1}{a-b+c\cos\theta_1} + \frac{1}{a-b+c\cos\theta_2} - \frac{2}{a-b+c\cos\theta_3}\right]b.$$

For definiteness let a pendulum with the following dimensions be assumed:

$$a = 3 \text{ inches}, \quad \theta_1 = 30°,$$
$$b = 2 \text{ inches}, \quad \theta_2 = -30°,$$
$$l = 2.5 \text{ inches}, \quad \theta_3 = 0°.$$

As a first approximation, let the eccentricity, c, be 0.50 inch. r, s and t must first be calculated from (10). Using these constants α is best obtained from (9) by the method of successive approximations. In order to obtain α with sufficient accuracy, seven-place tables of logarithms were necessary; hence, these tables were used for all of this work. α is found to be 113° 34′ 41.60″. Using (6), percent deviations are calculated at a sufficient number of points to give the curve, $c = 0.50$ inch, in Fig. 7. The approximation to linear performance is very good, for deviations are everywhere less than 0.015 percent of pendulum capacity.

It is interesting to observe the effect of increasing the eccentricity of the power sector from $c = 0.50$ to $c = 0.52$ inch. A complete set of deviations has been calculated for this

eccentricity which is represented by the curve, $c=0.52$ inch, in Fig. 7. An increase in the eccentricity of the power sector of 0.02 inch practically reverses the performance curve with respect to the capacity axis.

An interpolation between these two eccentricities results in an even nearer approximation to linearity. To test this, another set of deviations has been calculated for an eccentricity of $c=0.51$ inch. The plot for this set, shown also in Fig. 7, gives a maximum deviation from linearity of less than 0.0025 percent of pendulum capacity.

The curves in Fig. 7 are symmetrical about the one-half capacity point on the pendulum capacity axis. This is the result of taking θ_1 equal to 30° or, more generally, it is the result of balancing the travel of θ about the horizontal reference axis. If θ_1 is taken larger than 30°, which means that the pendulum must have a lower initial position, the deviations for the first half of pendulum travel are larger than when $\theta_1=30°$, while deviations in the second half are smaller than when $\theta_1=30°$. If θ_1 is taken smaller than 30°, just the reverse is true—deviations are less in the first half of travel and greater in the second.

To indicate these drifts in operating performance, data from two additional groups of deviations have been plotted in Fig. 8. For these

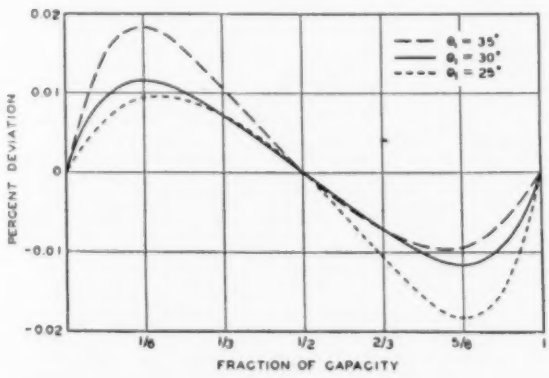

FIG. 8. Performance variations with respect to changes in initial pendulum position (constant eccentricity) for the pendulum of Fig. 6.

curves, $c=0.50$ inch, as for the first curve plotted in Fig. 7; a, b and l have the same values as previously; deviations are plotted for $\theta_1=35°$, 30° and 25°. There is a symmetry about the one-half capacity point of the capacity axis between

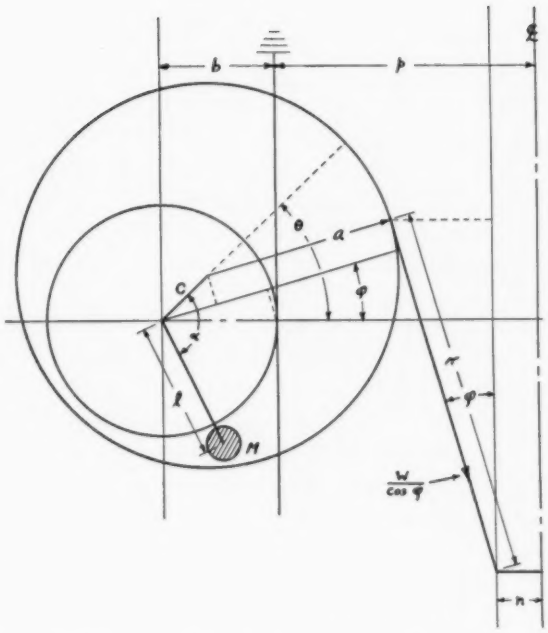

FIG. 9. An eccentric sector pendulum with nonvertical pull on the power sector.

the curves for $\theta_1=35°$ and $\theta_1=25°$. This symmetry is due to the symmetrical location of these two θ_1's about the position, $\theta_1=30°$. By observing the rates of change of curve ordinates with respect to changes in c and with respect to changes in θ_1, it is possible to select the pendulum constants in such a way that a performance curve of almost any shape can be obtained.

For pendulums connected to a system of levers, the power sector ribbons cannot always pull vertically because of sector eccentricity. The corrections which must be added for nonvertical pulling are not difficult to introduce, but they eliminate much of the symmetry observed in the performances of vertical pull pendulums.

A Nonvertical Pull Pendulum

An eccentric sector pendulum with a nonvertical pull on the power ribbon is sketched in Fig. 9. For a clear drawing, the angle, φ, which the power sector ribbon makes with the vertical is drawn larger than is ordinarily used. Referring to Fig. 3, the constant, p, is one-half the distance between pendulum fulcrums, while n is one-half the length of the lower ribbon connection. The other constants have the same significance as before. Equating moments, the characteristic

equation for equilibrium is given by

$$\frac{W}{\cos\varphi}[a-b\cos\varphi+c\cos(\theta-\varphi)] = M[b-l\cos(\alpha-\theta)],$$

or

$$W=\frac{M[b-l\cos(\alpha-\theta)]\cos\varphi}{[a-b\cos\varphi+c\cos(\theta-\varphi)]}. \quad (11)$$

φ is defined by

$$\sin\varphi=\frac{b+p-n-a\cos\varphi-c\cos\theta}{r}, \quad (12)$$

and r is given by

$$r=r_1+a[(\theta_1-\varphi_1)-(\theta-\varphi)]. \quad (13)$$

r_1 and φ_1 are the values for r and φ when $\theta=\theta_1$. (13) substituted in (12) gives

$$\sin\varphi=\frac{b+p-n-a\cos\varphi-c\cos\theta}{r_1+a[(\theta_1-\varphi_1)-(\theta-\varphi)]}. \quad (14)$$

φ is small enough that $\sin\varphi$ can by represented by φ and $\cos\varphi$ by $1-\frac{1}{2}\varphi^2$. Substituting these approximations in (14), φ finally becomes, to a second approximation,

$$\varphi=\frac{b+p-n-a-c\cos\theta}{r_1+a(\theta_1-\varphi_1-\theta)}\times\left[1-\frac{(b+p-n-a-c\cos\theta)a}{2[r_1+a(\theta_1-\varphi_1-\theta)]^2}\right]. \quad (15)$$

Again, φ is small enough that the second term in (15) can usually be neglected, leaving for φ,

$$\varphi=\frac{b+p-n-a-c\cos\theta}{r_1+a(\theta_1-\varphi_1-\theta)}. \quad (16)$$

Although the general procedure for obtaining the deviations from linearity for this nonvertical pendulum is the same as for the vertical pull pendulum, the labor involved is more tedious. φ must first be found as a function of θ from (16). Substituting values obtained from (16), (11) and (8) in (6) equated to zero, a slightly different equation for calculating α is given by

$$l(r\cos\alpha+s\sin\alpha)=t, \quad (9)$$

because r, s and t are now given as

$$r=\left[\frac{\cos\theta_1\cos\varphi_1}{a-b\cos\varphi_1+c\cos(\theta_1-\varphi_1)}+\frac{\cos\theta_2\cos\varphi_2}{a-b\cos\varphi_2+c\cos(\theta_2-\varphi_2)}-\frac{2\cos\theta_3\cos\varphi_3}{a-b\cos\varphi_3+c\cos(\theta_3-\varphi_3)}\right],$$

$$s=\left[\frac{\sin\theta_1\cos\varphi_1}{a-b\cos\varphi_1+c\cos(\theta_1-\varphi_1)}+\frac{\sin\theta_2\cos\varphi_2}{a-b\cos\varphi_2+c\cos(\theta_2-\varphi_2)}-\frac{2\sin\theta_3\cos\varphi_3}{a-b\cos\varphi_3+c\cos(\theta_3-\varphi_3)}\right], \quad (17)$$

$$t=b\left[\frac{\cos\varphi_1}{a-b\cos\varphi_1+c\cos(\theta_1-\varphi_1)}+\frac{\cos\varphi_2}{a-b\cos\varphi_2+c\cos(\theta_2-\varphi_2)}-\frac{2\cos\varphi_3}{a-b\cos\varphi_3+c\cos(\theta_3-\varphi_3)}\right].$$

α, so determined, will again insure zero deviation at the one-half capacity position of the pendulum travel.

To demonstrate the operation of a representative pendulum, the following group of constants has been selected from a pair of pendulums adjusted for operation in a scale:

$a=2.87$ inches, $M=3.027$ pounds,
$b=2.046$ inches, $\theta=35°$,
$c=0.39$ inch, $l=2.257$ inches.

φ is given as a function of θ, using the additional constants,

$p=2.125$ inches,
$n=0.812$ inch,
$r=6.543$ inches.

Performance is given by the curve, $c=0.39$ inch in Fig. 10. To indicate the effect of changing the eccentricity, deviations for a pendulum for which $c=0.40$ inch are also plotted in Fig. 10.

The capacity of the "$c=0.39$" pendulum is 5.33 pounds. If pendulums of this capacity (or very nearly this capacity) could be used in all scales, a pendulum could be designed which would give excellent linear response. However, it is desirable that this pendulum be used for capacities ranging from 5 to 15 pounds. The results on pendulum performance of varying pendulum capacities will be mentioned.

Increasing the weight on a pendulum stem increases capacity for two reasons: the primary increase is due to the increase in M, itself, while

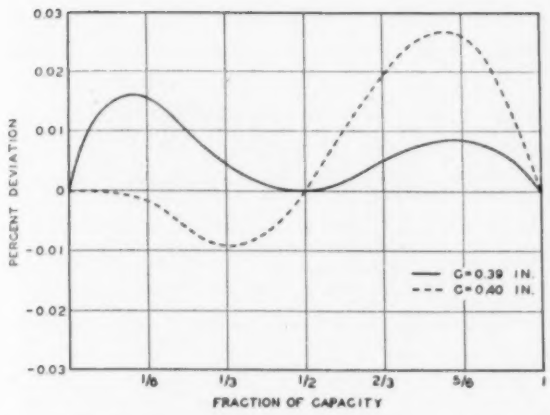

FIG. 10. Performance variations with respect to changes in eccentricity, c, for the pendulum of Fig. 9.

the secondary increase comes from an increase in l due to the increased M. For nonvertical pull pendulums an increasing l tends to distort the performance curve. To compensate for this distortion, a decrease in θ_1 has been found sufficient. Now α varies inversely with l according to (9), so that α decreases as l increases. The pendulum stems are always started from a vertical position; hence, θ_1 decreases as α decreases. Therefore, the distortion due to increasing l is partially corrected by the accompanying decrease in θ_1. However, the compensation is not complete because α does not change fast enough with respect to l. It seems best to maintain as narrow a range as possible for pendulum capacities.

Calculations have been made to learn the effect of changing φ. The results of these determinations show: first, the less φ changes with θ the better (r_1 should be as long as possible), and second, φ, all positive or all negative is definitely better than φ partially positive, partially negative. The conclusion seems to be that the eccentricity can better be adjusted to conform with φ than vice versa.

A thorough consideration of these variations in performance with changing values of parameters has shown clearly why a performance of the "$c=0.39$" type, in Fig. 10, is far more suitable for a pendulum of 5.33 pounds capacity than a performance of the "$c=0.40$" type. As pendulum capacity is increased, characteristic performance gradually changes from the "$c=0.39$" curve to a graph similar in contour to the "$c=0.40$" performance curve, hence, the reason for beginning with the former.

In the main, the search for better pendulum performance has been carried on by interpolating between the particular parameters which have differentiated two performances. This method may become quite tedious, and it is highly desirable that a procedure be found which would enable the calculator to obtain, directly, the best initial position, θ_1, the best eccentricity, c, and, at the same time, the correct value for α. Two procedures have been tried; namely, a method of minimizing the area under the curve of deviations and secondly, a method of solving, simultaneously, for two or more parameters. The first procedure soon becomes very cumbersome, and there is the further complication in that the curve of pendulum deviations crosses the capacity axis at more than one point as the "ideal" solution is approached. The second method develops into the simultaneous solution of third-degree equations. For these reasons, the method of interpolation has been found most satisfactory in seeking better performance. However, in developing a pendulum for a counting scale the second procedure, the simultaneous solution of parameters, has been found especially applicable. A brief description of this work follows.

A Counting Scale Pendulum

The number of units in a collection of units all of the same weight can be obtained, of course, by dividing the total weight by the unit weight. Counting scales have been developed to give this number directly. An important form of counting scale is one in which the capacity of the pendulum mechanism is made dependent upon the weight of one of the units being counted. The total number of parts placed on the platform can then be indicated directly on the chart of the scale.

For the scale, herein described, but one pendulum is used, and so arranged that the capacity is fixed for a particular count by attaching one of the units to the pendulum stem. In order that pendulum capacity of the correct amount be obtained when a unit is added to the stem, it is necessary that any pendular effect in the system of levers and pendulum be counter-

balanced when no unit is attached to the stem. This means, that without weight on the stem, the system must be free to rest in any position in which it is placed. Then, when weight is added to the stem, the system returns immediately to the zero position.

In this application of the pendulum it is advisable to substitute a single, fixed center pendulum for the floating double pendulums already described. However, it is still desirable that the graduations about the chart be uniformly distributed, and, as before, the requisite pendulum operation is obtained by placing the power sector center eccentric with respect to the center of pendulum rotation. Such a pendulum is sketched in Fig. 11. The constants have the same significance as previously except that θ is measured clockwise from the vertical through the center of rotation. Equating moments, the equation of equilibrium is given by

$$\frac{W}{\cos\varphi}[a+c\sin(\alpha-\theta-\varphi)]=Ml\sin\theta,$$

which becomes

$$W=\frac{Ml\sin\theta\cos\varphi}{a+c\sin(\alpha-\theta-\varphi)}, \tag{18}$$

where φ is defined by

$$\sin\varphi=\frac{x-a\cos\varphi-c\sin(\alpha-\theta)}{r} \tag{19}$$

and

$$r=r_1+a[(\theta-\theta_1)+(\varphi-\varphi_1)]. \tag{20}$$

Therefore, (19) and (20) give

$$\sin\varphi=\frac{x-a\cos\varphi-c\sin(\alpha-\theta)}{r_1+a[(\theta-\theta_1)+(\varphi-\varphi_1)]}. \tag{21}$$

Substituting φ for $\sin\varphi$ and $(1-\frac{1}{2}\varphi^2)$ for $\cos\varphi$, φ is given to a second approximation as

$$\varphi=\frac{x-a-c\sin(\alpha-\theta)}{r_1+a[\theta-\theta_1+\varphi_1]}\times\left[1-\frac{a}{2}\frac{[x-a-c\sin(\alpha-\theta)]}{[r_1+a(\theta-\theta_1+\varphi_1)]^2}\right]. \tag{22}$$

(6) can again be used for the equation of percent deviations, but in a much simplified form. From the fact that the entire system of levers and pendulum is nonpendular when the pendulum has zero capacity, it is clear that any weight added at a particular point of the pendulum stem will restore the pendulum to a position such that this point will come to rest directly beneath the center of rotation. If weight is always added at this point, the initial pendulum position will always be such that $\theta_1=0°$. From (18), W_1 must also be zero. These initial conditions simplify (6) so that it becomes

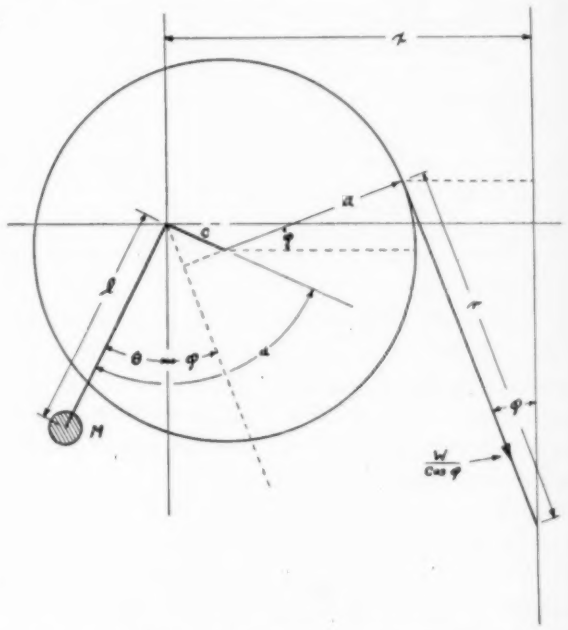

FIG. 11. A fixed center pendulum for a counting scale.

$$\%\ \text{Dev.}=\frac{100}{\theta_2 W_2}(\theta W_2-\theta_2 W). \tag{23}$$

If the angular rotation of the pendulum is again 60°, $\theta_2=60°$ and W_2 is obviously the capacity of the pendulum.

Now (23) is simplified enough that the two parameters, c and α, can be derived simultaneously. An approximation for φ, as a function of θ, must first be assumed, and later revised as more correct values for α and c are obtained.

Just as the percent deviations were independent of constant factors in the pendulum equations for the pendulums already analyzed, so the deviations for this pendulum are independent of constant factors. Therefore, (18) may be written

$$W=\frac{\sin\theta\cos\varphi}{a/c+\sin(\alpha-\theta-\varphi)}. \tag{24}$$

The parameters to be found simultaneously are now a/c and α.

The solution of these two parameters requires two equations. Let the two equations be obtained from the condition that percent deviations be zero at the four coordinates of pendulum travel, (θ_1, W_1), (θ_2, W_2), (θ_3, W_3) and (θ_4, W_4). (θ_1, W_1) is the position, (0, 0), while (θ_3, W_3) and (θ_4, W_4) are any two points between (0, 0) and (θ_2, W_2). Substituting, first the point (θ_3, W_3) in (23), then the point (θ_4, W_4) the two equations are

$$\theta_3 W_2 = \theta_2 W_3, \tag{25}$$

$$\theta_4 W_2 = \theta_2 W_4. \tag{26}$$

Expanding (25) and (26) then recollecting terms, simultaneous solution for α and a/c gives

$$\cot \alpha = \frac{tl - nr}{ns - lm} \tag{27}$$

and

$$\frac{a}{c} = \frac{r \sin \alpha + s \cos \alpha}{t}, \tag{28}$$

where

$$\begin{aligned}
r &= \left[\sin \theta_2 \cos \varphi_2 \cos (\theta_3 - \varphi_3) - \frac{\theta_2}{\theta_3} \sin \theta_3 \cos \varphi_3 \cos (\theta_2 - \varphi_2) \right], \\
s &= \left[\frac{\theta_2}{\theta_3} \sin \theta_3 \cos \varphi_3 \sin (\theta_2 - \varphi_2) - \sin \theta_2 \cos \varphi_2 \sin (\theta_3 - \varphi_3) \right], \\
t &= \left[\frac{\theta_2}{\theta_3} \sin \theta_3 \cos \varphi_3 - \sin \theta_2 \cos \varphi_2 \right], \\
l &= \left[\sin \theta_2 \cos \varphi_2 \cos (\theta_4 - \varphi_4) - \frac{\theta_2}{\theta_4} \sin \theta_4 \cos \varphi_4 \cos (\theta_2 - \varphi_2) \right], \\
m &= \left[\frac{\theta_2}{\theta_4} \sin \theta_4 \cos \varphi_4 \sin (\theta_2 - \varphi_2) - \sin \theta_2 \cos \varphi_2 \sin (\theta_4 - \varphi_4) \right], \\
n &= \left[\frac{\theta_2}{\theta_4} \sin \theta_4 \cos \varphi_4 - \sin \theta_2 \cos \varphi_2 \right].
\end{aligned} \tag{29}$$

Corresponding subscripts for φ and θ refer to φ for that particular θ. It is fortunate for this application that α is independent of the pendulum capacity.

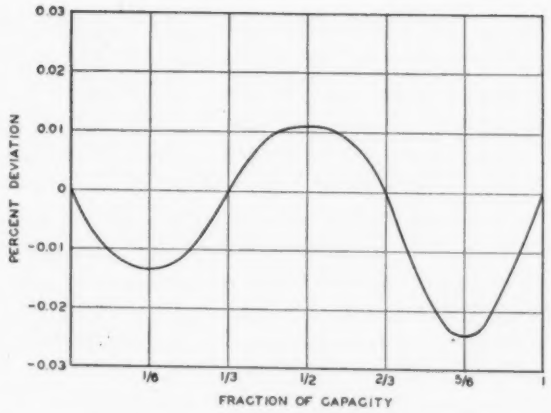

FIG. 12. Performance possible for a 60° travel of the counting scale pendulum of Fig. 11.

To demonstrate operation a pendulum of the following dimensions is selected: $a = 1.1875$ inches, $c = 0.6183$ inch, $x = 2.0000$ inches, $r = 13.000$ inches. φ is first obtained from (22) as a function of θ. A second approximation must be made for a very accurate calculation of pendulum performance. Using (27) and (28) and selecting $\theta_3 = 20°$ and $\theta_4 = 40°$, α and a/c are calculated. Then, (24) substituted in (23) gives the percent deviations which, when calculated and plotted, give the curve of Fig. 12. The maximum deviation is again less than 0.025 percent of pendulum capacity.

Discussion

In theoretical analyses it is often convenient to make certain simplifying assumptions in setting up descriptive equations. For a more refined solution, provision must either be made for these assumptions or it must be shown that by neglecting them, significant errors are not introduced. In this analysis equations were derived for a vertical pull on the power sector ribbon. For greater refinement, corrections were introduced to provide for pulling nonvertically.

However, several assumptions have been tacitly disregarded which may affect the linearity of performance, so that the equations may require further correcting. First, it has been assumed that there are no frictional forces in the system of levers and pendulums. Secondly, the

lower ribbon connection shown in Fig. 3 and drawn in Fig. 9 is coupled to the last lever in the system. The assumption has been made that the corrections necessary because of the very small horizontal component of motion thus transmitted to this connection have negligible effect on performance. Finally, no account has been taken either of ribbon thickness, of the energy required for bending the ribbons or of the ribbon elongations due to the applied stresses.

When all of the centers of movement in a scale are thoroughly cleaned, the combined effect on operation of all of the frictional forces is less than 0.01 percent of scale capacity. Hence, the first assumption is valid in that the effect of the frictional forces which are present can be made less than the tolerance allowed for operation.

To determine the order of error introduced by neglecting the small horizontal movement of the lower ribbon connection, careful tests were made on pendulum operation. The results indicate that corrections need not be added, for no differences can be observed between pendulum operation with the lower ribbon connection coupled to the last lever and operation without this coupling.

The ribbons used for mounting pendulums are 0.007 inch thick. One-half of the ribbon thickness should be added to the radius of each sector when calculating pendulum performance. However, the difference between the percent deviations calculated with this addition and deviations calculated without it is very small. Diminishing the sector eccentricity of 0.39 inch by 0.00067 inch would be more than equivalent to adding 0.0035 inch (one-half of 0.007 inch) to the radius of each sector and Fig. 10 indicates the change in performance when the eccentricity is changed by 0.01 inch. The bending moments for the ribbons are constant factors as are the ribbon elongations due to the applied stresses; hence, these two items affect not the linearity of performance but rather the capacity of the pendulums.

In order to check theoretical operation, careful experimental observations have been made on performance by using the regular pendulums with eccentricities of 0.39 inch. It has been found that the differences between the theoretical and the experimental operations are rarely greater than 0.01 percent of pendulum capacity. This is approximately the order of error to be expected in the observations.

Agreement between the calculated and the observed performances gives the assurance that operations calculated for other values of the pendulum parameters accurately describe pendulum operation. Since appropriate values for these parameters can be selected, analysis is placed on a firm footing as a tool in pendulum design.

Many theoretical performance curves have been calculated for the pendulums of Fig. 3. The results of these show that the eccentricity actually used, 0.39 inch, is probably the best that can be found, considering the wide range of capacities which these pendulums must possess. However, for a pendulum of 5.33 pounds capacity, the initial θ position (as pendulums are designed at present) is approximately 50°. This initial position unnecessarily introduces large deviations which, according to these same calculations, can be corrected by reducing θ_1 from 50° to 35°. This, in turn, means starting the pendulums from a position that is 15° higher. With this change in initial position, better operation also follows for the larger capacities. These predictions have been confirmed experimentally.

Although much remains to be done on the analyses of pendulums, it is hoped that a clearer explanation of pendulum performance will prevail as a result of this present study. The essential problem in designing pendulums lies in the selection of correct values for the parameters. Research in the immediate future will undoubtedly center around finding a more expedient means for making this selection.

Acknowledgment

The author wishes to take this opportunity to thank Professors H. M. Hansen, of the University of Michigan, T. H. Osgood, of the University of Toledo and M. F. Manning, now at the University of Pittsburgh, for their many helpful suggestions in connection with this research. The assistance given by Mr. M. A. Weckerly and the permission of the management of the Toledo Scale Company to publish this paper are sincerely appreciated.

The Development of Water-Cooled Quartz Mercury Lamps

By Edward B. Noel

Lamp Development Laboratory, General Electric Company, Nela Park, Cleveland, Ohio

From the Cooper-Hewitt mercury lamp of 1902, operating at a pressure of 0.0003 atmosphere and an efficiency of 18 lumens per watt, there have been developed lamps in hard glass and in fused quartz with pressures up to 200 atmospheres and efficiencies of 40 lumens per watt and above. At the highest pressures water-cooling is required, and a careful coordination of the designs of lamp, jacket, and ballast is required for successful operation. Brightness-distribution and spectral-energy data are given for the A-H6 and two experimental water-cooled lamps. Photoengraving, television, and searchlight applications of the A-H6 water-cooled lamp are discussed.

Introduction

MERCURY arcs are one of the older illuminants. Peter Cooper-Hewitt, in 1902, marketed one of the first practical lamps of this type, a self-rectifying direct-current arc in a glass tube about one inch in diameter and four feet long. It operated at an efficiency of about 18 lumens per watt which, compared to the 3 or 4 lumens per watt that could be obtained from the carbon filament incandescent lamp of that period, represented a great advantage in efficiency. Mercury arcs in quartz bulbs have also been known for a long time and have been used where a wealth of ultraviolet has been required. These lamps have been large, expensive, and required a graded seal or, as in some of the early ones, a complicated quartz-Invar-mercury-wax seal to bring the conducting leads through the low expansion quartz bulb.

Within the last six years, much smaller glass mercury lamps, operating on alternating current and consuming about 400 watts, have found use in industrial and highway lighting in this country and abroad.[1,2] These lamps produce light with an efficiency of 40 lumens per watt. One of the reasons for the increased efficiency is that these lamps operate at a pressure of 1.4 atmospheres, whereas the older Cooper-Hewitt lamps ran at 0.0003 atmosphere pressure. Bulb temperatures at this higher pressure were naturally much greater than in previous designs and were commercially possible only because new glasses with high softening points were available.

Workers in the vapor lamp field realized that small lamps consuming, say, 100 watts, and yet having a high efficiency, could be made if the temperature and the operating pressure of the mercury vapor could be raised.[3–6] To achieve this they had to replace the glass bulb with one of quartz, not in order to get the ultraviolet, but in order to withstand the high temperatures.

One remaining obstacle was that the small size of the proposed lamps left no room for the usual quartz-to-glass graded seal, and high temperature operation would not permit their use anyway. This problem was solved by the invention of a new type of glass of very high softening point and low expansion which formed tight bonds with quartz and also with tungsten.[7] With proper technique, seals could be made using only this one glass between tungsten and quartz. Such seals are not strain free at room temperature, but the strength of the glass and of the bonds is such that no difficulty with cracks is encountered. With the invention of this seal using the new glass, small quartz mercury lamps of from 40 to 250 watts, operating with high efficiency and at pressures from 4 to 30 atmospheres, appeared on the market.[8]

The new lamps operating at higher pressure also had a higher brightness of the arc core than previous lamps. It was realized by all workers in

the field, that still higher efficiencies and still higher brightness could be obtained by means of greater power input and water-cooling to prevent the softening of the bulbs.[3,4] The quartz water-cooled lamps, which are the subject of this paper, are thus the outgrowth of the search for a small source of high brightness and efficiency, and are possible because the industry now has available new glasses and sealing technique for quartz bulbs.

Early Work

Experimental work on the high pressure quartz lamps did not wait for a practical solution of the problem of a small metal-to-quartz seal. Both air-cooled and water-cooled models were made at first with what is known as a "ribbon seal." In this type of seal a ribbon of molybdenum about 10 mm long and 2 mm wide and having a thickness of only 0.005 mm carries the current through the quartz wall. Tungsten wires are welded at each end of the ribbon to serve as a lead and as a support for the electrode, and the assembly is supported vertically inside a tubular side-arm or extension of the discharge tube. While under vacuum, the walls of the side tube are melted down upon the ribbon and upon the ends of the tungsten wires. Once the seal is made the extra portion of the side tube is cut off. Upon cooling, the tungsten wire pulls away from the quartz because of the difference of expansion. Although the seal is broken at this point, the quartz supports the tungsten enough to prevent the relatively heavy lead being pulled away from the thin ribbon. The thin ribbon forms the actual seal. Being so extremely thin, it has little mechanical strength, and the expansion difference between it and quartz sets up stresses greater than the elastic limit of the molybdenum. The ribbon, therefore, deforms as required by the adjoining quartz. The bond between the two materials is not broken under these conditions, so the seal is tight.

This construction enabled the development engineer to work out the specifications for the new quartz lamps, but the difficulties with the ribbons were such as to discourage their use commercially. The ribbons are delicate, and great care must be taken in welding the tungsten wires to the ends to make a good weld which will carry the current, without burning the thin metal of the ribbon just around the weld. With such thin material, there is a tendency for it to stick to the welding jaws and tear away from the wire. If successfully welded, the resulting assembly must be handled very gently, as the welding operation recrystallizes the surrounding molybdenum and changes it from the ductile state to an extremely brittle condition. The quartz must be melted down on the ribbon under vacuum, which means additional pumping operations. In operation, such seals frequently burn off at the weld because the viscous quartz has not been pressed into perfect contact with the ribbon, and so does not carry off the I^2R heat from the ribbon as it should. If operated in air, these seals may fail prematurely due to oxidation of the ribbon by air seeping in along the wire.

When properly made, however, the seals are good. For extreme high temperature work, particularly in the air-cooled lamps, they are the only kind of seals that can be used because of the high temperatures encountered. However, two foreign companies have overcome the manufacturing difficulties to such an extent that they are today marketing small quartz lamps with ribbon seals.

The first water-cooled lamps, which were made with these ribbon seals, had tubular bulbs of quartz with a wall about 2 mm thick and an internal diameter $2\frac{1}{2}$ to 3 mm in diameter. The electrodes, which were spaced with a gap of 10 mm, consisted of tightly-wound coils which were slipped over the lead wire and coated with a small amount of BaO or SrO to serve as active material. Originally, only a drop of mercury was introduced and the starting gas was argon, neon, a neon-argon mixture, or helium at pressures of 100 to 500 millimeters of mercury. For a water jacket, a glass tube of about $\frac{5}{8}$" in diameter was used. The lamp was suspended by extensions of the lead wires which were run through rubber stoppers plugged into the ends of the tube. Water entered and left the jacket through side tubes.

Difficulties with these first lamps were many. The first trouble encountered was that, while they would operate satisfactorily as high pressure discharges when run in air at greatly reduced power input, they could not be made to "warm

One of four mercury-arc searchlights (right) which are used for decorative illumination of the General Electric Building in New York City (left). The insert shows the actual size of one of the mercury lamps.

up" when water-cooled, even though the power input was greatly increased.

When the arc is first struck in a high pressure lamp, the arc drop is from five to a hundred times less than under normal operation because, in the cold lamp, little mercury is in the evaporated state and the pressure is low. If there is sufficient heat from the initial arc to evaporate more mercury, the voltage drop across the lamp will increase due to the increase in mercury pressure. On a conventional power supply having a fixed value of reactance, the short circuit current is of the order of twice the lamp-operating current. Hence, at the start of a discharge, although there is more than normal current, because of the low value of arc voltage there is much less heat in the arc than when running at full pressure. If this heat is removed by the cooling medium without allowing much temperature rise in the coldest part of the bulb, the lamp never will develop a high pressure.

The first trouble experienced was of this nature. The conventional fixed reactance ballast with its two-to-one value of short circuit current was not supplying enough power in the initial stages of the arc to overcome the efficient removal of heat by the circulating water. A power supply was substituted which had several variable reactances whose value could be changed by shifting a lever. With this arrangement the ratio

of short circuit current to normal current was as much as ten to one, and lamps would frequently warm up. When they did, more frequently than not, the lamps burst due to excessive power input and pressure before the levers could be returned to the normal current position. When they did not run up, and the current was increased to the limit, the ribbon seals would frequently overheat and burn off, crack, or shatter. If the seals stood the abuse it was often found that there was such localized heat at the electrodes that opposite them the quartz bulb had become molten on the inner surface and deformed, even though the outer water-cooled surface hadn't become hot enough to form steam.

It was found that lamps which did warm up did so only once, and at that they couldn't be made to remain at high pressure. After the arc was struck the first time and the short circuit current slowly increased, at some critical value, which varied, the lamp would run up to pressure in a small fraction of a second. Within a minute the voltage would begin to drop. At first the drop could be counteracted by increasing the current, but soon this no longer helped and the lamp would slump. It could never be made to run up again. This phenomenon was traced to a cleaning up of the starting gas. Helium, which was used at first because it gave a high initial arc voltage drop, was the worst gas in regard to clean-up, as might be expected. Probably it was absorbed by, or penetrated through the quartz walls. The clean-up was not so rapid with neon, and even slower with argon.

Further experimenting was confined to the use of argon as a starting gas. When the amount of mercury introduced in the lamp was increased many fold, so that the "dead space" behind each electrode was entirely filled with mercury, the lamps no longer slumped completely, and they could be run up several times. It was in this "dead space" that the previous small drop of mercury had remained sheltered from the heat of the arc. After the starting gas had cleaned up, evidently not enough heat had been supplied the mercury, which was easily condensed, to maintain the pressure.

It was next found that if the inside diameter of the quartz tube were kept to about two millimeters or less, and enough mercury were introduced so that each end was filled to within less than a millimeter of the electrode tip that the lamps warmed up repeatedly and that a high short circuit current was no longer needed. From this time on, the conventional fixed-value high reactance type of transformer was used as a power supply. Troubles with gas clean-up and slumping also practically disappeared.

Lamps of this type would operate for an hour or so, during which time the quartz on the inside around the electrodes would devitrify so badly that the lamp would often crack through. When the electrode coil and the oxide coating were removed, leaving only a little tip of the bare tungsten lead wire projecting through the surface of the mercury to serve as an electrode, the extremely rapid devitrification disappeared, and the lamps lasted much longer.

By the time the development had gotten this far, the technique of using the new seal glass on

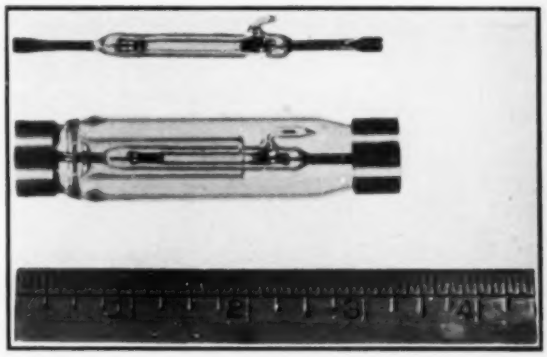

FIG. 1. An early lamp, and a lamp mounted in an early type of integral jacket. In this design, the assembled lamp and jacket is the replaceable element which is operated in a specially constructed socket.

tungsten wire for a seal in place of the molybdenum ribbon had been worked out for the air-cooled lamps, and attention was turned to making similar seals for the water-cooled types. This proved to be a matter of manufacturing technique, and when this was acquired, all the major development problems on the water-cooled quartz mercury lamps had been solved. There remained, of course, many minor, though important, problems affecting quality and life, and it was still necessary to decide upon a specific design and size which would be most universally acceptable to the trade.

The first experimental work had mostly been done on a 500-watt design running at 420 volts. From the commercial standpoint a 1-kw lamp seemed more desirable, so work was transferred to a lamp with twice the arc gap (20 to 25 mm) and an operating voltage of 840.[9] The current was the same for the two designs. It should be pointed out here that at present the current for which it is possible to design a satisfactory water-cooled high pressure quartz lamp can be varied only within narrow limits. Consequently the lamp wattage can be changed only by varying the lamp voltage, which means that for a given operating pressure the voltage and the wattage vary directly as the length of the arc.

Development of Commercial Types of Water Jackets

As has already been mentioned, the first jackets were glass tubes in which the lamp was suspended by its bare leads which were run through rubber stoppers, tied into the ends of the tube. While the disadvantages of this arrangement were many, it did serve reasonably well for the early experimental lamps which lasted but a short time. However, when the life increased to a matter of hours, the lead wires were eaten off by electrolysis, and attention was turned toward making a jacket that would be commercially acceptable.

In the design of the commercial water jacket there were three primary considerations: the cost of the jacket, the cost of the renewable lamp element, and the physical size. There was a fourth consideration which vitally affected the first three, and that was whether or not the leads to the lamp should be insulated from the cooling water.

Designs in which both leads were insulated from the water were a little cumbersome and expensive. Even in the simpler forms such designs made it necessary to discard the jacket along with the lamp when the latter failed.

Considerable simplification and improvement resulted when only one lead to the lamp was insulated. The other lead, which was in contact with the water, was connected to the grounded side of the transformer. With this construction it was possible to make a jacket which could be a permanent part of an installation, and in which only the lamp proper, or lamp plus a simple tube was the renewable element.[10] While jackets of this type were not as inexpensive as desired, the biggest objection was that this construction prohibited operation of lamps in a cluster with close spacing.

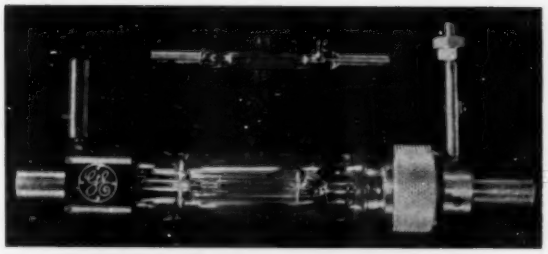

FIG. 2. The 1000-watt water-cooled quartz mercury lamp type A-H6 which is now on the market, and a Model 110-A single-unit glass water-jacket.

No difficulty had been experienced during the development program with lamps which had been run on alternating current with both leads in contact with the water, provided the electrical conductivity of the water between the two ends of the lamps was low enough. By reducing the cross section of the path of the cooling water along the length of the lamp, the resistance of the water circuit could be made sufficiently great with ordinary types of city water so that no trouble would result from this source. At the same time, this constriction made it possible to reduce the amount of cooling water because it was not the amount of water, but merely the surface velocity over the lamp that mattered. The criterion for proper cooling is that the speed of flow should be great enough to prevent the formation of any steam bubbles. With an annular passage about a millimeter wide around the lamp, a flow of approximately three liters per minute gave ample velocity and a temperature rise less than 3°C.

In Fig. 1 one of the early lamps is shown and beside it a lamp mounted in an early type of integral jacket. In this design, both ends of the lamp are in contact with the water which enters at one end and leaves at the other. Electrical connections are made at each end of the jacket on the brass rings. Single, double, and triple sockets were devised which clamped units of this type between rubber gaskets to make the water connection. Bronze fingers rubbing on the brass

ferrules made electrical connection. While satisfactory operation was obtained with this construction, it was dropped because it was felt that to discard a good jacket each time a lamp failed was unnecessarily expensive.

The cheapest possible replaceable element with the lowest possible cost was obviously the lamp itself. Simple bases were provided by cementing short lengths of $\frac{3}{16}''$ brass tubing over the two leads. With this as a starting point, a jacket of the type shown in Fig. 2, employing metal-to-glass seals, was worked out. By loosening the knurled nut, the lamp may be inserted in a removable holder. This end of the jacket is intended to be grounded, so is not insulated. The connection and the metal-to-glass seal at the other end are provided with insulating bushings so that when the rubber hose is in place one cannot accidentally come in contact with high voltage. This jacket has found wide use in industry.

FIG. 3. The No. 109 three-unit jacket which was designed as a projection source for photoengraving, photolithography, and searchlight applications.

From the first it was realized that operation of several lamps in a tightly grouped cluster would be required for many applications, and this was one of the factors which led to the adoption of the small, uninsulated, double-ended replaceable type of construction.

One of the first multiple units tested had three lamps lying side by side in a plane on $\frac{5}{16}''$ centers, and all within a single glass tube which served as a water jacket. Very short life was experienced with the center lamps, and it was later realized that this was due to the absorption by it of ultraviolet energy from its two neighbors with a consequent increase in its pressure and temperature.

In the three-unit jacket shown in Fig. 3, which was finally developed as a photoengraving projection source, this absorption was prevented by surrounding each lamp with "velocity tubes" of lead-bearing hard glass. In addition to acting as ultraviolet filters, these tubes also served to produce high water velocity over the lamp and to reduce the cross section of the water path so that the electrical resistance in parallel with the lamp would be high.

The combination of prolonged contact with water, high voltage, close spacing, and close dimensional tolerances made the design and choice of material for the insulator of this multiple jacket a very considerable problem. Few insulating materials were found to be satisfactory on all points. Isolantite was selected and experience has shown it to be an excellent choice for these difficult requirements.

Electrical Characteristics of the Lamps and Circuits

Since these lamps have a very steep volt-ampere characteristic, they must be run with an

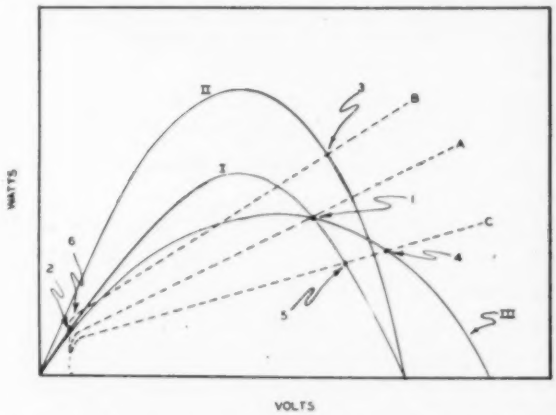

FIG. 4. Characteristic wattage-voltage curves for lamps and ballast. I. Normal characteristic of ballast. II. Ballast characteristic with high short circuit current. III. Ballast characteristic with low short circuit current and high open-circuit voltage. *A*. Characteristic of a normal lamp. *B*. Characteristic of a lamp with too little mercury or with too large an inside diameter. *C*. Characteristic of an old lamp.

accurately adjusted ballast. Experience has shown that the shape of the volt-ampere curve and of the wattage-voltage curve of the power supply markedly affect the life and performance of the lamps.

In Figs. 4, 5, and 6 the full-line curves represent the characteristics of the power supply and the dashed-line curves the characteristics of the lamp. Curve I may be considered the normal power supply, curve II one with high short circuit current, and curve III one with low short circuit current and high open circuit voltage. The normal new lamp has a characteristic which is denoted by "*A*." A lamp with too little mercury, or with too large a tube bore requires considerably more power to warm it up to the same voltage, and behaves as in "*B*." As lamps become old the electrode tips burn off a bit, and the tube walls devitrify and perhaps become a little blackened so that the mercury is heated

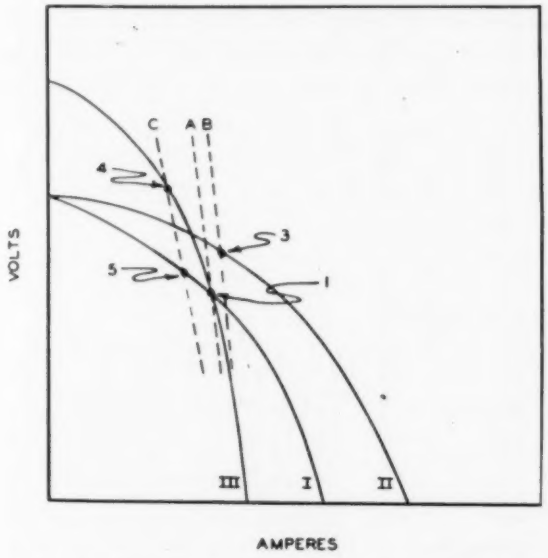

FIG. 5. Characteristic voltage-current curves for lamps and ballast. I. Normal characteristic of ballast. II. Ballast characteristic with high short circuit current. III. Ballast characteristic with low short circuit current and high open-circuit voltage. *A*. Characteristic of a normal lamp. *B*. Characteristic of a lamp with too little mercury or with too large an inside diameter. *C*. Characteristic of an old lamp.

hotter. The result is to shift the characteristic from "*A*" to "*C*."

Examination of Fig. 4 shows the point of normal operation to be point 1 at the intersection of the two normal characteristic curves,

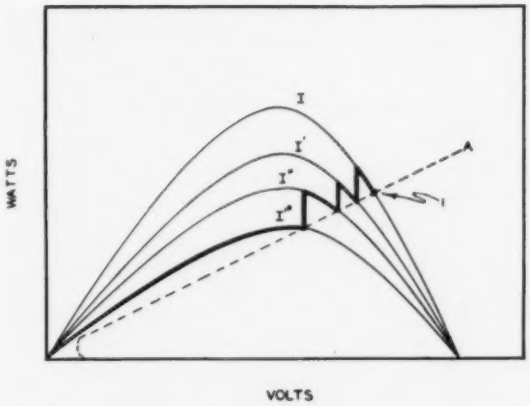

FIG. 6. Characteristic ballast curves for step-by-step starting. *A*. Characteristic of a normal lamp. *I'''* through *I*. Ballast characteristics with increasing short circuit current.

A and I. A lamp with too little mercury or with a large inside diameter and having a characteristic such as *B* will not run up on a normal power supply of type I. It will not get past the point 2 where a further increase in lamp voltage requires more power than the circuit can supply. If the short circuit current be decreased until this deficiency is overcome, as in II, the lamp will run up to point 3 which may represent more loading than the lamp can stand. Many of the difficulties encountered during the early stages of development were of this nature and can be explained by means of the curves of Fig. 4.

As shown in Figs. 4 and 5, two radically different ballast units such as I and III can be made to operate lamps of a given characteristic at the same voltage and current. However, since the lamp characteristic shifts during life, the performance on the two units will be greatly different. With III there will be considerable change of voltage but not much change in wattage during life, the operating point shifting from 1 to 4. Since almost full power is maintained up to the end of life and the quartz wall gradually gets weaker, failures are apt to occur earlier with this characteristic than with I. With I there will be a greater variation in wattage and a lesser variation of voltage during life than in the previous case. The operating point shifts from 1 to 5, and since the loading decreases as the tube becomes weaker, life is somewhat prolonged.

An open-circuit voltage greater than that required to insure starting is not desirable. The higher the open-circuit voltage, the steeper the

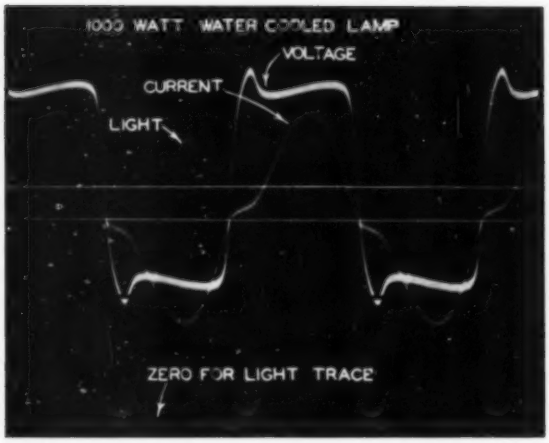

FIG. 7. Current, voltage, and light traces for a 1000-watt water-cooled mercury arc operating on a 60-cycle supply.

volt-ampere characteristic (Fig. 5). The lamp volt-ampere characteristic is also quite steep, and with the small angle of intersection of the two curves obtained with a high open-circuit voltage, minor differences in lamp characteristics produce wide changes in the operating values. It is not at all difficult to obtain a condition of extreme instability merely by using too high an open-circuit voltage.

As may be seen in Fig. 4, at one instant during the warming up process the lamps must pass through a state of peak power where the supply circuit delivers considerably more power than at the normal running condition. This explains why so many of the lamps which fail by bursting do so at starting. With lamps, which have a considerable factor of safety, such as the A-H6 which is now on the market, this momentary excess of power does no harm. With small lamps, and with highly loaded lamps consuming, say, 700 to 1000 watts per centimeter of arc, the limit of the quartz may be exceeded very easily. These lamps should be started with additional resistance or reactance in the circuit which can be cut out gradually or in steps, changing the characteristic from I''' to I, as shown in Fig. 6. In this case, the power supplied to the lamp will follow the jagged heavy curve, and the lamp will never be subjected to the peak power of the final operating characteristic.

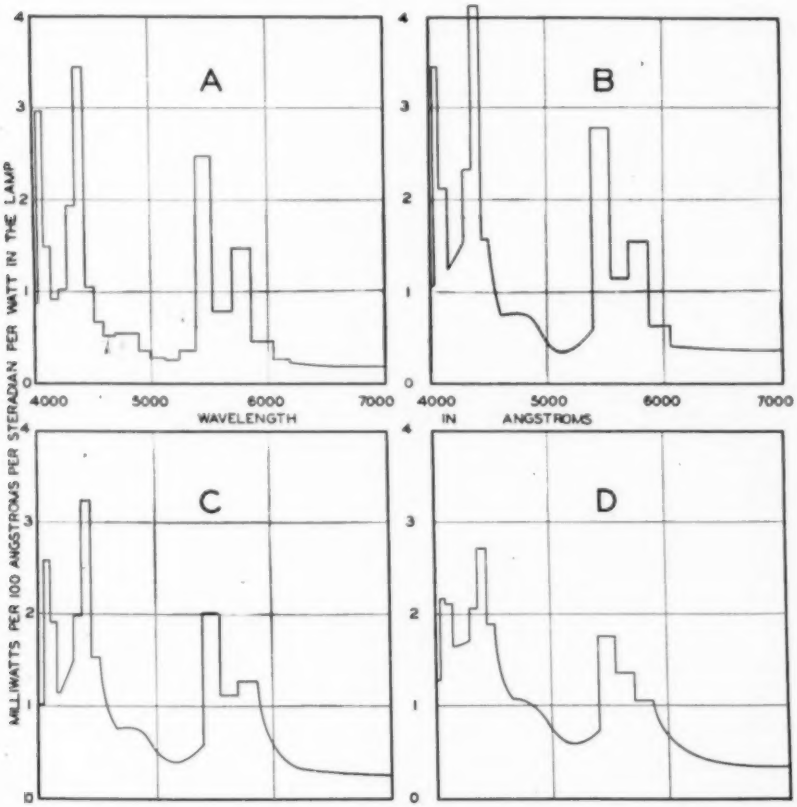

FIG. 8. Spectral energy distribution curves for various water-cooled quartz mercury lamps. *A*. Standard 1000-watt A-H6 lamp—inside diameter 2 mm, outside diameter 6 mm, arc gap 25 mm, gradient 330 v per cm. *B*. Experimental 2 amp. d.c. lamp—inside diameter 1.8 mm, outside diameter 4.0 mm, arc gap 17.0 mm, gradient 445 v per cm. *C*. Experimental a.c. lamp—inside diameter 1 mm, outside diameter 3 mm, arc gap 10 mm, gradient 600 v per cm. *D*. Experimental a.c. lamp—inside diameter 1 mm, outside diameter 3 mm, arc gap 10 mm, gradient 900 v per cm.

Examination of the oscillograph of Fig. 7 shows that the lamp current and voltage are not sine waves, which makes close calculation of circuit characteristics impossible. However, Dorgelo has been able to construct an equivalent circuit which permits considerable calculation and prediction of performance.[11]

On 60-cycle alternating-current operation there is a pronounced 120-cycle flicker, which is clearly evident in Fig. 7. Where this is of consequence, it can be eliminated in many applications by operating three lamps on a three-phase supply. Where only a single lamp is used, as for example as a light source for an oscillograph, it is necessary to run the lamps upon direct current.

Spectral Characteristics

The energy spectrum of a high pressure discharge consists of a continuous background upon which is superimposed broadened lines of the mercury spectrum. Examination of the radiation with a monochromator of high resolution and using narrow slits shows the lines to be sharp peaks and that the broadening due to pressure is greater on the side toward the red end of the spectrum than on the side toward the blue.[12–14] As the pressure is increased, the lines become broader and their peak lower, and at the same time the background radiation becomes more intense.[9,15] This can be seen in *A*, *C*, and *D* of Fig. 8. In this diagram, which gives the spectral distribution of one commercial and two experimental water-cooled lamps, the energy in regions close to mercury lines is plotted as a block in order to show to better advantage the continuous background radiation. The standard lamp of Fig. 8*A* operates with an internal pressure of approximately 80 atmospheres (over a half-ton pressure per square inch). There are no precise data on the pressure of the tiny experimental lamp whose spectrum is shown in Figs. 8*C* and 8*D* but extrapolation indicates that 8*C* corresponds to about 125 atmospheres and 8*D* to something between 150 and 200 atmospheres. The increase in the background radiation and the amount of red light with increase in pressure is readily apparent. It is interesting to note that, at the highest pressure, the yellow doublet and the green line of the low pressure mercury spectrum are merged completely with the background radiation. Because of this continuous background, the light from a water-cooled lamp does not distort colors to the extent which takes place with the more familiar low pressure

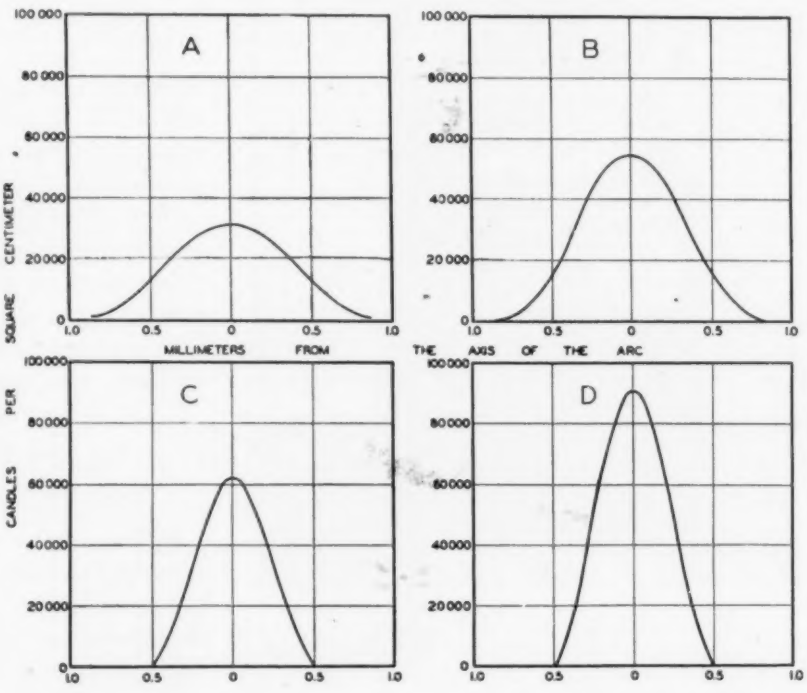

FIG. 9. Variation in brightness across the four arcs whose spectral energy distribution curves are given in Fig. 8. *A*. Standard 1000-watt A-H6 lamp—inside diameter 2 mm, outside diameter 6 mm, arc gap 25 mm, gradient 330 v per cm. *B*. Experimental 2 amp. d.c. lamp—inside diameter 1.8 mm, outside diameter 4.0 mm, arc gap 17.0 mm, gradient 445 v per cm. *C*. Experimental a.c. lamp—inside diameter 1 mm, outside diameter 3 mm, arc gap 10 mm, gradient 600 v per cm. *D*. Experimental a.c. lamp—inside diameter 1 mm, outside diameter 3 mm, arc gap 10 mm, gradient 900 v per cm.

mercury arcs, and its light appears bluish white. Fig. 8*B* gives the spectrum of an experimental lamp operating at approximately 100 atmospheres pressure. Because this lamp was designed to run on 2 amp. d.c., this spectrum is not directly comparable with the spectra of the a.c. lamps of Figs. 8*A*, 8*C*, and 8*D*.

The brightness of these water-cooled lamps is essentially constant along the length of the arc, but across the arc stream it varies as shown in Fig. 9 where the brightness of the same lamps previously mentioned in connection with Fig. 8 are given for the same conditions of operation as those for which the spectral energy-distribution are shown. The values of maximum brightness of 30,000 to 90,000 candles per square centimeter should be compared with the brightness of a 1000-watt tungsten projection lamp, which is 3100 candles per square centimeter, and that of a crater of a carbon arc, which ranges from 14,000 candles per square centimeter for the regular type to 50,000 to 86,000 candles per square centimeter for the high intensity type.

FIG. 10. A Douthitt Corporation photoengraving vacuum frame employing a single 1000-watt A-H6 water-cooled quartz mercury lamp.

The fact that the color and brightness of a mercury arc both improve with increase of pressure has focused attention on the desirability of operating at the highest feasible value. Unfortunately, life decreases rapidly as the pressure is increased, and economic considerations set the limit of usefulness. For example, the only lamp on the market in this country at present is the 1000-watt A-H6 which has a rated life of 75 hours. However, depending upon the cycle of operation, the life will be from a third to several times this value. In an appreciable proportion of the lamps the useful life will be terminated by the lamp bursting, and although the pressure at the time of failure is well over half a ton per square inch, nothing of consequence happens. The internal volume of the lamp is exceedingly small so the stored energy is likewise small. When a lamp breaks, the pressure impact transmitted by the cooling water to the jacket does not crack the glass except on rare occasions. With the extreme-pressure experimental lamps, life is but a fraction of that of the A-H6, and is nearly always terminated by the bulb bursting. The pressure impact on the water jacket in this case is such that the glass enclosure breaks more often than not.

When the small size of these water-cooled mercury arcs is considered in relation to the enormous amounts of power dissipated, it is surprising that any life worth mentioning is obtained at all. For example, to reach the highest values of brightness reported in this paper, operating pressures of the order of a ton per square inch were reached by dissipating nearly one kilowatt of power in an arc 10 mm long within a tiny bulb only one millimeter in inside diameter and having walls only a millimeter thick.

Commercial Uses for Water-Cooled Quartz Mercury Arcs

1000-watt water-cooled quartz mercury arcs operating at 80 atmospheres pressure have been commercially available in this country for less than two years, and within that time they have found considerable use in certain fields where

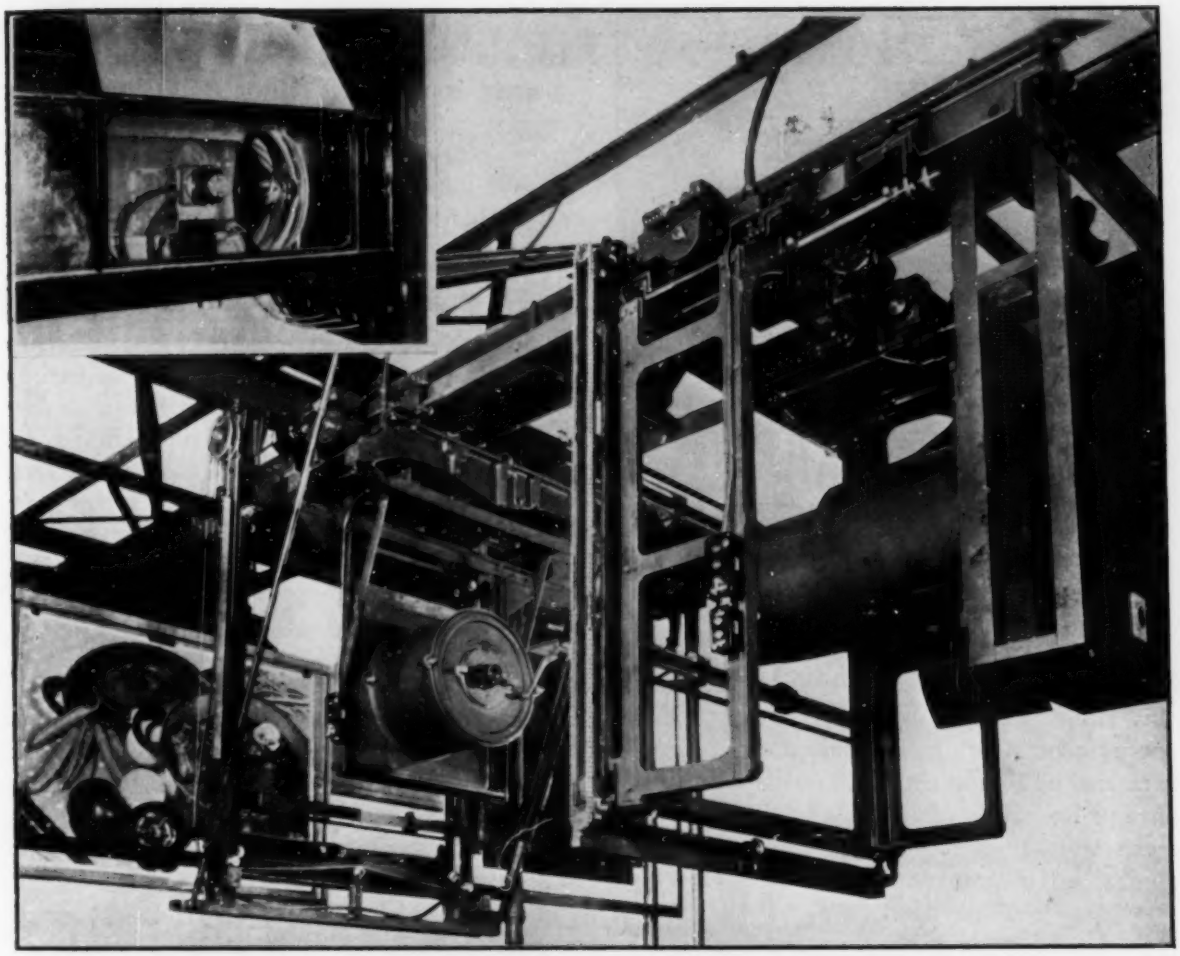

FIG. 11. For a projection source, three to five lamps can be used in a cluster giving reduced exposures and more output per machine. The above illustration shows a three-unit No. 109 jacket in use in a Lanston-Monotype camera.

the special advantages of this type of source are of value. Three outstanding characteristics of this type of lamp are the brightness of the source, its high actinic value, and the coolness of the light. In closing, some practical applications utilizing these special qualities will be mentioned.

The prime requirement of a source intended for searchlight service is that it have high brightness, and in this respect water-cooled quartz mercury lamps are outstanding. Single lamps were used in the sixteen searchlights whose beams crossed over the Court of Peace in the New York World's Fair. Three-lamp units of the type pictured in Fig. 3 are used in searchlights on top of several New York buildings. Page 327 shows one of the self-contained searchlight units used on the General Electric Building at 570 Lexington Avenue.

The abundance of blue light and long wave ultraviolet energy makes this source especially suitable for photochemical processes. It has been used for diazo printing, and in several universities has shown itself to be ideal for Wilson cloud-chamber illumination. It has found its widest application in photoengraving and in photolithography where reduced exposures and freedom from heat have been important advantages. In this service, the steadiness of the light also results in sharper halftone dots and better quality. Fig. 10 shows a single lamp installed in a vacuum frame, and Fig. 11 shows a three-lamp unit serving as a projection source in a precision camera.

FIG. 12. Water-cooled quartz mercury lamps in use in the General Electric Television station W2XBN. Three quartz lamps are clustered around the focal point in each of the deep-bowl reflectors. The absence of infra-red radiation makes it possible to obtain from 1000 to 5000 footcandles of illumination with minimum discomfort to the artists.

One of the most valuable characteristics of this lamp is the coolness of its light. Of the energy other than visible radiation, 77 percent is carried off by the circulating water. To supply an equal amount of light, only 42 percent as much wattage is required in the water-cooled quartz A-H6 lamp as with a 1000-watt high efficiency biplane tungsten-filament source. More important still is the fact that for equal light the mercury source emits but one-fourth the radiant energy of the filament lamp, which makes it possible to reach high levels of illumination with a minimum of discomfort from heat. In television studio lighting, where 1000 to 5000 footcandles are desirable, this cool source meets a great need. The General Electric's small television studio at the New York World's Fair was lighted with three 1000-watt water-cooled quartz mercury lamps in a trough reflector. The Schenectady station W2XBN employs twelve lamps in four deep-bowl reflectors of the type shown in Fig. 12.

While there are other commercial applications, the ones mentioned are those in which this lamp is finding wide use. Since the water-cooled quartz mercury lamp is a relatively new source, it may be expected that the near future may find it serving in still other fields.

Acknowledgments

The writer wishes to express his appreciation to the many people who aided in this work. He is especially indebted to Mr. G. E. Inman, to Dr. B. T. Barnes and D. D. Hinman for spectral measurements, and to Paul Davis for able assistance.

Bibliography

1. L. J. Buttolph, "The characteristics of gaseous conduction lamps and light," Trans. I.E.S. **30**, 147 (1935).
2. L. J. Buttolph, "High-intensity mercury and sodium lamps," J. Soc. Mot. Pict. Eng. **24**, 110 (1935).
3. Das Licht, April 15, 1935, No. 4, p. 84.
4. C. Bol. "Een Niewe Kwiklamp," Ingeniur **50**, 91 (1935).
5. Marden, Meister and Beese, "High-intensity mercury arc lamps," Elec. Eng. **55**, 1186 (1936).
6. L. J. Buttolph, "Mercury arcs of increased brightness and XXX efficiency," J. Soc. Mot. Pict. Eng. **28**, 43 (1937).
7. B. Jonas, "The sealing of metal leads through hard glass and silica," Philips Tech. Rev. April, 1938.
8. L. J. Buttolph, "High-efficiency mercury and sodium vapor lamps," J. Opt. Soc. Am. **29**, 124 (1939).
9. E. B. Noel and R. E. Farnham, "A water-cooled quartz mercury arc," J. Soc. Mot. Pict. Eng. **31**, 221 (1938).
10. E. G. Dorgelo, "Water-cooled mercury lamps," Philips Tech. Rev. June, 1937.
11. E. G. Dorgelo," Alternating-current circuits for discharge lamps," Philips Tech. Rev. April, 1937.
12. Barnes and Forsythe, "Characteristics of some new mercury arc lamps," J. Opt. Soc. Am. **27**, 83 (1937).
13. R. Rompe and P. Schulz, "Eigendruck un Elektronenstossverbreiterung in der Quecksilberhochdruckentladung in Abhangigkeit von der Stromstarke," Zeits. f. Physik **110**, 223–232 (1938).
14. P. Schulz, "Breite und Verschiebung von Spektrallinien in der Quecksilberhochdruckentladung," Zeits. f. Tech. Physik **12** (1938).
15. W. DeGroot, "Het Emissie en Absorptie-Spectrum van Kwikdamp Bij Z. H. Drukken," Ingenieur **50**, 92 (1935).

Resumés of Recent Research

Recent Experiments on the Thermionic Properties of Different Crystal Directions of the Same Metal

It has long been suspected that different crystal faces of the same clean metal have different thermionic and photoelectric properties. Photoelectric studies have substantiated this suspicion for several different metals. Electron projection tube data have shown in a qualitative way that the thermionic emission properties of pure metals vary with crystal direction.* It has also been clearly demonstrated that different crystal directions have markedly different powers for adsorbing caesium, barium, etc.

Martin[1] has shown, using a spherical tungsten crystal with a concentric spherical fluorescent screen, that all the thermionically important crystal directions for tungsten have indices of the form (*hhk*). Recrystallization studies by Johnson and Shockley[2] and later by Nelson[3] have shown that it is possible to obtain sizeable tungsten crystals in the form of fine wires. These crystals have one of their face diagonals [(110) crystal direction] in close coincidence with the wire axis. Thus if the (110) direction is parallel to the wire axis, all the directions of the form (*hhk*) are normal to the wire surface if it is smooth and round.

By using a method similar in principle to the Pintsch and to the Goucher commercial methods, Nichols[4] has been able to grow long single tungsten crystals in the form of wires. Quantitative measurements of the temperature dependence of the thermionic emission from the different crystal directions normal to the surface of one such crystal wire—i.e., directions having indices of the form (*hhk*)—were then made. These data

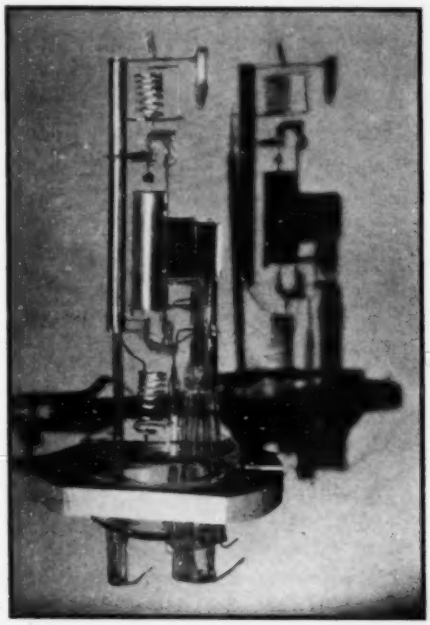

Apparatus used to measure quantitatively the thermionic constants of tungsten for the different crystal directions.

were fitted to the empirical relation

$$i_0 = A^* T^2 \exp(-e\varphi_0/kT),$$

giving values for the constants A^* (sometimes called the Richardson constant) and φ_0 (often called the thermionic work function) for the different thermionically important crystal directions.

The values of φ_0 ran from 4.35 volts for the (111) direction to 4.65 volts for the (112) and (110) directions. The (001) direction gave a φ_0 of 4.35 volts. The A^* varied from about 125 for the (001) and (112) directions to 15 for the (110) direction. This low value of A^*, together with the nature of the voltage dependence of the emission current from the (110) direction, indicates the existence on the surface normal to the (110) direction of a crystal face whose φ_0 is much larger than 4.65 volts.

* Until more is known about the surface structure of tungsten filaments, it is better to think of the thermionic data referred to here as associated with different crystal directions rather than with the ideal crystal faces normal to these directions because one cannot as yet be sure that the actual surfaces normal to these directions are "pure," i.e., that an actual surface normal to a given crystal direction is made up solely of the ideal crystal face normal to this direction.

[1] S. T. Martin, Phys. Rev. **56**, 947 (1939).
[2] R. P. Johnson and W. Shockley, Phys. Rev. **49**, 439 (1936).
[3] R. B. Nelson, M.I.T. Doctor's Thesis, 1939 (soon to be published).
[4] M. H. Nichols, Phys. Rev. **57**, 297 (1940).

These results show that the values of φ_0 and A^* obtained from the usual measurements on polycrystalline surfaces are characteristic of a weighted average of the properties of the various crystal surfaces occurring and have, therefore, only empirical value. This means that all attempts to relate observed to theoretical values of emission constants have, so far, nothing more than approximate significance. Furthermore, other fundamental thermionic phenomena must be reconsidered keeping in mind the fact that different crystal facets have different φ_0 and can therefore influence the thermionic behavior of their neighbors.

Electronic Work Functions by Contact Potential Measurement

If the work function of a single metal is known, measurements of contact potential differences are capable in principle of furnishing precise determinations of the work functions of all other metallic surfaces. The contact potential method does not require that the measured surfaces emit electrons and is, therefore, free from the temperature and sensitivity limitations inherent in the thermionic and photoelectric methods. It supplies, also, a powerful means of attack upon those surface phenomena, e.g. adsorption, to which the work function is such a sensitive index. Realization of these possibilities has been hindered by the lack of experimental methods, generally applicable to the common metals, which provide (1) a convenient technique for preparing the rigorously clean surfaces demanded in all work function studies, (2) the duplication of surfaces which is essential for establishing their reproducibility in any given measurement, and (3) the systematic organization of data which can be obtained only by measuring all the metals against a standard reference surface.

Development of the contact potential method along these lines has been undertaken at the State College of Washington by P. A. Anderson, whose latest results are reported in a paper on "The contact difference of potential between barium and zinc. The work function of zinc."[1] Utilizing his observation that the work functions of vaporized barium films are extraordinarily reproducible and constant, Anderson uses barium both for getting the sealed-off tubes in which his measurements are made and for the standard surface of known work function (2.52 ev) to which all his measurements are referred. Clean surfaces of both metals of the Ba-X pair are prepared in the measuring tube itself by first fusing and fractionally distilling the metals, then revaporizing the middle fractions. Each of the succession of films formed by the revaporizations is measured as it is laid down. Enough replica pairs of Ba-X surfaces can be prepared in a single tube to give repeated checks on the reproducibility and constancy of work function of each surface.

An unsolved problem, fundamental in all photoelectric and contact potential studies on cold surfaces, involves the question of whether work functions observed for such surfaces are not, in fact, affected by the films of residual gas which must form in even the highest attainable vacuum. By shortening to a few seconds the time lapse between the deposition and measurement of a fresh metal film, and showing that this time lapse is small relative to the time required to build an equilibrium film of gas on the metal, Anderson has been able to attack this problem and to show that his value for the work function of zinc, 4.28 ev, is probably characteristic of the clean metal.

[1] Paul A. Anderson, Phys. Rev. **57**, 122 (1940).

Calendar of Meetings

May	
1–3	American Society of Mechanical Engineers, Worcester, Massachusetts
6–10	American Foundrymen's Association, Chicago, Illinois
13–15	American Institute of Chemical Engineers, Buffalo, New York
June	
6–8	National Colloid Symposium, Ann Arbor, Michigan
9–14	Society of Automotive Engineers, White Sulphur Springs, West Virginia
10–14	American Medical Association, New York, New York
17–19	American Society of Heating and Ventilating Engineers, Washington, D. C.
17–21	American Society of Mechanical Engineers, Milwaukee, Wisconsin
18–21	American Physical Society, Seattle, Washington
20–22	American Physical Society, Pittsburgh, Pennsylvania
24–28	American Society for Testing Materials, Atlantic City, New Jersey
24–28	American Institute of Electrical Engineers, Swampscott, Massachusetts
27–29	Institute of Radio Engineers, Boston, Massachusetts
July	
24–26	American Society of Civil Engineers, Denver, Colorado
August	
27–30	American Institute of Electrical Engineers, Los Angeles, California

Here and There

Giant Cyclotron to be Built

For the construction of a cyclotron of 4,500 tons, the Rockefeller Foundation has made an appropriation of $1,150,000 to the University of California, with the stipulation that the University shall raise an additional sum of $250,000. The cyclotron is to be built under the supervision of Dr. Ernest O. Lawrence.

While plans are still very much subject to change, Dr. Donald Cooksey has made the following statement:

"The magnet will probably be made out of steel plates with a total weight of approximately 4,500 tons. The magnet will be actuated by copper windings weighing approximately 400 tons. The pole diameter is to be 184 inches and the gap in the vacuum chamber approximately 40 inches. The radiofrequency power will come onto the dees through resonant lines in the vacuum as is now done on our present 60-inch cyclotron. This scheme was originally suggested by J. R. Dunning of Columbia and has been modified in this laboratory. The outer envelope of these resonant lines will be 12 feet in diameter, and their length will depend on the wave-length at which we will be operating. This length will be something of the order of 33 feet as measured from the center of the magnet for a wave-length of 57 meters. At such a wave-length we should get fifty million volt deuterons. The inner conductor supporting the dee will be about four feet in diameter. The surface of this support and the inner surface of the envelope will be entirely of water-cooled copper. The charging currents on this equipment will be, as can be imagined, enormous, and hence these large areas are necessary, because, of course, naturally radiofrequency current flows on a very thin surface layer. As we become familiar with the operation of this equipment, the resonant lines will be shortened, and we feel confident that within a relatively short period we will reach 100 million volt deuteron energy, which will correspond to approximately 40 meters.

"There are large volumes that will have to be evacuated, and for this purpose we estimate that we will need a pumping speed of somewhere from one to two hundred thousand liters per second at the pump orifices. It is interesting that when dealing with such very high pumping speeds, small leaks become entirely negligible. This is already apparent in the 60-inch cyclotron. We will expect to have available approximately 2,500 KW for the operation of this machine.

"Another problem which may be of interest will be the selection of a location and the housing facilities. We expect to put up a building which will cover an area of approximately 17,000 square feet. The magnet will be in the center and will extend 25 feet above the floor level and 11 feet below. It will be 58 feet long and will rest on a heavy concrete footing. The outer envelope for the dee supports which will come in from opposite sides will run on tracks on the floor level. The operating controls will be approximately 150 feet from the center of the magnet. We are hoping to put this building on a hilltop somewhat remote from any other buildings and inset the control building into the face of the hill under ground. The main building itself will be of a type as flexible as possible so that we can readily add a wing in any direction that might in the future seem desirable. We are hopeful of being able to get the major part of this construction program completed within the course of three years and therefore feel that we might expect to have something to show for our efforts in the nature of high energy particles before four years have passed.

"The white streak coming from the side on the artist's drawing (shown on the front cover) is supposed to be a portion of the path of a 100-million-volt deuteron beam. It should have a range of approximately 140 feet at sea level in air. It will be understood, I hope, that our plans may diverge to some extent from these specifications."

★

Eighth American Scientific Congress

The Eighth American Scientific Congress which is to be held in Washington May 10 to 18 promises to be a brilliant occasion in bringing together a considerable number of the intellectual leaders of Latin America. In developing the program the Organizing Committee has made a special effort to obtain an adequate presentation of current scientific work in countries other than the United States. Papers from this country will be limited principally to discussions of general fields of work by outstanding leaders, with a few selected articles on work which is of particular interest in relation to Central and South America.

In the general program considerable emphasis has been given to humanistic, economic and social sciences. The physical and chemical sciences are grouped in one of the eleven sections of the Congress.

In that section Professor Albert Einstein will give a discussion of the fundaments of theoretical physics; Dr. Harlow Shapley will describe studies bearing upon the structure of the universe, with particular reference to recent work in the Southern Hemisphere; Professor Harold C. Urey will give a paper on isotopes; and Professor Manuel S. Vallarta one on cosmic rays. Other papers will deal with magnetism, variations of gravity, seismology, and the physics and chemistry of volcanoes.

Special sessions in which Latin American authors will take part are planned on astronomy, meteorology, radio transmission, and governmental standardizing and research laboratories. In the field of chemistry, papers have been scheduled on microchemical analysis, measurement of reaction velocities, and electrochemical theory.

The Congress will open and close with formal plenary sessions at which addresses will be made by high governmental officials and leaders of the delegations from several countries. There will be official social functions appropriate for such a gathering and also several special excursions, including trips to Mt. Vernon, Luray Caverns, and

Williamsburg, the latter by boat. After the Congress delegates will visit Philadelphia and New York, including the World's Fair.

More complete information will be supplied on request by the Secretariat of the Congress in the State Department, and detailed programs will be available at the end of April.

★

Photoelasticity Conferences

The Eleventh Eastern Photoelasticity Conference will be held May 24 and 25 at the Carnegie Institute of Technology, Pittsburgh, Pennsylvania. A program dealing with the latest developments in the field of photoelasticity is being arranged. Dr. Max M. Frocht, Associate Professor of Mechanics at the Carnegie Institute of Technology, is Chairman of the Committee on Arrangements.

The First Northwestern Photoelasticity Conference met under the auspices of the Department of Civil Engineering at the University of Washington, Seattle, Washington, on Saturday, March 30. The technical program included the following papers:

Elementary Theory and Practice of the Photoelastic Method, by R. WELLER;
Application of Photoelasticity to Soil Mechanics, by R. G. HENNES;
The Usefulness of Photoelasticity in Engineering Teaching,
(a) **Machine Design,** by B. T. MCMINN
(b) **Structures,** by F. B. FARQUHARSON;
Stresses Due to Secondary Bending, by B. J. RUFFNER;
Growing Problem of Stress Analysis in the Aircraft Industry, by ROBERT J. MINSHAL;
The Interferometer in Two and Three Dimensional Stress Analysis by J. H. A. BRATZ;
Photoelasticity Applied to Railroad Research, by W. LEAF;
Solution of the Torsion Problem by Photoelastic Analogy, by J. G. MCGIVERN.

★

National Research Fellowships Awarded

The award of five National Research Fellowships in physics was authorized March 16. The following were appointed:

Richard H. Bolt, who is being reappointed to a National Research Fellowship, is a graduate of the University of California in Los Angeles and will continue his studies at the Massachusetts Institute of Technology.

Robert A. Chipman was graduated from Cambridge University and will carry on research work at the University of Michigan.

Charles L. Critchfield, from George Washington College, will go to the University of California.

Myron H. Nichols, another National Research Fellowship reappointment and a graduate of Massachusetts Institute of Technology, has chosen Princeton for the continuation of his work.

George E. Valley, Jr., a graduate of the University of Rochester, has designated the University of California as his first choice for continued study.

★

Coffin Research Fellows Announced

Eight college graduates have been granted Charles A. Coffin Fellowships, totaling $5000, for use in carrying on advanced scientific research during the next school year, it was announced recently by W. W. Trench, Secretary of the Charles A. Coffin Foundation. These Fellowships were established by the General Electric Company in 1922 to honor its retiring president and founder. The 1940–1941 list of Charles A. Coffin Fellows, who will be distributed among five different educational institutions, is as follows: Marritt L. Kronberg, Baltimore, Maryland; Melvin L. Renquist, San Jose, California; Henry M. Foley, Birmingham, Michigan; Ernest C. Berkofsky, Madison, Wisconsin; LeRoy W. Apker, Rochester, New York; William H. Fenn, Berkeley, California; William J. Barclay, Palo Alto, California; and Robert J. Dwyer, Norwood, Ohio. Kronberg and Dwyer also received fellowships last year.

★

Lectures on Polarography

"The polarographic methods of chemical analysis" is the title of a course of six lectures to be given by Dr. A. Langer, Research Fellow, Westinghouse Electric and Manufacturing Company, and Lecturer in Physics, University of Pittsburgh, in a series of Wednesday afternoon lectures, April 17 to May 22, inclusive, at 4:30 P.M. in Thaw Hall at the University of Pittsburgh. This series is open to the public and is being sponsored by the Departments of Physics and Chemistry at the University of Pittsburgh. The subjects of the individual lectures are as follows:

April 17	General Principles of Polarography
April 24	Electrochemical Basis of Polarography
May 1	Applications of Polarography in Inorganic Chemistry and Metallurgical Analyses
May 8	Applications of Polarography in Organic and Biochemistry
May 15	Polarometric Titrations
May 22	Other Polarizable Electrodes and Their Uses.

★

Westinghouse Research Fellowships Granted

Appointment of the third annual group of five Westinghouse Research Fellows has been recently announced by the Westinghouse Research Laboratories, East Pittsburgh, Pennsylvania. The appointees were selected from a group of forty-two applicants for fundamental research in physics, chemistry, mechanics, and metallurgy. The men selected are: Dr. Jerald E. Hill, University of Rochester, for research in nuclear physics; Dr. Sidney Krasik, Cornell University, for research on fundamentals of velocity-modulated electron beams as generators of ultra-high frequency radiations; Dr. Walter Kauzmann, Princeton University, for research in application of the absolute reaction rate theory of chemical kinetics to liquid flow and solid plasticity problems; Dr. Frederick W. Stallman, University of Illinois, for research in nuclear physics; Dr. David P. Stevenson, California Institute of Technology, for research in chemical bond resonance energies with the aid of the mass spectrometer.

★

Advertising Club Honors Scientist

In honor of Dr. Katharine Blodgett as the person "whose work brought the most favorable attention to

Schenectady during 1939," a dinner was held by the Schenectady Advertising Club, February 29. Dr. Blodgett's work on molecular films resulted in the preparation of a glass surface which eliminates 99 percent of the reflection generally encountered. She was given a massive scrapbook filled with clippings about her discovery.

★

Summer Graduate Institute Planned

Armour Institute of Technology, Chicago, will conduct a three-term Summer Graduate Institute for engineers, professional men, industrialists, and educators in engineering and science beginning with the summer of 1940, according to the announcement made recently by Dr. L. E. Grinter, Vice President and Dean of the graduate division. The Institute plans to invite scientists of distinction to lecture each summer on modern developments in engineering and science.

The Summer Graduate Institute, arranged to provide an opportunity for graduate work is divided into seven separate and distinct sections, and will consist of three terms, each four weeks in duration. Work in advanced mechanics, chemical engineering and chemistry, civil and sanitary engineering, electrical engineering and physics, mechanical engineering, industrial engineering and applied mathematics will be offered. The division of electrical engineering and physics will offer the following courses:

June 17 to July 13

Matrix Properties and Application of Electric Circuits, MYRIL B. REED, *Armour Institute of Technology*
Communication Engineering, WILLIAM L. EVERITT, *The Ohio State University*

July 15 to August 10

Tensor Analysis of Electrical and Mechanical Engineering Problems, GABRIEL KRON, *General Electric Company*
Electrical Radiation and Radiating Systems for Radio Communication, WILLIAM L. EVERITT, *The Ohio State University*

August 12 to September 7

Physics of Electron Tubes, PAUL L. COPELAND, *Armour Institute o Technology*

★

Summer School Schedule Announced

The University of Chicago has scheduled 128 courses in the physical sciences to be offered in the 1940 summer session. Among the visiting professors will be P. Debye, Director of the Kaiser Wilhelm Institute for Physics. A regular session of the University year, the summer quarter is divided into two terms, one beginning Wednesday, June 19, and the second starting Monday, July 22. The quarter is planned to make all courses available in a three-year rotation schedule. The preliminary announcement of the summer program lists physics courses in the following fields: general physics, advanced experimental physics, classical mechanics, thermodynamics, electrodynamics, nuclear transformations, research in crystal structure, electron and nuclear physics, line spectra and atomic structure, band spectra and molecular structure, x-rays and electrons, cosmic rays, theoretical aspects of cosmic rays, statistical theories of thermodynamics.

Eighth Spectroscopy Program Offered

The George Eastman Research Laboratories of the Massachusetts Institute of Technology announce for 1940 the Eighth Summer Program on Spectroscopy and Its Applications. The Program is divided into three sections: Spectroscopy Conference, July 15–17; Courses in Practical Spectroscopy, June 10–July 20; Spectroscopic Research, June 1–August 1.

The Spectroscopy Conference this year will repeat to a considerable extent the type of program presented at the conferences held during the past seven summers. A series of papers and discussions is being prepared on the following topics, among others: Analysis by the emission spectrum; Absorption spectrophotometry; Photographic photometry; Industrial applications of spectroscopy; Biological and chemical effects of spectral radiation; Spectroscopy of the ultraviolet and the infra-red; and Analysis of spectra, and Measurement of wave-lengths. The course on practical spectroscopy is being offered in the regular Institute Summer Session and will deal principally with applications of spectroscopy to biology, chemistry, geology, metallurgy, physics, and other branches of science. The Institute is again extending its invitation of the last six summers to properly qualified noncommercial investigators to make use of its spectroscopic facilities in connection with their researches.

★

Modern Pioneer Awards

At the time of the 150th anniversary of the founding of the American Patent System, the National Association of Manufacturers made Modern Pioneer awards to many outstanding inventors. The committee on Modern Pioneer Awards consisted of Drs. Karl T. Compton, Chairman; Forest R. Moulton; George B. Pegram; John T. Tate; Edward R. Weidlein; and Frank C. Whitmore. Those who have received awards and who are also members of the American Physical Society are listed below:

National Awards: William David Coolidge, Charles Franklin Kettering, Irving Langmuir, and Vladimir Kosma Zworykin.
New York Area: William David Coolidge, Alfred Norton Goldsmith, William Nelson Goodwin, Jr., Alan Hazeltine, R. A. Heising, B. W. Kendall, Irving Langmuir, Edward C. Wente, Willis R. Whitney, Browder J. Thompson, Harry C. Thompson, and Humboidt W. Leverenz.
Baltimore Area: A. Herman Pfund and S. Karrer.
Boston Area: Harold E. Edgerton, Arthur Cobb Hardy, Edgar D. Tillyer, and William S. Wilson.
Chicago Area: Roscoe Henry George, Paul E. Klopsteg, and Carl Pfanstiehl.
Cincinnati Area: Games Slayter.
Cleveland Area: Lars O. Grondahl and Charles Baldwin Sawyer.
Detroit Area: Charles F. Kettering.
Los Angeles Area: Frederick Bedell, Herbert Thomas Kalmus, and Evald Anderson.
Philadelphia Area: Newcomb Kinney Chaney, Thomas Randolph Harrison, Morris Evans Leeds, Vladimir Kosma Zworykin, and Irving Wolff.
Rochester Area: Loyd A. Jones, C. E. Kenneth Mees, and Leopold K. Mannes.
San Francisco Area: E. O. Lawrence.

★

Dr. Peter I. Wold, Professor of Physics and Head of the Department at Union College, has been made Chairman of the division of science in succession to Dr. Edward Ellery.—*Science*

Contributors to This Issue

G. R. Carley

F. Offner

L. A. Dean

K. C. D. Hickman

S. S. Ballard

F. H. Miller

Kenneth C. D. Hickman was born in London, England, and received his Ph.D. degree from London University. From 1925 to 1939 Dr. Hickman was employed with the Eastman Kodak Company, and since 1939 he has been Vice President and Director of Research for Distillation Products, Inc.

Glenn R. Carley has been employed since 1936 by the Toledo Scale Company on various engineering and research problems. He was graduated from the California Institute of Technology with the B.S. degree in physics in 1936.

Jesse W. M. DuMond has been on the staff of the Physics Department at the California Institute of Technology since 1921, with the exception of a brief period as acting Associate Professor at Stanford in 1931. His research activities have been chiefly in the field of x-rays, atomic physics, and the natural atomic constants. Dr. DuMond's picture has appeared in the *Journal of Applied Physics* on p. 289, Vol. 9, No. 5, 1938.

Franklin Offner is at present engaged in the development and manufacture of laboratory apparatus. He received his Ph.D. degree in 1938 from the University of Chicago where he was research assistant from 1936–1938.

Stanley S. Ballard, Assistant Professor of Physics at the University of Hawaii, is also Collaborator in Chemistry and Soils in the Hawaii Agricultural Experiment Station. He received his A.B. degree from Pomona College in 1928, and his Ph.D. degree from the University of California in 1934.

Pictures and biographical sketches of the following contributors have appeared in previous issues of the *Journal of Applied Physics:*

Richard Burt Dow, p. 350, Vol. 8, No. 5, 1937.
C. E. Fink, p. 106, Vol. 10, No. 2, 1939.

E. B. Noel has been associated with the development of electric discharge lamps in the Nela Park Division of the General Electric Company since 1933, in which year he was transferred there from the Engineering General Department of the Company. He holds the B.S. and M.S. degrees from the University of Illinois.

L. A. Dean received his B.S. degree from the University of Hawaii in 1931, and his Ph.D. degree in soils from the University of Wisconsin in 1934. He spent the year 1935–36 at the Rothamsted Experimental Station, England, as a National Research Council Fellow. Dr. Dean is at present Associate Agricultural Chemist with the Hawaii Agricultural Experiment Station.

E. B. Noel

Frederic H. Miller has been an Instructor in Mathematics at Cooper Union and at Columbia University and has been an Assistant Professor of Mathematics at Cooper Union since 1932, in which year he received the Ph.D. degree from Columbia University. He is the author of *Calculus* and co-author of *Advanced Mathematics for Engineers.*

Contributed Original Research

A Note on Heaviside's Expansion Theorem

F. H. Miller
Cooper Union Institute of Technology, Cooper Square, New York
(Received November 7, 1939)

1. Introduction

In the solution of certain physical problems, mathematically formulated as linear differential equations (either ordinary or partial) coupled with suitable initial and boundary conditions, operational methods often serve to shorten the labors of computation. A particularly powerful tool is the operational calculus initiated by the engineer Oliver Heaviside.[1]

Heaviside's methods and results, some of which were originally of doubtful validity, have been critically examined by a number of writers. Many others have, in addition, extended the techniques and content of the operational calculus so as to give it greater practicability.

This note is concerned with the latter phase of the subject, and accordingly the treatment is entirely formal. Justification of the processes employed presents no difficulty.

2. Definitions and Elementary Formulas

The operator basic to Heaviside's work is the differential operator usually denoted by p. If the independent variable is t, commonly representing time, then p operating on a function $g(t)$ yields the derivative function:

$$p\cdot g(t)=\frac{d}{dt}g(t)=g'(t). \tag{1}$$

However, the more fundamental operator is the inverse of p; namely, p^{-1}, denoting a definite integration:

$$p^{-1}\cdot g(t)=\frac{1}{p}\cdot g(t)=\int_0^t g(t)dt. \tag{2}$$

Also by definition, we have for n any positive integer,

$$p^n\cdot g(t)=\frac{d^n}{dt^n}g(t)=g^{(n)}(t), \tag{3}$$

$$p^{-n}\cdot g(t)=\frac{1}{p^n}\cdot g(t)=\int_0^t\int_0^t\cdots\int_0^t g(t)(dt)^n. \tag{4}$$

If, in particular, $g(t)=1$, (4) gives us

$$p^{-n}\cdot 1=\frac{t^n}{n!}. \tag{5}$$

Using this relation, a number of frequently occurring operational formulas are readily established. For example, we have

[1] See Heaviside's *Electromagnetic Theory* (The Electrician, 1893–1912, 3 volumes).

$$\frac{p}{p-b}\cdot 1=\frac{1}{1-bp^{-1}}\cdot 1=(1+bp^{-1}+\cdots+b^np^{-n}+\cdots)\cdot 1$$

$$=1+bt+\cdots+\frac{b^nt^n}{n!}+\cdots=e^{bt}. \tag{6}$$

Likewise, by expansion in negative powers of p, or by partial differentiation of relation (6) with respect to b, there is obtained the formula

$$\frac{p}{(p-b)^m}\cdot 1=\frac{t^{m-1}e^{bt}}{(m-1)!}, \tag{7}$$

where m is any positive integer.

3. Heaviside's Expansion Theorem

When a physical problem leads to a system of ordinary linear differential equations with real constant coefficients, as in elementary electric circuit theory, the operators that arise are expressible as rational functions of p. Let such an operator function be denoted by $f(p)/F(p)$, where $f(p)$ and $F(p)$ are polynomials with real constant coefficients. Suppose the degree of $f(p)$ to be less than or equal to that of $F(p)$, and suppose further that the roots $a_1, a_2, \cdots, a_r$ of $F(z)=0$ are distinct and different from zero. Then one form of Heaviside's expansion theorem may be written as

$$\frac{f(p)}{F(p)}\cdot 1=\frac{f(0)}{F(0)}+\sum_{k=1}^{r}\frac{f(a_k)}{a_kF'(a_k)}e^{a_kt}. \tag{8}$$

This theorem is easily proved by means of the algebraic identity

$$\frac{f(z)}{F(z)}=\frac{f(0)}{F(0)}+\sum_{k=1}^{r}\frac{f(a_k)}{a_kF'(a_k)}\frac{z}{z-a_k} \tag{9}$$

together with formula (6).

The expansion theorem is sometimes given in a second form,

$$\frac{f(p)}{F(p)}\cdot e^{bt}=\frac{f(b)}{F(b)}e^{bt}+\sum_{k=1}^{r}\frac{f(a_k)}{(a_k-b)F'(a_k)}e^{a_kt}, \tag{10}$$

where b is any constant distinct from the r roots $a_1, a_2, \cdots, a_r$. This may be obtained as follows. Replacing e^{bt} by its operational equivalent (6), we have

$$\frac{f(p)}{F(p)}\cdot e^{bt}=\left[\frac{f(p)}{F(p)}\frac{p}{p-b}\right]\cdot 1.$$

Now (8) applies, with $pf(p)/(p-b)F(p)$ as the new rational operator acting on unity. Formula (10) follows immediately.

Various extensions of the Heaviside expansion theorem have been given. For instance, Gotō,[2] dealing with form (10), has considered the case in which b is equal to some a_k, and the case in which $F(z)=0$ has multiple roots.

4. Complex Zeros of $F(z)$

In the application of Heaviside's theorem to specific problems, the occurrence of complex quantities among the a_k in (8) often introduces awkward and lengthy computations. The following process was developed to meet this practical difficulty.

[2] Mochinori Gotō, "Extension of the Heaviside expansion theorem," Researches of the Electrotechnical Laboratory, No. 201, Tokyo, June, 1927.

We remark first that only pure imaginary numbers need be considered; for, the real part of a complex number may be disposed of at once. Let an operator $\psi(p)$ be expressed as a series in powers of p^{-1},

$$\psi(p)=\sum_{k=0}^{\infty}\frac{c_k}{p^k},$$

and consider the operation $\psi(p-b)\cdot e^{bt}$. Using (6), we get

$$\psi(p-b)\cdot e^{bt}=\left[\psi(p-b)\frac{p}{p-b}\right]\cdot 1=\sum_{k=0}^{\infty}\frac{c_k}{(p-b)^k}\frac{p}{p-b}\cdot 1=\sum_{k=0}^{\infty}\frac{c_k p}{(p-b)^{k+1}}\cdot 1=\sum_{k=0}^{\infty}\frac{c_k t^k}{k!}e^{bt}$$

from (7). Hence, from (5), $\psi(p-b)\cdot e^{bt}=e^{bt}\psi(p)\cdot 1$, or

$$\psi(p)\cdot 1=e^{-bt}\frac{p\psi(p-b)}{p-b}\cdot 1. \tag{11}$$

This is the well-known shifting formula. If, therefore, b is the real part of a conjugate complex pair among the a_k in (8), the application of formula (11) yields a new operator whose denominator has a corresponding pair of pure imaginary zeros.

Suppose, then, that the denominator of our operator has the form $F(p)=\phi(p)(p^2+\alpha^2)$, where α and the roots $a_1, a_2, \cdots, a_{r-2}$,[3] of $\phi(z)=0$ are all real and distinct from zero, and the a_k are different. We have, by identity (9),

$$\frac{f(z)}{\phi(z)}\frac{1}{z^2+\alpha^2}=\frac{f(0)}{\phi(0)}\frac{1}{z^2+\alpha^2}+\sum_{k=1}^{r-2}\frac{f(a_k)}{a_k\phi'(a_k)}\frac{z}{(z-a_k)(z^2+\alpha^2)}.$$

But from (8), or by other means, the results of operating on unity with $1/(p^2+\alpha^2)$ and with $p/(p-a_k)(p^2+\alpha^2)$ are easily obtained, whence there is found

$$\frac{f(p)}{\phi(p)(p^2+\alpha^2)}\cdot 1=\frac{f(0)}{\alpha^2\phi(0)}(1-\cos\alpha t)+\sum_{k=1}^{r-2}\frac{f(a_k)}{a_k\alpha(a_k^2+\alpha^2)\phi'(a_k)}(\alpha e^{a_k t}-\alpha\cos\alpha t-a_k\sin\alpha t). \tag{12}$$

5. Trigonometric Operands

In many physical problems, notably in the treatment of electrical networks, the operand encountered is $\sin\omega t$ or $\cos\omega t$ instead of unity. In such circumstances it is usual to employ either (10) with b complex, or the result of operating on unity together with the so-called superposition theorem. However, by means of the same device used in obtaining (12), coupled with the familiar and easily derived operational relations

$$\frac{\omega p}{p^2+\omega^2}\cdot 1=\sin\omega t,\quad \frac{p^2}{p^2+\omega^2}\cdot 1=\cos\omega t,$$

we may find suitable formulas.

Suppose first that all r roots of $F(z)=0$ are real, different, and distinct from zero. Then, by (9),

$$\frac{f(p)}{F(p)}\frac{\omega p}{p^2+\omega^2}\cdot 1=\frac{f(0)}{F(0)}\frac{\omega p}{p^2+\omega^2}\cdot 1+\sum_{k=1}^{r}\frac{\omega f(a_k)}{a_k F'(a_k)}\frac{p^2}{(p-a_k)(p^2+\omega^2)}\cdot 1,$$

and

$$\frac{f(p)}{F(p)}\frac{p^2}{p^2+\omega^2}\cdot 1=\frac{f(0)}{F(0)}\frac{p^2}{p^2+\omega^2}\cdot 1+\sum_{k=1}^{r}\frac{f(a_k)}{a_k F'(a_k)}\frac{p^3}{(p-a_k)(p^2+\omega^2)}\cdot 1.$$

[3] The cases in which $r<3$ are trivial here, and we therefore assume now and hereafter that $\phi(z)$ is not merely a constant.

Performing the indicated operations on unity, we get

$$\frac{f(p)}{F(p)}\cdot\sin\omega t=\frac{f(0)}{F(0)}\sin\omega t+\omega\sum_{k=1}^{r}\frac{f(a_k)}{a_k(a_k^2+\omega^2)F'(a_k)}(a_ke^{a_kt}-a_k\cos\omega t+\omega\sin\omega t), \tag{13}$$

$$\frac{f(p)}{F(p)}\cdot\cos\omega t=\frac{f(0)}{F(0)}\cos\omega t+\sum_{k=1}^{r}\frac{f(a_k)}{a_k(a_k^2+\omega^2)F'(a_k)}(a_k^2e^{a_kt}+a_k\omega\sin\omega t+\omega^2\cos\omega t). \tag{14}$$

It may be noticed that (14) is obtainable from (13) by differentiation with respect to t.

Next suppose, as in §4, that $F(p)=\phi(p)(p^2+\alpha^2)$, with α, a_1, a_2, $\cdots$, a_{r-2} real and distinct from zero and the a_k different. When $\alpha\neq\omega$, we get

$$\frac{f(p)}{\phi(p)(p^2+\alpha^2)}\cdot\sin\omega t=\frac{f(0)}{\alpha(\alpha^2-\omega^2)\phi(0)}(\alpha\sin\omega t-\omega\sin\alpha t)$$
$$+\omega\sum_{k=1}^{r-2}\frac{f(a_k)}{a_k\phi'(a_k)}\left[\frac{a_ke^{a_kt}}{(a_k^2+\alpha^2)(a_k^2+\omega^2)}+\frac{\omega\sin\omega t-a_k\cos\omega t}{(a_k^2+\omega^2)(\alpha^2-\omega^2)}+\frac{a_k\cos\alpha t-\alpha\sin\alpha t}{(a_k^2+\alpha^2)(\alpha^2-\omega^2)}\right], \tag{15}$$

$$\frac{f(p)}{\phi(p)(p^2+\alpha^2)}\cdot\cos\omega t=\frac{f(0)}{(\alpha^2-\omega^2)\phi(0)}(\cos\omega t-\cos\alpha t)$$
$$+\sum_{k=1}^{r-2}\frac{f(a_k)}{a_k\phi'(a_k)}\left[\frac{a_k^2e^{a_kt}}{(a_k^2+\alpha^2)(a_k^2+\omega^2)}+\frac{\omega^2\cos\omega t+a_k\omega\sin\omega t}{(a_k^2+\omega^2)(\alpha^2-\omega^2)}-\frac{\alpha^2\cos\alpha t+a_k\alpha\sin\alpha t}{(a_k^2+\alpha^2)(\alpha^2-\omega^2)}\right]. \tag{16}$$

As before, we may derive (16) from (15) by differentiating with respect to t.

Finally, suppose that $\alpha=\omega$, that is, take $F(p)=\phi(p)(p^2+\omega^2)$, with ω, a_1, a_2, $\cdots$, a_{r-2} real and distinct from zero and the a_k different. This situation occurs in connection with the phenomenon of resonance. Then by passing to the limit, as α approaches ω, in (15) and (16), or by direct evaluation, we find the formulas

$$\frac{f(p)}{\phi(p)(p^2+\omega^2)}\cdot\sin\omega t=\frac{f(0)}{2\omega^2\phi(0)}(\sin\omega t-\omega t\cos\omega t)$$
$$+\omega\sum_{k=1}^{r-2}\frac{f(a_k)}{a_k\phi'(a_k)}\left[\frac{a_ke^{a_kt}}{(a_k^2+\omega^2)^2}-\frac{(a_k^2-\omega^2)\sin\omega t+2a_k\omega\cos\omega t}{2\omega(a_k^2+\omega^2)^2}-\frac{t(a_k\sin\omega t+\omega\cos\omega t)}{2\omega(a_k^2+\omega^2)}\right], \tag{17}$$

$$\frac{f(p)}{\phi(p)(p^2+\omega^2)}\cdot\cos\omega t=\frac{f(0)}{2\omega\phi(0)}t\sin\omega t$$
$$+\sum_{k=1}^{r-2}\frac{f(a_k)}{a_k\phi'(a_k)}\left[\frac{a_k^2e^{a_kt}}{(a_k^2+\omega^2)^2}-\frac{a_k(a_k^2-\omega^2)\sin\omega t+2a_k^2\omega\cos\omega t}{2\omega(a_k^2+\omega^2)^2}+\frac{t(\omega\sin\omega t-a_k\cos\omega t)}{2(a_k^2+\omega^2)}\right]. \tag{18}$$

Again, relation (18) is merely the result of differentiating (17) with respect to t.

Using methods similar to those of Gotō, it is possible to derive generalizations for cases in which two or more pairs of complex zeros of $F(z)$ occur, but such relations are extremely cumbersome and have little practical value.

A Recorder for Electrical Potentials

The Damping of Piezoelectric Systems

FRANKLIN OFFNER
Departments of Physics and Physiology, University of Chicago, Chicago, Illinois
(Received August 31, 1939)

I. INTRODUCTION

THE expense, inconvenience, and delay of continuous photography of bioelectric potentials can be eliminated by an ink-writing oscillograph, provided the frequencies to be recorded are within its range. Dr. R. W. Gerard and the writer described a piezoelectric crystal actuated ink writer[1] with range great enough to record many of the potentials encountered in biology. A study of the theory of operation of this instrument has led to several improvements in design.

A diagram of the improved instrument appears in Fig. 1. Two rectangular Rochelle salt plates *A*, cut as described by Sawyer,[2] are mounted symmetrically. Three corners of each plate are clamped between rubber blocks *B* and steel ball pivots *C*. The link *D* transmits the motion of the fourth corner through the segment *E* and pulley *F* to the pen shaft. For strength, rigidity, and lightness, the pen lever *G* is a Duralumin stamping 6.5 cm long. It supports the ink tube *H* and writing point *J* which are fed ink through the small rubber tube *K*. Friction is minimized by keeping a film of ink between pen and paper. The paper is driven at speeds up to 25 cm/sec.

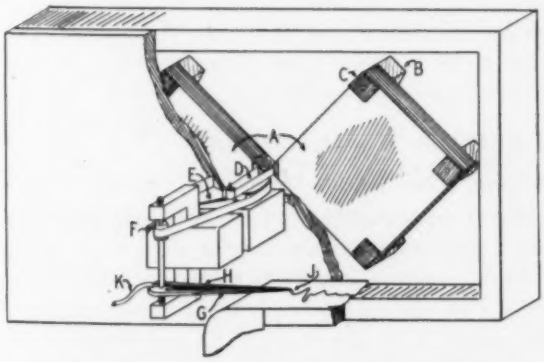

FIG. 1. Diagram of the crystal ink writer.

[1] F. Offner and R. W. Gerard, Science **84**, 209 (1936).
[2] C. B. Sawyer, U. S. Patent 1,803,275. Fig. 13.

The symmetrical placement of the crystals, which are electrically paralleled so that they act mechanically in push-pull, has several advantages. First, the doubling of power increases the product of resonant frequency and maximum displacement by $\sqrt{2}$ (Eq. (1), below). Second, even-order harmonics are canceled; and third, a pure torque is imparted to segment *E*, thus preventing lost motion due to any play in its bearings. The total motion magnification is 65-fold from driving point to record.

II. THEORY OF THE INK WRITER

a. Units and notation

Mason's derivation[3] of the equivalent electrical circuit of a piezoelectric crystal used as a transducer has been followed in deriving the equivalent circuit of the ink writer. This has facilitated the analysis of the instrument's action.

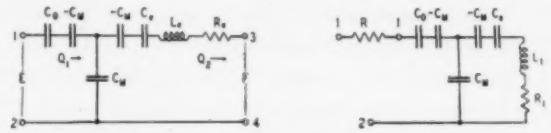

FIG. 2. (a) The electric circuit analog of a piezoelectric transducer. (b) The equivalent circuit of the ink writer.

The electrical analog of a crystal is shown in Fig. 2(a), where 1, 2 represent the electrical terminals; E the applied potential; Q_1 the electrical charge; and 3, 4 the mechanical driving points of the crystals, to which the mechanical load may be connected. Table I shows force, displacement, and velocity of the driving point to be analogous to an electrical potential F, a charge Q_2, and a current i_2, respectively. The compliance C_e is the displacement per dyne applied at 3, 4 with 1, 2 open-circuited. Con-

[3] W. P. Mason, Proc. I. R. E. **23**, 1252 (1935).

versely, the electrostatic capacity C_0 is the charge entering 1, 2 per unit potential developed with 3, 4 open-circuited (i.e., with the crystal clamped). The mutual capacitance-compliance C_m is the ratio of charge to force with 3, 4 open; or the ratio of displacement at 3, 4 to potential developed at 1, 2.

If mechanical dissipation is treated as analogous to an electrical resistance, the latter must in general be a function of i_2. This difficulty is not serious since friction is kept low and will usually be neglected. Fig. 2(b) shows the resultant equivalent circuit of the instrument with the mechanical system connected to the crystal driving points (terminals 3, 4). L_1 is the total mass, as reflected to the driving points; R_1 is the mechanical resistance. The electrical resistance R will be discussed below.

The radian frequency of mechanical resonance is

$$\omega_0 = 1/(L_1 C_e)^{\frac{1}{2}}. \tag{1}$$

If the motion magnification of the mechanical system is increased in the ratio $\phi : 1$, as for example by increasing the pulley to segment diameter ratio, the effective mass of the pen reflected back to the driving points of the crystals is increased in the ratio $\phi^2 : 1$. Because of the relatively minute motion of the remainder of the mechanical system as compared with that of the pen, the mass of the former may be neglected in computing L_1. Thus L_1 is proportional to ϕ^2, and by Eq. (1) $\omega_0\phi$ is constant. Increase in pen excursion obtained by raising the motion magnification therefore results in a proportionate lowering of the resonant frequency.

b. The fidelity problem

Any e.m.f. may be expressed by the Fourier integral

$$E(t) = \int_{-\infty}^{\infty} F(f) e^{j2\pi f t} df$$

and a recorder reproducing all frequencies undistorted would give a facsimile of any wave form. The amplitude-frequency and phase-frequency response curves are thus a criterion of fidelity. These will be discussed in Section II-c.

Another criterion which has been used is the response form for a known signal; e.g., critical damping, which will be discussed in Section II-d.

TABLE I. *Electromechanical units.*

Mechanical Quantity	Electrical Analog	Symbol	Defining Equation
Force	Potential	F	
Displacement	Charge	Q_2	
Velocity	Current	i_2	$i_2 = dQ_2/dt$
Mass	Inductance	L_e	Kinetic Energy $= \frac{1}{2} L_e i_2^2$
Compliance	Capacitance	C_e	$C_e = Q_2/F$
Resistance	Resistance	R_e	
Mutual Capacitance-Compliance		C_m	$C_m = Q_1/F = Q_2/E$
Coefficient of Coupling		k	$k^2 = C_0 C_e / C_m^2$

These two criteria are not equivalent. Consider (for simplicity) a transient $\delta(t) = 0$ for $t \neq 0$, and of unit integrated area.[4] Then

$$E(t) = \delta(t) = \int_{-\infty}^{\infty} e^{j2\pi f t} df$$

and faithful recording of all frequencies would reproduce the original signal. A system cutting off sharply at f_0 gives the recorded wave.

$$\int_{-f_0}^{f_0} e^{j2\pi f t} df = \sin(2\pi f_0 t)/\pi t.$$

i.e., a decrementing sine wave of frequency f_0. On the other hand, a critically damped recorder would give a broadened and shortened, but nonoscillating, spike. Apparently critical damping gives the better reproduction; but if the essential components of the signal lie below f_0, and the damped system fails to transmit some of these, the sharp cut-off system would give the greater accuracy. In practice, the ink writer's cut-off frequency is above the range necessary for many purposes, whereas some desired frequencies would be attenuated by critical damping (e.g. mechanically).

In view of the above, it is well to test a recorder's fidelity by comparison of a signal of the type to be studied with a facsimile (e.g., from a cathode-ray oscillograph).

c. Response to sinusoidal e.m.f.

Some conclusions may be drawn from a qualitative consideration of the equivalent circuit's sinusoidal behavior (Fig. 2(b)).

First, assume potential to be applied at 1, 2 (R out of the circuit). R_1 being assumed small, the effect of it and L_1 may be neglected at low frequencies, and the network appears as a pure

[4] Such a signal is obviously physically unrealizable but would be approached by a very brief spike.

capacitance. The input current i_1 and the resultant velocity i_2 are then both proportional to frequency. But

$$i_2 = dQ_2/dt = \omega Q_{max} \sin \omega t.$$

so that the resulting excursion is independent of frequency. However, with increasing frequency L_1 appreciably reduces the net capacitive reactance, and i_1 and i_2 both increase more rapidly than the frequency. Thus the pen excursion increases with frequency up to resonance;[5] it diminishes beyond.

An interesting possibility results from the simultaneous increase of i_1 and i_2. Apply the potential at 1′, 2 (R in the circuit). If the value of R is properly chosen, the input impedance of the crystal at low frequencies will be much greater than, and in quadrature to, R; the latter then has little effect on the 1, 2 voltage (i.e., that applied to the crystal). As the frequency increases, the input impedance decreases and becomes more nearly resistive; the fractional voltage drop in R thus increases. At resonance the impedance is a minimum and purely resistive; R is here most effective in reducing the crystal voltage. Thus the drop in the 1, 2 potential parallels the natural increase in deflection with frequency, and a much more nearly constant amplitude results. This effect is verified by a quantitative treatment.

The response of the instrument may be calculated from the mesh equations. If E, the impressed e.m.f., is of radian frequency ω, and R_1 is assumed negligibly small, these equations are

$$pE = i_1(pR + 1/C_0) - i_2(1/C_m). \quad (2)$$

$$0 = -i_1(1/C_m) + i_2(p^2L_1 + 1/C_e), \quad (3)$$

where $p = j\omega$. Then

$$Q_2 = i_2/p = k^2\omega_0^2 C_m E/[(1-k^2)\omega_0^2 - \omega^2 + j\omega RC_0(\omega_0^2 - \omega^2)]$$

with k, the coefficient of coupling, defined by

$$k^2 = C_0C_e/C_m^2$$

and, by Eq. (1), $\omega_0^2 = 1/L_1C_e$. When $\omega = \omega_0$ the second term of the denominator is zero for any R; i.e., $i_1 = 0$, and ω_0 is the anti-resonant frequency.

[5] As shown below, this electrical resonant frequency is $(1-k^2)^{\frac{1}{2}}$ times ω_0, the frequency of mechanical resonance.

If $R = 0$, the amplitude becomes infinite at

$$\omega^2 = (1-k^2)\omega_0^2 = \omega_1^2.$$

ω_1 is the resonant frequency of the circuit. The amplitude factor is then

$$k^2\omega_0^2 C_m/[(\omega_1^2 - \omega^2)^2 + R^2\omega^2 C_0^2(\omega_0^2 - \omega^2)^2]^{\frac{1}{2}} \quad (4)$$

and the phase shift is

$$\tan \delta = R\omega C_0 \frac{\omega_0^2 - \omega^2}{\omega_1^2 - \omega^2}. \quad (5)$$

Thus, plotted against ω/ω_1 the undamped ($R = 0$) phase-shift and (except for a constant factor) amplitude characteristics are independent of k. The undamped and damped response curves as given by Eqs. (4) and (5) are illustrated in Fig. 5(a) and (b); these are described in Section III-a.

Another interpretation of ω_0 and ω_1 is this: if a mechanical transient is applied, ω_0 will be the frequency of oscillation with the electrical terminals open-circuited, and ω_1 that when short-circuited.

d. Transient response

It has been shown that the sinusoidal response is improved by a series electrical resistance. But can the system be damped critically in this way? That is, can the oscillatory terms in the transient response be eliminated by resistance in the first (electrical) mesh alone?

The natural (force-free) modes, p, of the network of Fig. 2(b) (R_1 again negligibly small) are given by the roots of coefficients of the i's in Eqs. (2) and (3); that is, by the roots of

$$p^3RL_1 + p^2L_1/C_0 + pR/C_e + 1/C_0C_e - 1/C_m^2 = 0$$

or

$$p^3 + p^2/RC_0 + p\omega_0^2 + \omega_0^2\lambda/RC_0 = 0 \quad (6)$$

with $\lambda = 1 - k^2$. If the damping is to be critical or greater, all roots of this cubic must be real. The condition for this is that

$$b^2/4 + a^3/27 \leqq 0,$$

where

$$a = (\omega_0^2/3)(3 - 1/x^2),$$
$$b = (\omega_0^3/27x)(2/x^2 + 27\lambda - 9)$$

and

$$x = RC_0\omega_0.$$

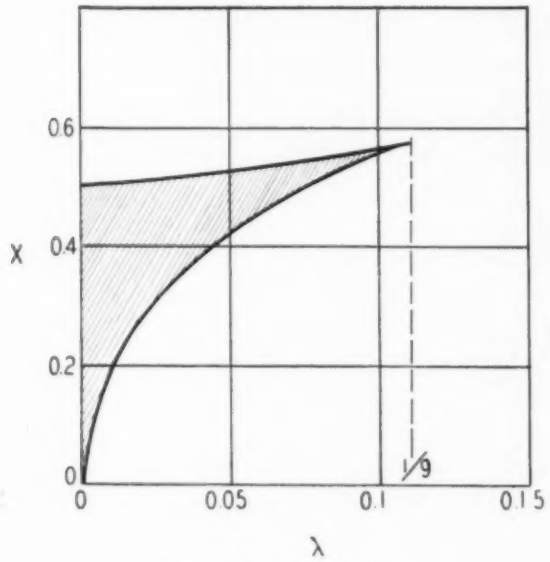

FIG. 3. The damping locus.

Substituting, we have after simplification

$$y = 4x^4 + 3x^2(9\lambda^2 - 6\lambda - \tfrac{1}{3}) + 4\lambda \leqq 0. \qquad (7)$$

The values of λ (in the range $1 \geqq \lambda \geqq 0$) for which there exist real positive values of x satisfying this inequality are shown by the shaded area of Fig. 3. The boundary curve gives the value of x for critical damping at the corresponding λ, while points enclosed by the curve correspond to over-damping. It is seen that critical damping is possible only when

$$\lambda = 1 - k^2 \leqq \tfrac{1}{9},$$
$$k \geqq 0.943.$$

Thus critically damping by insertion of resistance in the first mesh alone is impossible unless k is greater than 0.943. The coefficient of coupling k is a property of the crystal plate, depending only on the composition, orientation with respect to the crystallographic axes, and temperature. Values for a typical Rochelle salt element (as a function of temperature) are given in Fig. 4, for which the author is indebted to Dr. Mason.[6] Since the highest k attained is approximately 0.83, complete damping by this means should be impossible. Partial experimental verification of this is given in Section III.

[6] W. P. Mason, personal communication.

III. Experimental Tests of Fidelity

Partial confirmation of the foregoing theoretical results has been obtained by several experiments.

a. The equivalent network

To check the circuit theory developed, the electrical network (Fig. 2(b)) was examined oscillographically. Furthermore, it is more practical to investigate the effect of circuit parameters empirically than by a detailed study of the circuit equations.

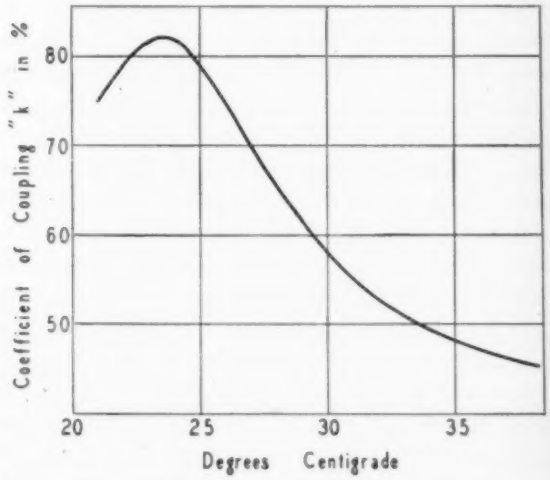

FIG. 4. The variation of the coefficient of coupling of a typical Rochelle salt plate with temperature.

In realizing the circuit, the negative and adjoining positive capacitances were combined into two positive condensers; a cathode-ray oscillograph showed the potential across the condenser formed from C_e and $-C_m$. Since this potential is proportional to Q_2, it is a measure of the displacement of the electromechanical system.

Table II shows the experimental results for the values of k appearing in the first column. The second and third columns list the approximate values of $x = R\omega_0 C_0$ for best transient and sinusoidal fidelity, respectively.

The best frequency response and damping are attained with approximately the same resistance. Fig. 5(a) illustrates the amplitude-frequency, and Fig. 5(b) the phase-frequency characteristics, both with and without damping; the amplitude response has been calculated by Eq. (4), and verified experimentally. The improvement in

linearity effected by the resistor is obvious. The phase shift has been calculated by Eq. (5). With $R=0$, it is zero up to ω_1, where it shifts through 180°. In practice, there is always some dissipation in each mesh, and appreciable phase shift below ω_1; damping then improves the phase response below ω_1 as well.

The apparent critical damping with k as low as 0.9 probably results from the inability to detect a small oscillation in the presence of a large exponential term.

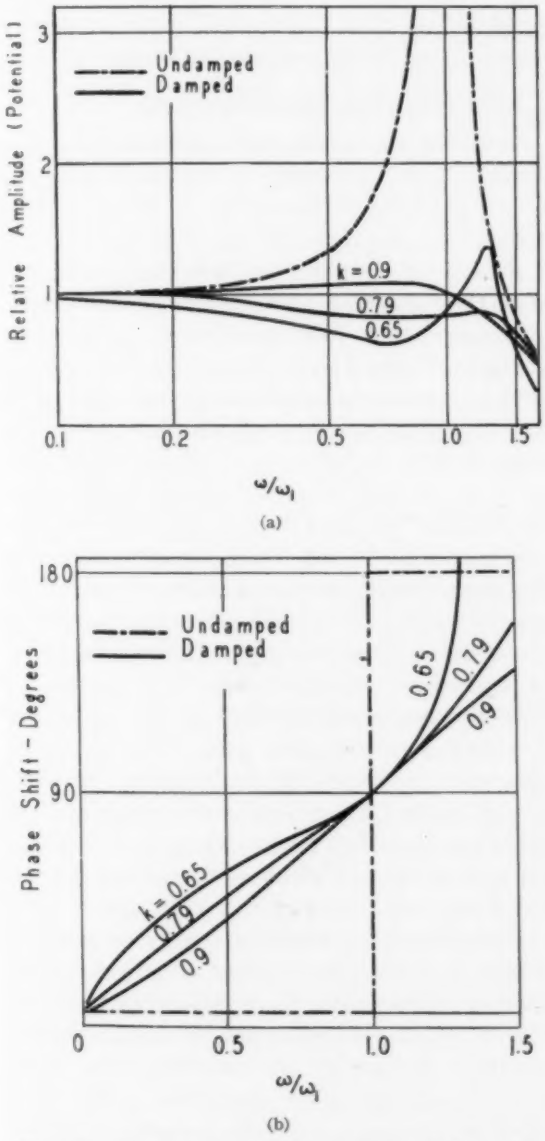

FIG. 5. Theoretical response characteristics of the equivalent network (Fig. 2(b)). (a) Amplitude-frequency. (b) Phase-frequency.

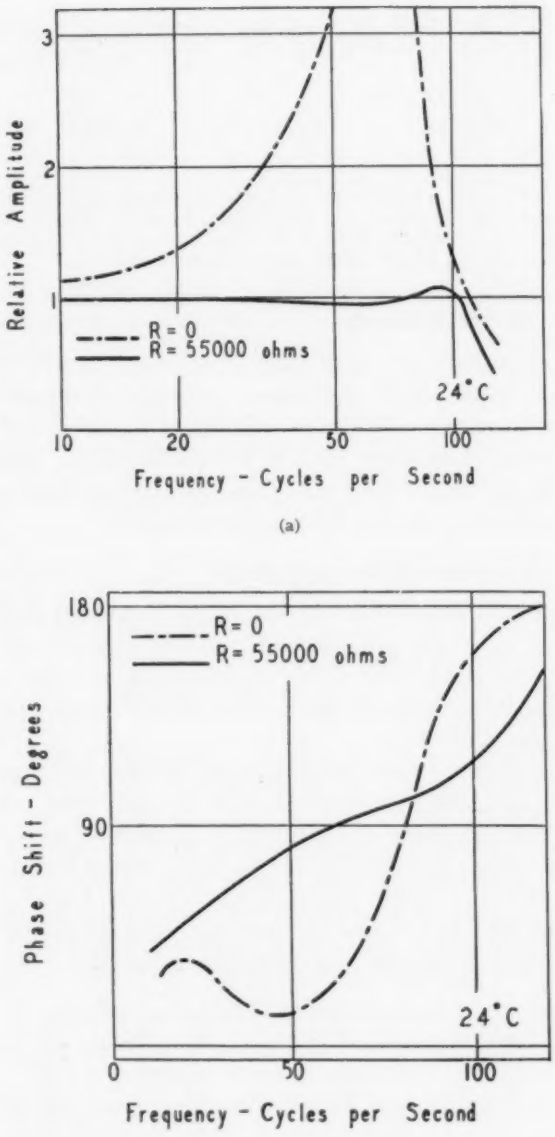

FIG. 6. Experimental response characteristics of the ink writer. (a) Amplitude-frequency. (b) Phase-frequency.

TABLE II. *Response of the equivalent network.*

k	$x = R\omega C_0$ FOR TRANSIENT*	$x = R\omega C_0$ FOR SINUSOIDAL†	REMARKS
0.90	0.72	0.51	Appears critically damped
0.79	1.2	1.2	Small transient oscillation
0.65	1.9	2.1	Larger transient

* Experimentally determined to give least oscillation.
† Gives most nearly uniform frequency response (Fig. 5(a)).

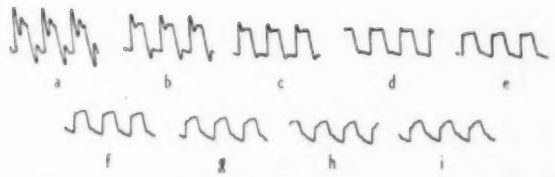

FIG. 7. Electrical damping of transient response. a. $R=0$, b. $R=10{,}000$ ohms, c. $R=20{,}000$ ohms, d. $R=30{,}000$ ohms, e. $R=40{,}000$ ohms, f. $R=50{,}000$ ohms, g. $R=60{,}000$ ohms, h. $R=70{,}000$ ohms, and i. $R=80{,}000$ ohms.

b. Crystal currents

Transient potentials were applied to a Rochelle salt plate, and the input currents examined oscillographically as the damping resistor and temperature were varied. As predicted by the theory, at no time was it possible to eliminate completely the oscillatory components.

c. Response of the instrument

Figure 6 (a) shows the amplitude-frequency and Fig. 6(b) the approximate phase-frequency response of the ink writer described in Section I. The improvement effected by the series resistor is again evident.

Figure 7 illustrates the damping of transients by the input resistor. It may be seen that no value of resistor completely suppresses overshooting (a residual oscillation). Here again, about the same damping gives most faithful transient and frequency response. In practice the resistor is adjusted so that a d.c. pulse and a 60-c.p.s. wave of the same voltage give the same pen excursion.

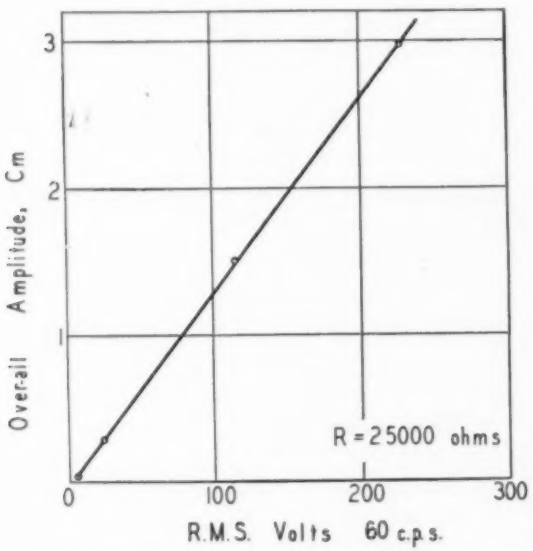

FIG. 8. Voltage-amplitude linearity of the ink writer.

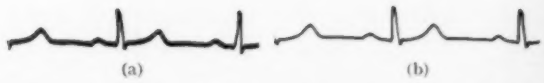

FIG. 9. A human electrocardiogram. (a) Cathode-ray oscillograph record. (b) Ink writer record.

The voltage-amplitude linearity characteristics measured at 60 c.p.s., is shown in Fig. 8. At very low frequencies and large amplitudes Rochelle salt shows a hysteresis effect similar to the magnetism of ferromagnetic materials. This seems to cause no appreciable error in the frequencies usually encountered in biological work.

d. Recording of electrocardiograms

As mentioned before, probably the best test of fidelity of any recorder is comparison of the records obtained with a known wave form of the type to be studied. Electrocardiograms must frequently be recorded in biological work, and since they have a wide range of component frequencies, they have been used to check the accuracy of the instrument. Fig. 9 shows the same human electrocardiogram, as recorded by the cathode-ray oscillograph at *a* and by the ink writer at *b*.

IV. Summary and Acknowledgment

A piezoelectric ink-writing oscillograph has been found useful in the recording of bioelectric potentials. The analysis of the electromechanical system of the instrument is simplified by deriving the equivalent electrical network. From this the phase-frequency, amplitude-frequency, and transient characteristics can be calculated. While these are all improved by inserting a series resistor, critical damping cannot be achieved by this means alone in a piezoelectric device because the necessary coefficient of coupling, greater than 0.943, is unobtainable in a crystal.

Critical damping and best frequency response are not necessarily equivalent. The best test of fidelity is comparison of records with the wave form of the applied potential. Such comparisons have been made with the instrument described.

I wish to express my gratitude to Dr. Carl Eckart for his assistance in the theoretical portion of this investigation, and to Dr. R. W. Gerard for his encouragement.

Computation of Some Physical Properties of Lubricating Oils at High Pressures

I. Density

R. B. Dow and C. E. Fink
School of Chemistry and Physics, The Pennsylvania State College, State College, Pennsylvania
(Received October 24, 1939)

From a survey of available data on the density of fluid lubricants as a function of pressure and temperature, the following empirical equation has been derived:

$$\rho = \rho_0(1+ap-bp^2)_t.$$

ρ is the density at a given pressure (gage) p and temperature t; ρ_0 is the corresponding density at atmospheric pressure. The constants a and b are evaluated over a temperature range extending from 20° to 220°F and the density equation is valid over a pressure range of 50,000 lb./in.^{2}. While the equation was derived from data on mineral oils it has been found to hold equally well for animal, vegetable, and fish oils. The variation of density with pressure is independent of the nature of the oil.

IN order to compute the thermodynamic characteristics of an oil at high pressure it is necessary that the specific volume or density be known as a function of temperature and pressure. Moreover, in problems of lubrication design it is often necessary to convert from the dynamic to the kinematic coefficient of viscosity, and vice versa, and in order to do this at high pressures the oil densities must be known over the range of pressure involved. It is the purpose of this paper to present a practical means for calculating density over a pressure range up to 50,000 lb./in.^{2} at temperatures between 20 and 220°F. These ranges of pressure and temperature are those commonly encountered in many problems of lubrication in the fields of engineering and applied physics, and although data could be obtained readily at higher pressures, provided that the temperature was also raised so that the oil would remain fluid, the investigation would then become one of academic interest rather than of practical importance.

Densities of five petroleum lubricants have been measured by Hyde[1] at 104°F over a pressure range of 25,000 lb./in.^{2}. Similar data were obtained on four petroleum oils by Dow[2] at 77°F, 104°F, and 167°F at pressures up to 50,000 lb./in.^{2}. Dow and Fenske[3] obtained data on an oil at 104°F and 167°F at pressures up to 50,000 lb./in.^{2}, and then fractionated the oil into narrow-boiling cuts and obtained data on ten of these cuts.

The striking result of all these investigations is the fact that, within the range of experimental error, all of the oils have the same compressibility. Thus the oils studied in Europe by Hyde, who used the moving piston type of apparatus to make his measurements, showed the same behavior in this respect as the oils studied in this country by Dow who used the sylphon apparatus. Furthermore, the work of Dow included extreme types of oils such as a typical Pennsylvania oil which is noted for its high paraffinicity and low temperature coefficient of viscosity, and a typical Gulf Coast oil which is characterized by the fact that it contains large amounts of naphthenic and aromatic types of molecules and has a relatively high temperature coefficient of viscosity. The work of Dow and Fenske, moreover, shows that the generality in regard to compressibility may be extended to narrow-boiling fractions which vary considerably in boiling point and molecular weight. This insensitivity of compressibility, within the range of experimental error, among the wide variety of oils studied is strikingly different from other properties that have been studied under pressure, as, for example, viscosity.[4]

From an experimental standpoint, therefore,

[1] J. H. Hyde, Proc. Roy. Soc. **A97**, 240 (1920).
[2] R. B. Dow, J. Wash. Acad. Sci. **24**, 516 (1934).
[3] R. B. Dow and M. R. Fenske, Ind. and Eng. Chem. **27**, 165 (1935).
[4] R. B. Dow, J. App. Phys. **8**, 367 (1937).

the available density data for oils at high pressure appear to be adequate for present needs. The fact that all of the oils studied show the same compressibility indicates the desirability of constructing standard density-pressure curves. The practical means adopted by the writers to express these curves in a form convenient for calculation of density at high pressure is an empirical equation that reproduces the standard curves that were drawn as averages of the experimental data. Interpolation and extrapolation were used, as explained later, to amplify and extend the range of usefulness of the equation.

Details of Computation

The pressure-density data of Hyde,[1] Dow,[2] and Dow and Fenske[3] were plotted on graph paper of large enough scale that the coordinates of any point could be read to four significant figures. To facilitate computation, density ratios ρ/ρ_0 were plotted against pressure. ρ is the density in g/cm³ at any fixed temperature and pressure and ρ_0 is the corresponding density at the same temperature and atmospheric pressure. Temperature is expressed in degrees Fahrenheit and pressure in pounds per square inch gage. Curves were constructed for temperatures of 77°, 104° and 167°F. They were found to have the same general shape as those obtained by Bridgman[5] for many pure liquids; i.e., the density increases quite rapidly as pressure is first applied but at a slower rate at higher pressures. For example, in the case of oils at 104°F the density increases by about 5.3 percent for the first 15,000 lb./in.² but only by an additional 3.2 percent for the next 15,000 lb./in.².

The distribution of points with reference to the curves is of importance in determining the relative precision of the data. The three studies gave density values for twenty oils at various temperatures and pressures. Four of the oils had been studied at all three temperatures, five at 104° only, and eleven at 104° and 167°F. It is evident that the data are not enough for a critical study of accuracy by the method of least squares. Consequently, curves were drawn in such a way that they passed through the averages of all the plotted points. At 77° the maximum deviation of any point from the average was 0.1 percent; at 167°, 0.7 percent; and at 104°F, the most representative since data from all three studies were available, 0.9 percent.

Table I illustrates the distribution of the densities measured at 10,650 lb./in.² for a temperature of 104°F. Three investigators, working with twenty different oils, are represented by the data. The arithmetic average is seen to be 1.039 as compared with 1.040 obtained graphically, indicating that the graphic method of averaging is sufficiently accurate. The average deviation from the mean of a single observation is seen to be ±0.002 and the percentage deviation of the mean is ±0.04.

Table I. *Density ratios of twenty oils at 10,650 lb./in.² and 104° F.*

Oil	Observer	Density Ratio, ρ/ρ_0
1	Dow and Fenske	1.035
2	Dow	1.035
3	Dow	1.037
4	Dow	1.037
5	Dow	1.037
6	Dow and Fenske	1.037
7	Dow and Fenske	1.037
8	Dow and Fenske	1.038
9	Dow and Fenske	1.038
10	Dow and Fenske	1.038
11	Dow and Fenske	1.038
12	Hyde	1.039
13	Dow and Fenske	1.039
14	Hyde	1.040
15	Dow and Fenske	1.040
16	Dow and Fenske	1.040
17	Hyde	1.041
18	Hyde	1.042
19	Dow and Fenske	1.043
20	Hyde	1.045
	Average	1.039

The absolute error involved in the measurements is probably somewhat greater than the precision might seem to indicate. Both the piston displacement and the sylphon methods of measuring volume change are quite complicated in comparison with the simple and accurate method of weighing with a specific gravity bottle at atmospheric pressure. Furthermore, the measurement of the absolute pressure in the system introduces errors which are not involved in ordinary atmospheric gravity determinations. Bridgman[5] indicates that the absolute error involved in the measurement of density under pressure might generally be expected to be 2 or 3

[5] P. W. Bridgman, Proc. Am. Acad. A & S **66**, 185 (1931).

percent at constant temperature. The fact that there is good agreement between the data of Hyde, who used the piston displacement method, and that of Dow, and Dow and Fenske, who used the sylphon method, would seem to indicate, however, that the absolute error involved in the measurements under consideration at constant temperature might be somewhat less than what would otherwise be expected.

Probably the source of greatest error lies in the interpolation and extrapolation. Data were available at only three temperatures; namely, 77°, 104°, and 167°F. By interpolation and extrapolation of these data, a system was evolved by means of which densities can be calculated at intervals of 10° between the limits of 20° and 220°F. The method employed was to construct relative density-temperature isobars at atmospheric pressure, 10,000 lb./in.², and 20,000 lb./in.² by reading off the relative densities at 77°, 104° and 167°F from the relative density-pressure curves already described. While only three points were used to determine these isobars, the uncertainty in locating the curves accurately was not as great as might be expected at first thought. Relative density increases slowly with temperature at constant pressure, and for the experimental range considered here does not depart greatly from linearity. Moreover, the isobar at atmospheric pressure could be located with extreme accuracy with the aid of the National Bureau of Standards tables[6] that show the change in density of petroleum oils with temperature at atmospheric pressure. At this point it is to be noted that the National Bureau of Standards tables indicate that oils in the range of specific gravity of the present ones under consideration have a thermal coefficient of expansion of 40×10^{-5} per °F at atmospheric pressure. The averages of the corresponding values reported by Dow,[2] and by Dow and Fenske[3] were 37×10^{-5} and 41×10^{-5}, respectively. This variation of the coefficient can be taken as the possible error in the temperature measurements, since the apparatus used at the National Bureau of Standards was doubtless better suited to measuring the atmospheric isobar than the sylphon apparatus used by these other investigators. Thus the atmospheric isobar was first corrected to bring it into line with the National Bureau of Standards values, and the other isobars were then corrected correspondingly. By using this system of correction, the actual shape of the density-pressure curves was left unchanged, and the intercept on the density axis was corrected only to bring the atmospheric densities into line with the National Bureau of Standards tables.

[6] National Bureau of Standards Circular C410, United States Government Printing Office, Washington, D. C. 1936.

Density Equation

In order to express the graphical results in a simple form that can be used readily for the calculation of density at various pressures and temperatures when the density at atmospheric pressure is known at a particular temperature, the following empirical equation was developed,

$$\rho=\rho_0(1+ap-bp^2)_t. \qquad (1)$$

In this equation ρ is the density in g/cm³ at any stated temperature t and pressure p, and ρ_0 is the density at the same temperature at atmospheric pressure. Temperatures are expressed in degrees Fahrenheit and pressures in pounds per square inch gage. The symbols a and b represent constants at any given temperature. Values for a and b are given in Table II.

Table II. *Density constants a and b as functions of temperature.*

Temp. °F	a	b	Temp. °F	a	b
20	3.96×10^{-6}	7.3×10^{-11}	130	4.50×10^{-6}	5.3×10^{-11}
30	4.02	7.0	140	4.53	5.1
40	4.08	6.8	150	4.56	5.0
50	4.14	6.6	160	4.59	4.9
60	4.19	6.4	170	4.61	4.8
70	4.24	6.2	180	4.63	4.7
80	4.29	6.0	190	4.64	4.6
90	4.34	5.8	200	4.66	4.5
100	4.38	5.7	210	4.67	4.4
110	4.42	5.5	220	4.68	4.4
120	4.46	5.4			

The method used to compute the values of a and b is readily explained. For each of the temperatures listed values of ρ/ρ_0 were taken from the isobars constructed as described in a previous section, and a and b were evaluated using simultaneous equations of the type of Eq. (1). The values so calculated were then plotted as shown in Fig. 1 and Table II was constructed

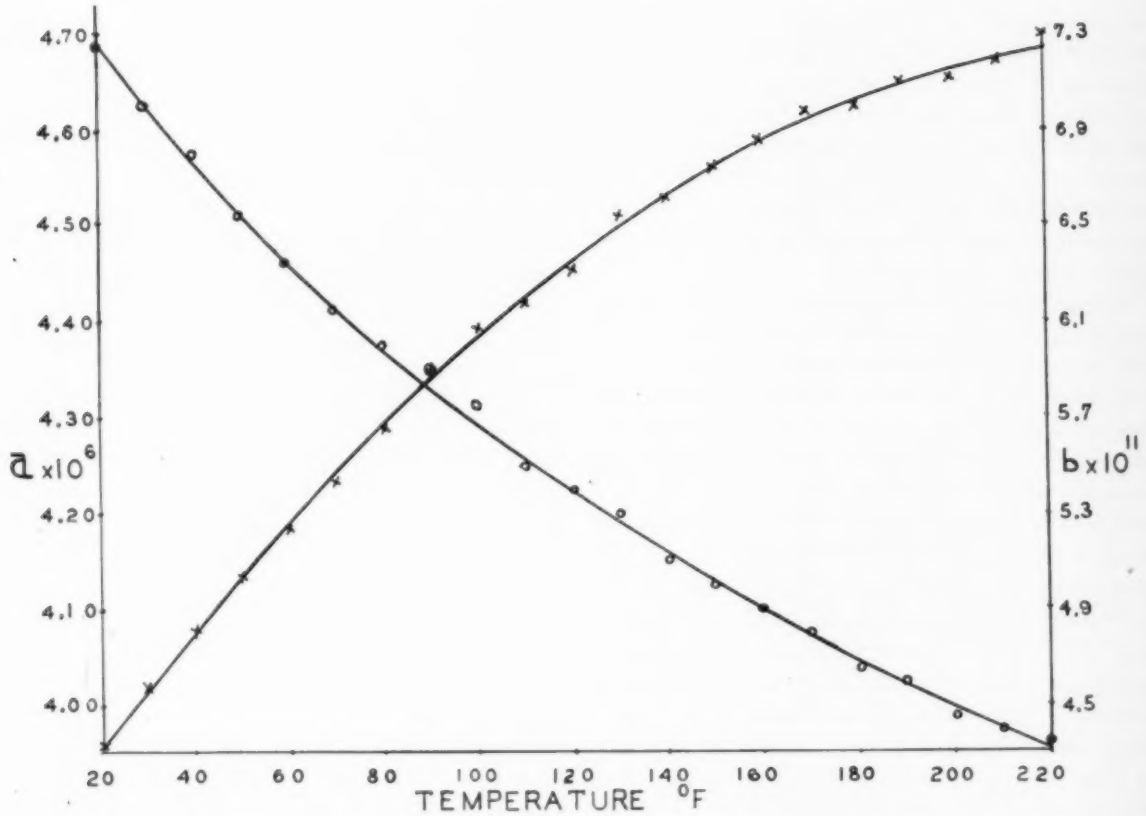

FIG. 1. Calculated values of a and b as functions of temperature; ax, bo.

from values read from smooth curves through these plots.

If the density of an oil is known at atmospheric pressure and it is desired to calculate its density at some other pressure, it is only necessary to refer to the values of a and b of Table II at the temperature under consideration and make the calculation by means of Eq. (1). If the known atmospheric density is at a temperature different from that required in the final answer, the atmospheric density is first adjusted to the desired temperature by means of one of the methods already known to the petroleum industry, as, for example, the National Bureau of Standards tables[6] referred to already.

DISCUSSION

It is the belief of the writers that the system developed in this paper offers the best means so far described for the calculation of density of lubricating oils at various pressures from their known densities at atmospheric pressure. Taking all of the possible sources of error, discussed in a previous section, into account, it is believed that the error in any density computed by this system is not above 3 to 5 percent.

While the density equation, as given above, was derived from data on mineral oils, it is of interest to note that it has been found to hold equally well, using the same table of values for the constants a and b, for animal, vegetable, and fish oils, insofar as there are data available. Hyde[1] obtained data at one temperature on castor oil, trotter oil, rape oil, and sperm oil. Dow[2] obtained data at three temperatures on lard oil and sperm oil. Using the atmospheric densities reported by these investigators for their oils, a number of density computations were made at various pressures and temperatures using Eq. (1). The values so obtained were then compared with the experimental values reported by Hyde and Dow. For ten such calculations made, the equation reproduced the experimental

data to within 0.5 percent in nine cases, and to within 1.0 percent in all cases. While the data are not sufficient to show definitely that the method of calculating densities developed in this paper is applicable to these other types of oils, there seems to be good indication that it is.

Two thermodynamic quantities of interest, the isothermal compressibility and the thermal expansivity, can be calculated from the data of this paper. The compressibility can be obtained by differentiation of the density equation at the temperature corresponding to the constants a and b, and, if computed at two pressures, shows the normal decrease with increase of pressure. On the other hand, if the compressibility is calculated at two temperatures, it will be found to increase with temperature. The thermal expansivity can be calculated by applying the density equation at two temperatures at constant pressure. If computations are made at two pressures it will be found that the expansivity decreases also with increase of pressure. In regard to these derived quantities it should be noted that they cannot be calculated to an accuracy claimed for the basic density data. However, this lack of accuracy becomes important only at the lowest pressures where possible inaccuracy in measuring pressure by means of the manganin coil is recognized.

An X-Ray Method of Determining Rates of Diffusion in the Solid State

JESSE DUMOND AND J. PAUL YOUTZ
California Institute of Technology, Pasadena, California
(Received November 7, 1939)

Gold and copper were simultaneously deposited in vacuum by vaporization on a plate of glass, the copper being deposited at a uniform rate while the gold was deposited in one hundred stratified layers in the copper by alternately raising and lowering the temperature of the molybdenum vaporizing trough containing the boiling gold. The translucent deposit so formed had a total thickness of about 10,000A and hence an average interplanar distance of 100A. In an especially constructed x-ray spectrograph selective diffraction of Mo K radiation from these stratified films was observed corresponding to the artificially imposed periodicity of the stratification and the intensity of this diffracted image relative to the direct beam was found to fall off with time so as to indicate a "half-life" for the stratified structure of about two days. This suggests a general method for the study of average rates of diffusion and the determination of diffusion coefficients of solids in solids by utilizing the decay of such stratified films. Simple theoretical considerations indicate that such an artificial stratification should, through the action of diffusion alone, rapidly and automatically lose the higher Fourier harmonics of its periodic density distribution function and retain the fundamental in such a way as to render the determination of the diffusion coefficient quite accurate. The observed behavior of the diffracted maxima seem to support these expectations as does also the absence of any intensity in higher orders than the first. This purification by diffusion probably takes place principally during the depositing process itself while the temperatures are still quite high. Formulae are derived relating the observed rate of decay of the diffracted intensity, the artificial "grating constant" of the strata, and the diffusion coefficient. The method seems especially promising for substances and temperatures where diffusion is so slow as to be otherwise quite unobservable because the diffusion time varies as the square of the distance over which atoms must migrate and in this method these distances are many orders of magnitude smaller than in any other.

I. INTRODUCTION

WHEN the experiments here described were started[1] our purpose in trying by controlled evaporation in vacuum to produce artificially stratified layers of two different substances (gold and copper) was to develop, if possible, a technique of measuring the absolute wave-length of x-rays by a type of diffraction more nearly resembling Bragg reflection than is the case in the

[1] See J. DuMond and J. P. Youtz, Phys. Rev. **48**, 703 (1935), also for unsuccessful attempts to produce artificial Bragg reflectors see H. Koeppe, Dissertation Gieszen 1923, W. Deubner, Ann. d. Physik **5**, 261 (1930).

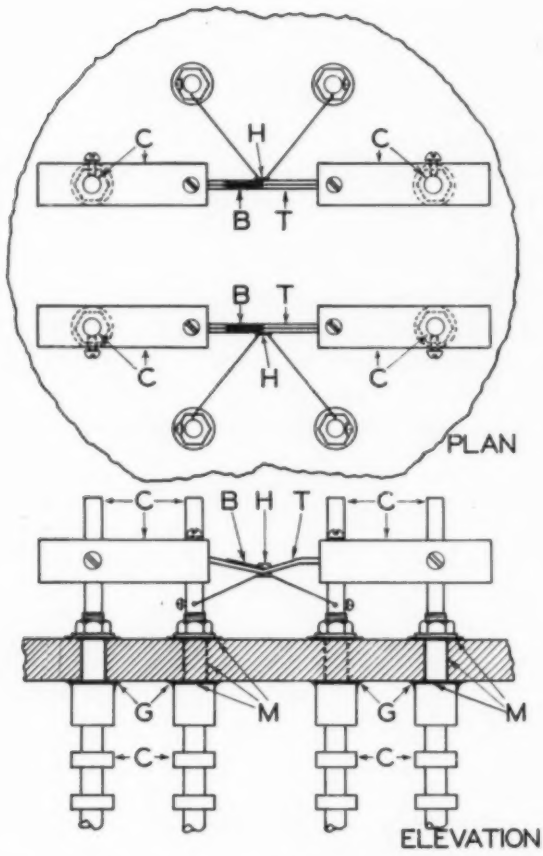

FIG. 1. Showing plan and elevation views of small, V-shaped, molybdenum troughs, *T*, heated by electrical conduction in which gold and copper were vaporized. The thermojunction, *H*, with its heat receiver is shown.

well-known method of grazing incidence on ruled gratings. We had hoped to count the number of artificial strata in process of deposition and to measure the total thickness by optical interference methods in order to ascertain the grating constant in terms of visible light. The many difficulties which one encounters in an effort to get, by evaporation methods, uniformity of layer spacing comparable to the ruling of a good grating have led us to abandon the original project. A by-product of this work, however, may prove to be of some utility in the study of the rate of diffusion at ordinary temperatures of one solid through another. This is suggested by our observation that the x-ray diffraction maxima formed by selective interference in the stratified films gradually diminished in intensity, and fell off to half-value in about two days. This must be interpreted as meaning that the *amplitude* of the periodic functions representing the distribution of the two components as a function of depth in the deposit fell off with time, and that the one component diffused into the other so as to go from a stratified structure toward an increasingly uniform mixture.

The transfer of atoms of kind *A* will occur by diffusion at every point at a rate jointly proportional to their density gradient and the diffusion coefficient so that information as to the form of the periodic density function is important if the diffusion coefficient is to be determined from the rate of decay of the intensity of the selective reflection. Now by a fortunate circumstance it appears that such stratified films should and do by the simple process of diffusion alone rapidly approach and for a considerable fraction of their lives retain a sinusoidal distribution function. For such a function the calculation of the diffusion coefficient is simple. An attractive feature of this method is the fact that the x-ray diffraction reveals the diffusion process for extremely minute displacements of the diffusing atoms. Thus the process of diffusion can be followed without much delay at much lower temperatures than would otherwise be feasible.

II. METHOD OF DEPOSITING STRATIFIED FILMS

The evaporating apparatus

The evaporating apparatus consisted of a flat steel disk 15 inches in diameter supported as a horizontal table on steel legs and provided with a two-stage glass mercury diffusion pump and liquid-air trap below the disk and between the legs. Eight large brass electrical terminals (shown at *C* in Fig. 1) pass through the disk insulated therefrom with mica washers and sleeves *M* and made vacuum tight with glyptal lacquer *G*. Air-cooling fins are provided for these terminals. A glass cylinder 12 inches in diameter closed at the top by a metal disk waxed onto it forms the bell jar for enclosing the work. The lower edge of this cylinder previously lapped flat against a plane steel plate with abrasive stands on the steel disk, the joint being made tight with beeswax.

The glass plate, 2 inches square, on one side of which the stratified deposit was made, was held above the boiling sources of metal vapor in a

small brass frame supported by a fork from the metal top on the glass cylinder. A small vane pivoted to the supporting frame could be swung in a horizontal plane by means of a magnet so as to cover progressively more and more area on one corner of the glass plate. This vane was shifted after every 25 layers had been deposited so as to form a "staircase" in the layered deposit with steps each 25 layers high. Our purpose here was to check by interferometry the uniformity of deposition and also to determine to what extent the phase change of the light reflected by the metal film might be influenced by the varying proximity of the glass backing.

An electrical discharge was maintained while the system was being pumped down to suitable vacuum for evaporation. The discharge from a 15,000-volt transformer occurred between the lower steel plate and the metal frame supporting the glass plate on which the layered deposits were to be made. J. Strong has used this method of the gas discharge which very effectively removes by ion bombardment the last traces of grease, or other organic impurity from the surface to be coated.

The resistance troughs or boilers

The containers for the boiling metals gave some trouble. The metals gold and copper were chosen originally for the evaporated films because the atoms have much external similarity but widely different atomic numbers and hence very different x-ray scattering power. The melting points of these metals are slightly above 1000° C and they must be made considerably hotter to boil at a sufficient rate in the vacuum. Molybdenum was one of the few substances which we found capable of containing either the boiling gold or copper without amalgamation. The boilers were made by bending a strip 5 mils thick and 0.1 inch wide cut from sheet molybdenum so as to form 90-degree V-shaped troughs each 5 cm long. Each trough ran nearly horizontally between two of the heavy air-cooled current terminals, *C*, (Fig. 1) and was heated by passing an alternating current of 50 amperes through it, furnished by a step-down transformer. At the point where the molten metal lies in the trough the resistance of the conductor is so much diminished that the bulk of the vaporization occurs at the two ends of the melt adjacent to the hot empty trough. If the trough is nearly horizontal the melt becomes unstable, oscillating back and forth along the length of the trough in an irregular way, impelled apparently by surface tension forces and often breaking into two halves which find their way to the cool regions of the trough at its ends. The consequent heating and cooling of the trough gives a very irregular rate of vaporization which is most undesirable. This we avoided by providing the trough with a definite kink in the middle so that it sloped downward toward this point from either terminal. The metal to be melted, *B*, was placed *on one side only* of this kink. As the vaporization progressed from the hot spot where the lower end of the melt was adjacent to the hot empty trough the metal lost by evaporation would be replaced by fresh metal running slowly down the incline. The rate of evaporation was thus practically constant over a good fraction of the life of the charge. Fig. 1 shows the troughs at *T*.

Chromel-Alumel thermocouples were introduced into the vacuum chamber with heat collectors *H* close to the trough to permit of checking the constancy of the temperature in any given run.

The copper was maintained at as constant a rate of evaporation as possible throughout the run which lasted generally an hour and forty minutes. The periodic vaporization of the gold controlled by a clock mechanism was accomplished by alternately closing and opening a vacuum mercury tilting switch sealed in glass, which short-circuited a resistance in series with the heating current on the boiler containing the gold, increasing the power supply for periods of 28 seconds alternating with periods of reduced power supply of 28 seconds duration. The reduction in power supply was only just enough to inhibit vaporization of the gold. In this manner a total of one hundred spurts of gold would be applied. Distances from boiling metal to the glass plate were varied in different runs from 10 cm to 20 cm. The total deposits were all translucent. They however reflected considerably more visible light than they transmitted.

It is most probable that our technique could be much improved in the matter of boilers by going to more trouble than we have taken. A massive molybdenum boiler heated by electron bom-

bardment and completely enclosed except for a relatively small opening for the vapor jet would give much more uniform results.

Control circuit for periodic deposition

The mercury tilting switch for heating and cooling the boiling gold was operated as a relay actuated by a clock pendulum. The appropriate swing of the pendulum was selected by a magnetically driven ratchet wheel. The clock pendulum which made and broke an electrical contact (on for one second, then open for one second) caused the ratchet wheel to advance one tooth every second by a solenoid actuated ratchet. Pins on this wheel after 28-second intervals closed circuits permitting the next swing of the pendulum alternately to open then 28 seconds later to close the solenoid operated mercury tilting switch. Fig. 2 showing the circuit diagram is self-explanatory.

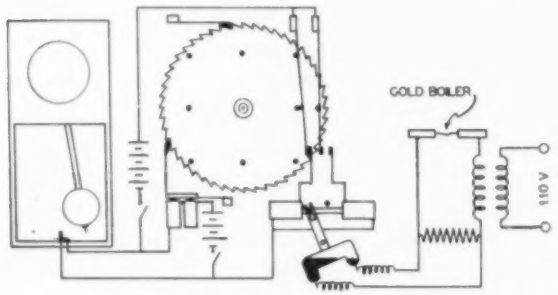

FIG. 2. Control circuits, relays, and ratchet by means of which a pendulum clock was made to control the heating and cooling of the trough containing the gold so as to deposit one hundred approximately uniform layers of that metal in a matrix of copper.

III. X-RAY DIFFRACTION STUDIES WITH STRATIFIED FILMS

The diffraction camera

It occurred to us that the surface of the polished glass plate on which the layered deposits are made is, from the point of view of x-ray wavelengths, probably very far from flat. As the successive layers of gold are deposited in the matrix of copper it is more than likely that the initial irregularities of the surface may be augmented by the random nature of the vaporization so that the strata higher up in the deposit may also be very far from plane. X-rays reflected from such surfaces might well give images as blurred as that of the moon seen reflected in a choppy sea. To avoid this difficulty we resorted to the well-known device of Bragg in which the crystal is rocked through a small range of angles, the photographic emulsion and the effective source of x-rays (slit or focal spot of x-ray tube) being stationary and equidistant from the center about which the crystal is rocked (Bragg "focusing" condition). The geometry whereby this focusing condition minimizes the blurring of the diffracted maxima caused by angular distortions of the diffracting planes and emphasizes only the *periodicities* responsible for the selective diffraction is too well known to require repetition here.

We expected our first-order diffraction angle to be very small from a rough estimate of the grating constant made by laying an optically flat glass plate on the stratified film. Interference fringes could be seen presenting discontinuous lateral displacements where they crossed the steps 25 layers high in the stratified deposit which we had made with the movable shielding vane in the process of deposition. We estimated the total thickness of the deposit at roughly 10,000A and from this the "grating constant" of our artificial strata would be 100A. For the Mo K x-rays we used whose wave-length is about 0.7A this calls for a diffraction angle in the first order of about $\theta = 12$ minutes of arc. It seemed interesting however to explore at larger angles for higher orders and to look for diffraction effects from the atomic structure of the deposit if such might exist.

At such small grazing angles as 12 minutes of arc it becomes a problem to prevent fogging of the photographic emulsion by primary radiation transmitted directly past the stratified deposit without reflection therein. To prevent such fogging we provided a lead wedge confronting the stratified deposit supported by a lever mechanism designed to make the opening between the wedge and the deposit increase as the grazing angle of incidence and reflection of the x-rays increased. Fig. 3 shows a plan and an elevation of the spectrograph with the linkage for moving the wedge W. This linkage is designed so that over the entire range of angles the opening left by the

wedge permits a little less than the entire surface of the stratified deposit to be illuminated by x-rays. To insure against leakage of direct x-rays past the glass plate on which the stratified deposit was laid, a long pivoted brass paddle, *P*, shown in Fig. 3, was provided. This paddle extended through the pivot *q* to within a few millimeters of the photographic film and the glass plate *S* with its stratified film was supported in a square hole in the paddle so that the reflecting surface was quite accurately in the plane of the paddle. Paddle and crystal were rocked together by means of a cam, *C*, cut on the end of a cylinder, consisting of two equal right- and left-hand helical arcs. The small schema at bottom of Fig. 3 shows the geometry of reflection and shielding for two different angles.

In such a Bragg focusing diffraction camera the width of the source determines the width of the spectral lines. Instead of defining this width of source by a slit we have, as shown in Fig. 3, turned the target surface of the x-ray tube at such an angle as to give effectively a very thin line source situated so as to fulfill the Bragg focusing condition.

Diffraction photographs and control tests

Throughout the exposures the x-ray tube was operated at 40 kilovolts and 10 milliamperes. For each of the exposures we show here the cam *C* made four revolutions in a time interval of 28 minutes. Only a rough estimate can be made of the fraction of this time effective in reflecting the

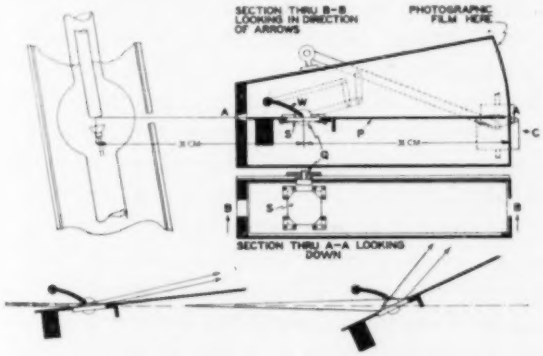

FIG. 3. The x-ray spectrograph used for examining the stratified deposits.

diffracted lines observed on our spectra. From the geometry of the apparatus and the width of the diffracted line this fraction seems to be about 1/100 so that the effective time of reflection for each exposure is apparently about 17 seconds.

While the time and intensity of each exposure was sensibly the same, another factor, the geometry of the alignment of the focal spot in the x-ray tube with the paddle *P* and lead wedge *W*, when these are nearly in contact at one extreme end of their travel, has a strong influence on the width and intensity of the undeflected direct beam and we believe that variations in this geometry account for the greater width of the direct beam in the first and last exposures shown in Fig. 4. This figure is a reproduction of the

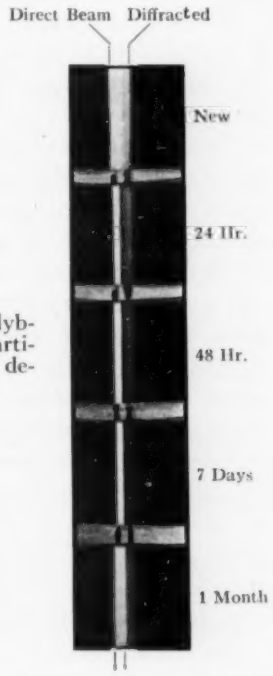

FIG. 4. X-ray spectra of molybdenum *K* radiation made with artificially stratified metal films deposited by evaporation.

spectra we have obtained from one of our best stratified deposits.

The decay in the intensity of the diffracted maximum relative to the directly transmitted intensity with increasing age of the deposit is apparent. This decay, in itself, is strong internal evidence that the observed effect is indeed diffraction from the artificially produced stratification and not some vagary of the glass or metal surface or some imperfection in the camera. To be absolutely sure, however, that we were not mistaken in this interpretation we ran control exposures with the stratified deposit replaced by: (1) clean glass, (2) a pure evaporated copper

deposit on glass, (3) a copper plate, (4) nothing whatever in the square hole in the paddle, (5) a calcite crystal cleavage surface. Nothing resembling the diffraction maxima from the stratified deposit was observed in any of these control exposures.

While the results here shown represent admittedly only very rough qualitative work there is not the slightest doubt as to the reality of the decay of the diffracted intensity with age of the deposit.

Absence of orders of reflection higher than the first and our interpretation thereof

We were struck by the complete absence of higher order reflection than the first in all the diffraction photographs. The diffraction angle indicated in our photographs checks very well with our estimate of the 100A "grating constant" for the stratification assuming this to be a first-order reflection. A sinusoidal distribution of the density of gold atoms in the copper (as a function of depth) is the only one incapable of diffracting the x-ray intensity in other orders than the first. Our method of producing the intermittent vaporization of the gold should give layers with more or less diffuse boundaries. Furthermore, since the displacement of the gold into the pure copper regions is proportional to the density gradient of the gold and the time rate of change of the quantity of gold in any region is proportional to the second space derivative of the density function *one would expect the process of diffusion itself to render the density function rounded and sinusoidal* rather than angular and discontinuous. Indeed as we shall show immediately, if the periodic density function be represented by a Fourier series the process of diffusion will obliterate all the higher harmonics so much faster than the fundamental that in a very short time it should become quite strictly a simple harmonic function and no higher order reflections should then be observed. It is this circumstance which in our opinion renders the decay of reflected x-ray intensity from artificially stratified films a promising method of studying diffusion and diffusion coefficients in the solid state for if the concentration function automatically becomes a simple harmonic function it is a very simple matter to compute the diffusion coefficient from the grating constant and the time rate of decay of the diffracted intensity.

Behavior of the images with time

Beside the absence of higher order reflections we think our spectra, shown in Fig. 4, exhibit other slight evidences of this tendency for the density distribution function to become and remain for some time a simple harmonic grating. In the spectrum from a so called "new" deposit in Fig. 4, the width of the direct beam prevents a satisfactory estimate of the structure of the diffracted image for this case but judging from the exposure of a deposit 24 hours old compared to those for two and for seven days there seems to be a little sharpening of the diffracted image with time. The time required to remove the plates from the vaporization machine, load them in the x-ray diffraction camera and take the x-ray exposures would prevent any of our observations from being made on strictly "new" deposits. The rate of decay of the higher harmonics in the distribution function will be especially rapid during the deposition itself and for a short time thereafter because of the much higher initial temperature of the deposit, exposed as it is to radiation from the molten metal and to the hot metal vapor condensing on its surface. The diffraction from so called "new" deposits must therefore be regarded as coming from strata which already have passed through a substantial portion of the diffusion process whereby the higher harmonics are suppressed.

After very long times one expects the fundamental simple harmonic distribution function itself to disappear from one or both of two causes. First, the so called fundamental period made by the intermittent vaporization of the gold may be superposed on weaker subharmonics of longer period caused by mal-functioning of the vaporization technique. Just as the fundamental should persist much longer than any of the higher harmonics so such subharmonics should persist long after the fundamental has become negligible by comparison. Second, given a perfect simple harmonic distribution function decaying in amplitude with time this amplitude will eventually reach a value of the same order as the accidental fluctuations in density to be expected in a "uniform" mixture of gold and copper upon

statistical fluctuation theory. The artificial periodicity will then be completely submerged and obliterated. The diffraction exposure of a stratified deposit one month old seems to show that either or both of the last two processes may have occurred.

IV. Theoretical Relations Between Rate of Decay of the Diffracted Line, Grating Constant and Diffusion Coefficient

We shall confine our theory so as to agree with the following simplifying assumptions.

In a binary mixture of components A and B (gold and copper in our case) we assume that over the range of concentrations obtaining in the stratified deposit the average volume per atom of a given kind is sensibly constant independent of the relative concentration of the two components.[2] We also assume that, save for the artificially imposed stratification, no structure exists (such as a crystal structure characteristic of the components) and that the mixture is free from voids.

Let $\rho_A(x,t)$ represent the mass of atoms of kind A per unit volume *of the mixture*, ρ_B being the corresponding quantity for B atoms. We shall frequently refer to these as the density distribution functions for atoms of kinds A or B. They are of course not to be confused with the densities characteristic of A or B atoms in the pure solid state.

The number n_A of atoms A per unit volume of mixture will be proportional to ρ_A; $n_A=\rho_A/\mu_A$; $n_B=\rho_B/\mu_B$ where μ_A is the mass of an atom A, μ_B the mass of an atom B.

Let $V_A=1/\rho_{0A}$ represent the net volume (a constant) occupied in the mixture by unit mass of atoms of kind A with a corresponding definition for V_B. Evidently ρ_{0A} would be the density of the pure, void-free, amorphous solid A if, even in the complete absence of B, the atomic volume remained unchanged.

Now $V_A\,\rho_A$ is the volume of atoms of kind A in unit volume of mixture with corresponding significance for $V_B\,\rho_B$ and hence

$$V_A\,\rho_A(x,t)+V_B\,\rho_B(x,t)=1;$$

or

$$\rho_A(x,t)/\rho_{0A}+\rho_B(x,t)/\rho_{0B}=1. \tag{1}$$

It is clear then that $\rho_A(x,t)$ is a linear function of $\rho_B(x,t)$. Also $n_A(x,t)$ and $n_B(x,t)$ are linearly related to each other and to the preceding two functions.

We now assume that the diffusion equation

$$\partial\rho_A/\partial t=K\partial^2\rho_A/\partial x^2 \tag{2}$$

holds; with K a constant independent of ρ_A[3] over the range[2] obtaining in the stratified deposit. On account of the linear relationship expressed by Eq. (1) it is evident that a diffusion equation of the same type as (2) with the same numerical

[2] The justification for this assumption will increase as the amplitude of the periodic density distribution becomes small compared to the constant term in the later stages of decay of the stratified deposit.

[3] It is a well-known fact that the diffusion coefficient for solids is not in all cases a constant but is in fact a function of the concentration. In this more general case the diffusion equation must be written

$$\frac{\partial c}{\partial t}=\frac{\partial}{\partial x}\left(K\frac{\partial c}{\partial x}\right)$$

or

$$\frac{\partial c}{\partial t}=\frac{dK}{dc}\left(\frac{\partial c}{\partial x}\right)^2+K\frac{\partial^2 c}{\partial x^2}.$$

Matano has shown, Jap. J. of Phys. **8**, 109 (1933) how to obtain a solution to this equation for the special boundary conditions obtaining at an initially sharp interface. The solution for the periodic case here discussed is difficult when the amplitude of the concentration is large but such a case is perhaps not very significant. Both Matano in the above reference and R. F. Mehl, J. App. Phys. **8**, 174 (1937) adduce evidence by Matano's method for variation of K with concentration, the former for diffusion of copper in nickel, the latter for copper in aluminum. The diffusion coefficient increases, they find, in the first case with increasing proportions of copper and in the second case with increasing proportions of aluminum. Over a considerable range of concentrations, however, K can be treated as a constant. This variation of the diffusion coefficient with concentration is of considerable interest and we believe it might be studied by the x-ray observations of the decay of artificially stratified films. In order that the considerations here set forth shall apply to the case where K depends on concentration it is only necessary to wait until the amplitude of the periodic concentration function shall have decayed to a point such that the total range of variation of concentration embraced in the periodic part of the distribution shall correspond to a negligible variation in K. The concentration distribution function can be made to consist of a periodic component superposed upon a uniform mixture with the latter in any desired proportions, by proper control of the evaporation ratio. By preparing a number of samples with different average proportions of the components and taking the rate of decay toward the end of the life of the stratification it should be possible to study the variation of K with concentration. An approximate curve of $K(c)$ and from this of dK/dc coming from the experiment itself could be used to decide whether the appropriate smallness of concentration amplitude had been realized or whether a correction would be required.

coefficient K will characterize the diffusion of ρ_B and obviously this same equation will also hold with n_A or n_B as the dependent variable.

In Fowler's *Statistical Mechanics*[4] (1936) that author following Einstein derives a diffusion equation of the type of Eq. (2) (with the number density as the dependent variable) *from statistical considerations alone* without regard to the state of the diffusing atoms. Fowler's principal assumption for this purpose is that the chance of an atom migrating from a point x at a time t to a point x' at a time t' depends on the intervals $(x'-x)$ and $(t'-t)$ and nothing else. This seems to be tantamount to the assumption of constant K.

We further assume that the density distribution functions $\rho_A(x,t)$, $\rho_B(x,t)$ can be represented with sufficient accuracy by a terminating Fourier series periodic in x with period "d" whose coefficients (save for the constant terms which we shall call ρ_A' and ρ_B') are exponentially decaying functions of the time. These series terminate with harmonics N' of wave-length large compared to the statistical fluctuations of density arising from the atomic nature of the deposit so that the series represents only the *artificially imposed* periodicities. Let ρ_A^* denote the fluctuating part of ρ_A so that $\rho_A=\rho_A^*+\rho_A'$ and

$$\int_x^{x+d} \rho_A^* dx = 0.$$

Since the series is finite we may safely differentiate it term by term without examining the convergence of the derivatives. The series is

$$\rho_A(x,t) = \sum_{n=0}^{N'} S_n e^{-\sigma_n t} \sin 2\pi nx/d + C_n e^{-\gamma_n t} \cos 2\pi nx/d. \quad (3)$$

in which σ_n and γ_n are to be determined while the C_n and S_n characterize the shape of the periodic fluctuations of the distribution profile. On substitution into Eq. (1) this solution is justified and the resulting identities give

$$\sigma_n=\gamma_n=4\pi^2n^2K/d^2$$
or
$$K=\sigma_n d^2/(4\pi^2n^2)=\gamma_n d^2/(4\pi^2n^2). \quad (4)$$

[4] Fowler, *Statistical Mechanics* (Cambridge, second edition, 1936), p. 770.

Now the important thing to notice is that the decay constants of various harmonic components of the films are proportional to n^2 the square of the ordinal number of the harmonic.

Thus if the ratio of the amplitude of the *fundamental* at some time $t=\tau$ to the amplitude at $t=0$ is

$$R_1=e^{-(4\pi^2K/d^2)\tau},$$

then the corresponding ratio representing the decay of the second harmonic in the same time will be

$$R_2=e^{-(4\pi^2 4K/d^2)\tau}=R_1^4,$$

while for the third harmonic it will be R_1^9 etc. Thus when the fundamental has decayed to one-tenth of its initial value the second harmonic will have only one-ten-thousandth of its initial amplitude, the third harmonic only one-billionth of its initial amplitude and so on with all the higher harmonics decaying to infinitesimals of higher order. This purifying process continues with time until the fundamental amplitude has decayed to a value comparable with the accidental statistical fluctuations of density caused by the atomic nature of the film.

The diffracted x-ray intensity to be expected from such a stratified deposit will be proportional to the square of the amplitude of the periodically varying part of the electron density function. Let Z_A and Z_B be the atomic numbers of the components, W_A and W_B their atomic weights, N Avogadro's number, and n the number density of electrons per unit volume which consists of the sum of a periodic term n^* and a constant term n' so that

$$n=n^*+n'.$$

Then evidently

$$n=\rho_A Z_A N/W_A+\rho_B Z_B N/W_B$$

and since from Eq. (1)

$$\rho_B=\rho_{0B}-(\rho_{0B}/\rho_{0A})\rho_A,$$

it follows that

$$n=\rho_A[Z_AN/W_A-(\rho_{0B}/\rho_{0A})Z_BN/W_B] + \rho_{0B}Z_BN/W_B. \quad (5)$$

The last term of this expression is constant and

contributes nothing to n^* the fluctuating part of n. Denoting by $\rho_A{}^*$ the periodic part of ρ_A we have

$$(n^*)^2=(\rho_A{}^*)^2[Z_AN/W_A - (\rho_{0B}/\rho_{0A})Z_BN/W_B]^2. \quad (6)$$

The diffracted x-ray intensities will therefore be jointly proportional to the square of the amplitude of the density fluctuations and to the square of the difference in the parenthesis in (6). Since Z_AN/W_A is practically constant, materials of very different densities will give the strongest reflections as might be expected.

The intensities reflected in the different orders will be proportional to the squares of the amplitudes of the various Fourier harmonics of the density distribution function and it is obvious that all orders above the first will also decay very rapidly in the same way as described above for the amplitudes of the density distribution.

Determination of the diffusion coefficient K

Assuming that the function $\rho^*(x,t)$ has by the diffusion process purified itself to a simple harmonic function of x we observe the ratio R_{21} of the intensities I_2 and I_1 of the diffracted radiation for a time t_1 and for a later time t_2

$$R_{21}=I_2/I_1=e^{-(8\pi^2K/d^2)(t_2-t_1)}.$$

Solving this for K we obtain an expression for the diffusion coefficient entirely in terms of measurable quantities

$$K=-\frac{d^2\log_e I_2/I_1}{8\pi^2(t_2-t_1)}. \quad (7)$$

The value of d may be measured directly from the diffraction angle and the wave-length of the x-rays used or it may be obtained by measuring the total thickness of the film by interferometry and dividing this by the number of layers. Our present rough results indicate $K=5\times10^{-20}$ cm^2 sec.$^{-1}$ for the diffusion coefficient of gold through copper at room temperature.

It is worth noting that for reasonable time intervals (t_2-t_1) because of the factor d^2 in Eq. (7) values of K many orders of magnitude smaller can be measured by this method than by methods requiring diffusion over macroscopic distances d. The time for observable diffusion over a distance of $\frac{1}{10}$ mm is a hundred million times as great as it is for the 100A involved in this experiment.

ACKNOWLEDGMENTS

We wish gratefully to acknowledge our indebtedness to Dr. Leon L. Watters of New York City for the funds which have supported this work.

The Use of Radioactive Phosphorus in Soil Studies*

STANLEY S. BALLARD[1] AND L. A. DEAN[2]
Hawaii Agricultural Experiment Station, Honolulu, Hawaii
(Received September 8, 1939)

Some uses of radioactive phosphorus in soil and fertilizer studies have been investigated. The necessary apparatus, the technique, and the accuracy of determining radioactive phosphorus in soils, solutions and plant ashes are described and discussed, and several examples of its application in agricultural problems are given. These include measurements of the rate of sorption of phosphorus by soils, fertilizer-placement studies, and measurements of the movement of applied phosphorus through a soil.

I. INTRODUCTION

IT has been known for many years that phosphorus is one of the several elements essential to plant growth. In fact phosphorus is one of the three elements around whose sale the fertilizer industry has been built. Some seventy million dollars are spent annually for phosphate fertilizers in the United States, and a great deal of research has been done to determine the best method of applying phosphates, as well as their subsequent fate in the soil, their rate of uptake by plants, and their particular function in the plant. This work has been done by standard chemical methods and lately also by specialized and more rapid methods. Many of these methods have proved satisfactory, but their chief weakness lies in the fact that it has never been certain that the phosphorus taken up by the plant was the *same* phosphorus added in a specific fertilizer treatment, since all soils contain certain amounts of phosphorus.

With the advent of artificial radioactivity, a new class of tools has been placed within the reach of the agricultural chemist. It is the purpose of this paper to describe the use of one of these; namely, radioactive phosphorus. Among the advantages of radioactive phosphorus in soil studies are the ease and directness of its use, the simplicity of the equipment needed, and particularly the certainty that the phosphorus detected and measured in the soil or in the plant is the *same* phosphorus that was added to the soil at the beginning of the experiment.

II. APPARATUS

In the experiments reported here, a Lauritsen quartz-fiber electroscope was employed in obtaining quantitative measurements of radioactivity. Fig. 1 shows the experimental set-up, which consists of the electroscope, a small vacuum-tube rectifying charging unit, and a movable stage on which can be placed a dish containing the material to be tested—a soil, a solution (such as a soil extract), or a plant material ash. The total cost of the equipment was about fifty dollars.

Several variables are encountered in making such radioactive measurements. First may be mentioned the rapid increase in electroscope deflection rate as the sample is brought closer to the electroscope window. As a result of this rapid change, the distance from window to sample must be noted carefully and kept constant throughout a series of determinations. The importance of this adjustment can be illustrated by an example: Working with soils whose free surface was at a distance of 2 cm from the electroscope window, a variation of 1 mm in this distance was found to cause a change in deflection rate of 4 percent. The height adjuster and indicator shown in Fig. 1* facilitated accurate height settings. The small disk, at the same level as the index at the meter stick, is used to set on soil surfaces, while the sharp point, which is 4 mm below disk level, is used to set on liquid surfaces.

In experiments using containers which were smaller than the electroscope window dimensions it was found that when all other variables were

* Published with the permission of the Director, as Technical Paper No. 51 of the Hawaii Agricultural Experiment Station.
[1] Assistant Professor of Physics, University of Hawaii.
[2] Associate Chemist.

* Constructed by Mr. S. Okubo in the University Physics Department shop.

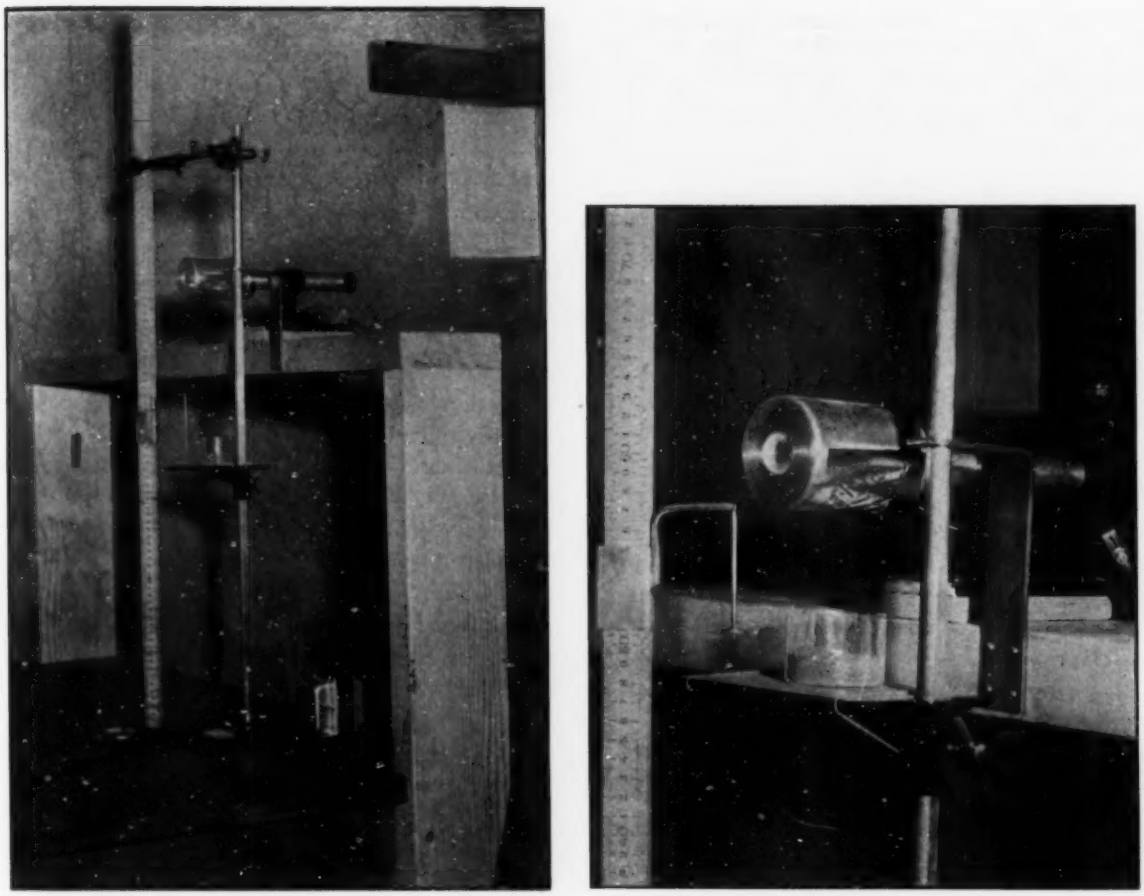

(a) (b)

FIG. 1. Electroscope and accessories for measuring the radioactivity of soils, solutions, and plant ashes. (a) General view of set-up, showing vacuum-tube charging unit on table. (b) Close-up view showing detail of height adjuster and indicator.

held constant the radioactive strength indicated for a given material varied directly and linearly with the surface area of the sample. By holding the surface area and height constant but varying the depth of material in the dish, a relationship between depth and measured radioactivity such as that shown in Fig. 2 was obtained. A number of similar test graphs for both soils and solutions were drawn, and in these it was found that no increase in tested strength ever occurred for depths of material greater than 15 mm.

From 3 to 10 electroscope deflection rate readings were averaged to obtain any individual radioactive strength. The time was measured for deflection between two specified points on the scale, thereby eliminating errors due to scale non-linearity. An example of the accuracy obtained when dealing with solutions is afforded by a series of tests of different dilutions of a solution containing radio-phosphorus. The results are

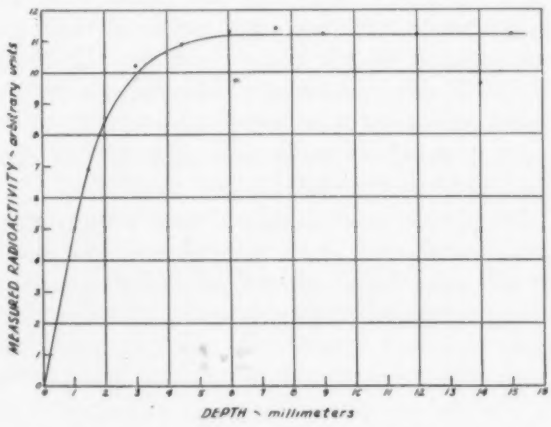

FIG. 2. Measured radioactivity of a soil plotted against depth of soil in a cylindrical dish.

TABLE I. *Results of testing a series of dilutions of a solution containing radio-phosphorus.*

D DILUTION	*R* MEASURED RADIOACTIVITY (ARBITRARY UNITS)	*R/D*	ABSOLUTE DEVIATION FROM MEAN	PERCENT DEVIATION FROM MEAN
1	18.7	18.7	+.1	0.5
2/3	12.4	18.6	0	0
3/5	11.2	18.7	+.1	.5
1/2	9.26	18.5	−.1	.5
2/5	7.56	18.9	+.3	1.6
1/3	6.02	18.1	−.5	2.7
3/10	5.67	18.9	+.3	1.6
1/4	4.57	18.3	−.3	1.6
1/5	3.71	18.6	0	0
1/6	3.12	18.7	+.1	.5
1/8	2.30	18.4	−.2	1.1
		mean 18.6		mean .97

presented in Table I. The greatest deviation from the mean encountered here was less than 3 percent, while the average deviation from the mean was 1 percent. These errors also included the errors encountered in preparing the dilutions. The $\frac{1}{2}$ dilution, which was the second solution to be run, was run again at the end of the series, some 2 hours later, with the resulting strength of 18.4 as against the original result of 18.6; that is, a difference of about 1 percent. The average of these two results is used in Table I.

The technique for handling soils consisted in filling the dish full to overflowing and then leveling off the surface with a straightedge. This gave a smooth surface with a random distribution of particle size. By careful handling, packing was avoided. In Table II is given an example of the accuracy with which measurements on a soil were repeated, using this technique. The soil was remixed between each series of readings, the various results given in Table II being obtained over a period of 2 hours, with measurements on several other samples intervening. The greatest deviation from the mean in this case was less than 2 percent.

The plant material ashes tested were usually quite weak and small in volume. Therefore, rather than being placed in a dish of small enough diameter to give a depth of 15 mm they were spread as evenly as possible over the bottom of a larger, shallow dish and brought up very close to the electroscope chamber. This method introduced the possibility of greater errors.

In work of this sort it appears unnecessary to give results (i.e., measured radioactive strengths) in absolute units, if indeed such were always possible. Therefore arbitrary units, such as divisions per minute of electroscope deflection, are used throughout. One must, of course, be sure that the geometrical conditions under which the samples are tested are constant throughout the series. If a series of observations lasts more than a few hours, corrections must be made for the radioactive decay of the phosphorus (in approximately 5 hours its strength will decrease by 1 percent). This can be done by the usual exponential methods, using the known value of the radioactive decay constant of radio-phosphorus. A problem which is perhaps more important in the tropics, where the humidity is ordinarily in the eighties and may vary rapidly, is that of a changing electroscope background. In making measurements of weak, near-background samples, it was found advisable to take background readings every half-hour.

III. SOME APPLICATIONS OF THE METHOD

A. Determination of the half-life of radio-phosphorus

A series of 26 observations, extending over a period of 6 weeks, was made on the strength of a certain test sample of activated sodium phosphate. As a result, the half-life of the radioactive phosphorus was computed to be 14.3 days. This value is in good agreement with values quoted in the literature.

B. Studies of the sorption of phosphorus by soils

The factor mentioned above, that only the top 15 mm of a soil or solution contribute to the measured radioactivity, made possible the ready

TABLE II. *Repeat results on the measured radioactive strength (in arbitrary units) of a soil. Each result is the mean of three electroscope deflection-rate readings.*

STRENGTH	ABSOLUTE DEVIATION FROM MEAN	PERCENT DEVIATION FROM MEAN
41.4	−0.4	0.9
42.0	+ .2	.5
41.6	− .2	.5
41.6	− .2	.5
42.5	+ .7	1.7
mean 41.8		mean .8

determination of the rate of sorption of phosphorus by soils. The apparatus consisted of a large test tube which could be filled with 75 cc of a sodium phosphate solution, and a mechanical agitator. The radioactivity of this solution was tested with the electroscope, after which 10 g of soil were added. The test tube was stoppered and was agitated slowly by mechanical means. After a few minutes of agitation, the test tube was placed in a vertical position so that the soil would settle to the bottom. Within 3 or 4 minutes all but the finest particles had settled, and the radioactivity of the solution was again tested. This measure was less than that before the addition of the soil because of the sorption of the phosphorus by the soil particles. Periods of slow agitation were repeated for several hours, with tests of radioactivity made at appropriate intervals, and gave a series of data which could be plotted as in Fig. 3. The two curves of Fig. 3 show the rate of sorption of the phosphorus and also the total percentage of phosphorus sorbed, for a low and for a high fixing soil; namely, 20 percent and 95 percent sorption, respectively.

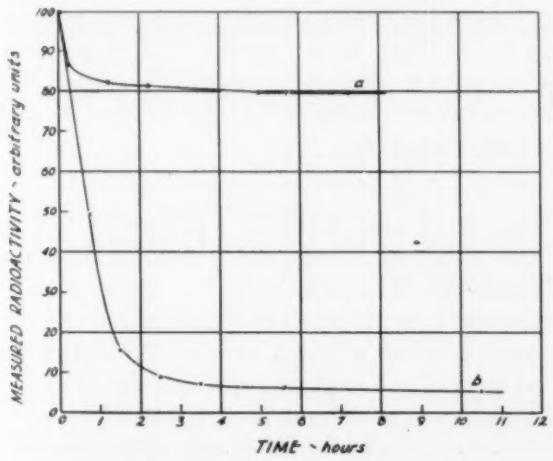

FIG. 3. Graphs of the radioactive strength of a solution from which a soil is sorbing radio-phosphorus. Measured radioactivity of the solution is plotted against time, for (*a*) a low fixing soil, (*b*) a high fixing soil.

C. Phosphate fertilizer placement experiments

An important problem to agriculturists is that of the proper placement of fertilizers in order to obtain maximum absorption by the plant. This problem can be studied readily by the use of the radio-elements, if their half-life periods are sufficiently long. With phosphorus, the half-life of which is approximately 2 weeks, it is preferable to use a rather fast-growing plant. To date three series of phosphate placement experiments have been carried out, one of which is described

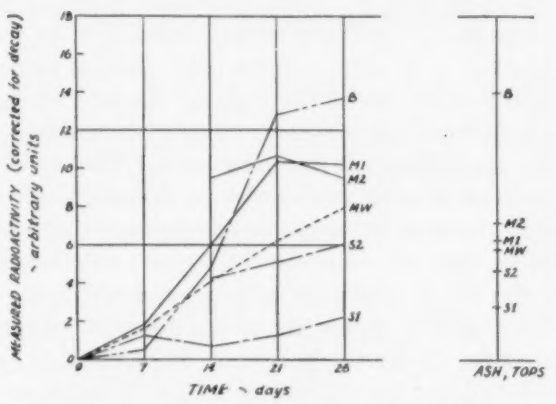

FIG. 4. Plot of the accumulation of radioactive phosphorus by tomato plants. *S* = surface placement, *M* = mixed through soil, *MW* = mixed through soil and the soil washed, *B* = bottom placement. At extreme right: Relative strengths of the ashed tops of the same plants.*

below. Tomato plants were transplanted to individual pots in the high fixing soil mentioned above. Equal weighed portions of activated sodium phosphate were added to each pot, but with three methods of application. In the "surface" treatment (pots *S*1 and *S*2), a small amount of sodium phosphate was placed in a lump just under the soil surface; in the "bottom" treatment (pot *B*), the phosphate was placed at approximately root level but to the side, at the time of transplanting; in the "mixed" treatment (pots *M*1 and *M*2), the phosphate, in solution, was mixed through the soil as completely as possible. A variation of the last method was the "mixed and washed" treatment (pot *MW*), in which the soil, after being mixed with the radio-phosphorus, was washed with water in an attempt to leach out all soluble phosphorus.

The rate of uptake of radio-phosphorus by the plants was followed in a semi-quantitative fashion. The entire plant, in the pot, was placed under the electroscope so as to bring the small cluster of young, rapidly growing leaves up against the electroscope chamber window (pro-

* For ease of comparison, the values of ash radioactivity were adjusted by a constant factor so that the strongest one, *B*, matches the corresponding plant value.

tected by a piece of light cardboard). A sheet of lead placed over the top of the pot shielded the electroscope from soil radioactivity. The values obtained were plotted against the time elapsed since planting, as shown in Fig. 4. In this case the experimental values were first corrected to eliminate the factor of radioactive decay. At the extreme right of Fig. 4 are indicated the radioactive strengths of the tops as determined by testing the ash of the total green material at the conclusion of the experiment. The values given cannot of course be compared directly with those of the growing plants, but it will be noted that the order for the various treatments is the same. This fact, which was borne out in other series, shows that the progress of the phosphorus accumulation of a plant can be followed without the necessity of removing leaves for test or of harvesting one of a number of duplicates.

Very little discussion of the graphs of Fig. 4 is needed. It will be seen that the plants receiving the "surface" treatment took up the least phosphorus. No explanation is offered for the wide difference in results between plants *S*1 and *S*2, although it might be stated that plant *S*1 never grew to as large a size as did the others. The position of the *MW* graph relative to the *M* graphs suggests that the small amount of phosphorus in the latter soils was more available, and hence was taken up more rapidly.

TABLE III. *Comparative radioactive strengths of soil layers in pots after 4 weeks.*

TREATMENT	SURFACE	SURFACE	SURFACE	BOTTOM
DESIGNATION	NO PLANT	*S1*	*S2*	*B*
Top 3 cm	100.	84.	81.	0
Middle 3 cm	0.4	0.2	3.1	0.5
Bottom 3 cm	0.2	0.1	0.5	96.

It appears that the development of the root system of plant *B* was such that 2 weeks elapsed before the roots started feeding on the radiophosphorus. Plants *S*2 and *M*2 were not tested the first week, and their graphs are not drawn through to the origin, to prevent misinterpretation of the 1-week data.

D. Studies on the movement of applied phosphorus through the soil

Information on the rate of movement of phosphorus through soil was obtained by testing the top, middle, and bottom 3-cm layers of the soil of each of the above-mentioned pots, after removing as many roots as possible. So far as the "mixed" and "mixed and washed" pots were concerned, no significant differences in radio-phosphorus concentration among the three levels were observed. In the case of the "surface" and "bottom" treatments, however, high gradients were encountered. The data taken from these three pots, along with those taken from a fourth pot which had "surface" treatment but no plant growing, are shown in Table III. These data are adjusted so that the radioactive strength of the strongest layer of the "no plant" control pot is 100. The known property of phosphorus of staying almost exactly where it is placed in a soil, is well illustrated by the results of this simple experiment.

IV. ACKNOWLEDGMENTS

We wish to acknowledge with thanks the cooperation of Professor E. O. Lawrence, Director of the Radiation Laboratory of the Department of Physics of the University of California, and the gift of two samples of radiophosphorus. The interest and encouragement of Dr. John H. Lawrence have been greatly appreciated.

KODACHROME FILM
FOR SCIENTIFIC PHOTOGRAPHY

KODACHROME FILM combines the advantages of full-color photography with the simplicity in exposure of black-and-white films and plates. It provides transparencies that do not have screen pattern or grain. There is a size and type of Kodachrome Film for every requirement of color reproduction for scientific purposes—"still" pictures . . . motion pictures . . . photomicrographs . . . projection slides.

KODACHROME PROFESSIONAL FILM Cut-sheet film, supplied in two types—*Type B*, for artificial light; *Daylight Type*. Sizes—from 45 x 107 mm. to 11″ x 14″.

KODAK KODACHROME FILM "Miniature" film in rolls, supplied in two types—*Type A*, for artificial light; *Regular*, for daylight. Sizes—35 mm. (image, 24 x 36 mm.); Bantam (image, 28 x 40 mm.). Ideal for projection slides.

CINÉ-KODAK KODACHROME FILM Motion-picture film, supplied in two types—*Type A*, for artificial light; *Regular*, for daylight. Sizes—16 mm. and 8 mm.

Visit the Kodak Building at the New York World's Fair

EASTMAN KODAK COMPANY, ROCHESTER, N. Y.

Announcing: the Second Volume of an Important Two-volume Text

INTRODUCTION TO ELECTRICITY AND OPTICS

By NATHANIEL H. FRANK
Associate Professor of Physics
Massachusetts Institute of Technology

In press—ready in June

This textbook, together with the author's *Introduction to Mechanics and Heat*, constitutes a two-volume series in physics for the introductory technical course. *Introduction to Electricity and Optics* gives a logical exposition of the fundamental principles, emphasizing field theory and the elementary application of these principles to circuits and to the electrical, magnetic, and optical properties of matter. The treatment is quantitative throughout and modern atomic ideas are stressed along with the more classical modes of presentation.

INTRODUCTION TO MECHANICS AND HEAT

By NATHANIEL H. FRANK. *Second edition.* 384 pages, 6 x 9. $3.00

Send for copies on approval

McGRAW-HILL BOOK COMPANY, Inc.

330 West 42nd Street **New York, N. Y.**

Innovations in Instruments

Instrument for Concentration Measurements

An addition to the line of Solu-Bridge test instruments has been recently marketed by Industrial Instruments, Inc., 156 Culver Avenue, Jersey City, New Jersey. Model RD-3, illustrated in the accompanying figure, is designed primarily to determine the concentration of alkali washing solutions of the type generally used in the dairy, brewery and soft drink industries, as well as in the field of metal products when surfaces must be cleansed. This instrument covers a concentration range from zero to thirty parts per million and is provided with a temperature compensation dial with a range from 64° to 190°F.

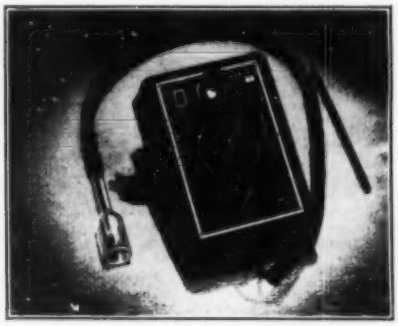

Monitor Speaker with Wide Frequency Range

A new monitoring loudspeaker employing a newly-designed permanent magnet mechanism and housed in a modernistic cabinet which permits an unusually wide angle of sound distribution has been announced by the RCA Manufacturing Company. The loudspeaker (Model 64-B) is designed primarily for broadcast control room monitoring, but it is also well suited for many other applications where high quality is of prime importance, such as audition rooms, public rooms, offices, etc. All the frequencies between 60 and 10,000 cycles are faithfully reproduced with exceedingly low distortion through a combination of RCA's double voice coil speaker mechanism with a folded horn cabinet. Diffusing vanes are located in front of the cone and effectively spread the high frequency radiation over a 100-degree arc at 10,000 cycles. The 64-B is rated at 10 watts and has a 15-ohm input impedance.

Moisture Teller

The Harry W. Dietert Company of Detroit, Michigan, is manufacturing a new size moisture teller which takes a sample pan $2\frac{3}{4}$" in diameter and $1\frac{1}{4}$" in depth. This pan is light and may be weighed on a sensitive analytical balance for accurate moisture determinations. The bottom of the sample pan is made of 500-mesh monel filter cloth. The sample to be dried is placed in the pan under the heated air outlet of the moisture teller. An adjustable thermostat controls the temperature of the drying air. Since the air is above the steaming point of water, the moisture contained in the sample is flashed to steam and blown through the bottom of the pan. For many materials a sample can be dried to constant weight in as short a period as one minute. A descriptive leaflet may be obtained from the manufacturer.

Circuit Tester

A new circuit tester for use in individual measurements on all types of control and signal equipment and electronic apparatus, has been announced by Weston Electrical Instrument Corporation, Newark, New Jersey. Known as the Model 785 circuit tester, this relatively inexpensive device has 27 complete ranges for voltage, current and resistance measurements. It provides d.c. voltage measurements at a sensitivity of 20,000 ohms per volt in ranges of 0–1, 0–10, 0–50, 0–200, 0–500 and 0–1000 volts; a.c. voltage measurements at a sensitivity of 1000 ohms per volt in ranges of 0–5, 0–15, 0–30, 0–150, 0–300, and 0–500 volts; d.c. current measurements in ranges of 0–50 microamperes; 0–1, 0–10, 0–100 ma; 0–1, and 0–10 amp.; a.c. current measurements in ranges of 0–0.5, 0–1, 0–5, and 0–10 amp.; and resistance measurements in ranges of 0–3000, 0–30,000, and 0–300,000 ohms; 0–3, and 0–30 megohms. The instrument accuracy on d.c. voltage and current measurements is within 2 percent (excluding the 1000-volt range, which has an accuracy within 3 percent). A.c. voltage accuracy is within 3 percent; a.c. current ranges give accuracy within 3 percent on 60-cycle approximate sine wave measurements; the accuracy on all resistance ranges is within 2 percent of the linear arc length on the ohmmeter scale.

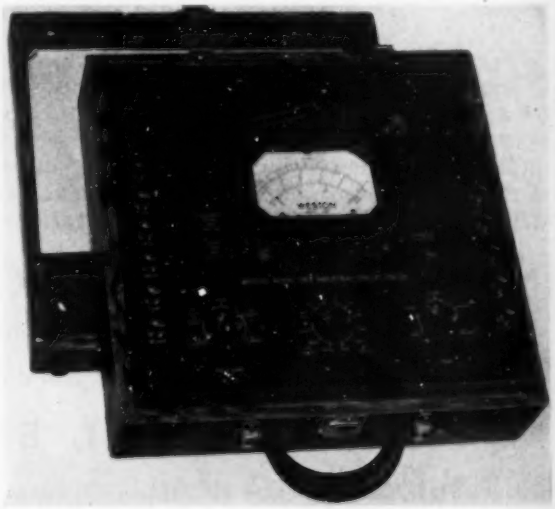

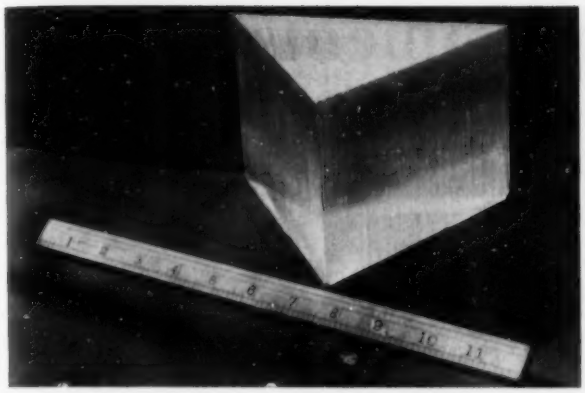

An eight pound rock salt prism blank cut from a twenty-five pound single crystal

SYNTHETIC CRYSTAL OPTICS

For infrared and ultraviolet spectroscopy and for polarizing optics. . . . Single crystals of Lithium Fluoride, Sodium Chloride, Sodium Nitrate, and Potassium Bromide. . . . Write for information.

THE HARSHAW CHEMICAL CO.
SPECIAL PRODUCTS DIVISION CLEVELAND, OHIO

JAGABI *"Lubri-tact"* RHEOSTATS

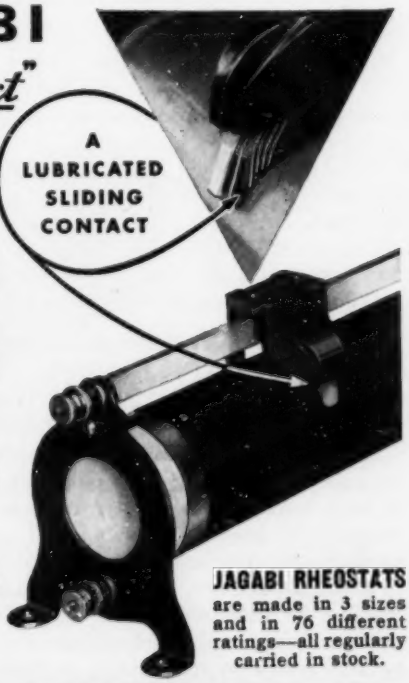

have a graphited carbon lubricator associated with the contact brushes. Eliminates scratching and abrasion—gives smoother operation and a better contact. Makes Jagabi Rheostats *better* rheostats.

Write for Bulletin 1620-R which lists new lower prices.

JAGABI RHEOSTATS are made in 3 sizes and in 76 different ratings—all regularly carried in stock.

JAMES G. BIDDLE CO.
1211 ARCH STREET *Electrical and Scientific Instruments* PHILADELPHIA, PA.

EPPLEY THERMOPILES *for* RADIANT ENERGY MEASUREMENTS

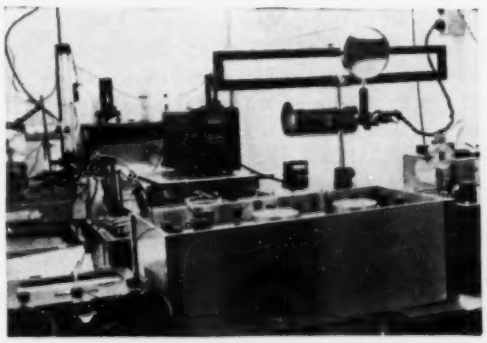

A view of some of the apparatus used for calibrating thermopiles at the Eppley Laboratory, Inc.

Adequate manufacturing, testing and calibrating equipment in the hands of our skilled and experienced technicians insures satisfaction to the users of Eppley Thermopiles.

We are prepared to furnish thermopiles of either bismuth-silver or copper-constantan, mounted in vacuum or air type cases. We also furnish thermopiles and mountings especially designed to meet individual needs. A card will bring you our Bulletin R–3 which contains illustrations, sample curves, complete descriptive matter, prices, references, etc., with regard to Eppley Thermopiles.

EPLAB
THE EPPLEY LABORATORY, INC.
SCIENTIFIC INSTRUMENTS
NEWPORT, R.I.
U.S.A.

Innovations in Instruments *(continued)*

Outdoor Turbine-Generator

The first hydrogen-cooled turbine-generator for outdoor installation is being built by the General Electric Company for a new station at the city of Glendale, California. It is estimated that this plant will be built at a substantial saving over the conventional type because of the absence of heavy building structures. The boilers and firing aisle are to be enclosed with stucco-covered light-steel frame housing, and the turbine-generator unit will be located upon an open deck and served with a traveling gantry crane. Basically, the Glendale unit will be the same as a hydrogen-cooled turbine-generator built for installation indoors, except for a welded sheet-steel housing over the high-pressure end of the turbine proper. Control panels will be located in the station basement.

Rated 20,000 kw, 13,800 volts at 3600 r.p.m., the unit will operate at 0.8 power-factor and have a total output of 25,000 kva. It will use steam at 600 lb. gage pressure, with a back pressure of two inches of mercury absolute. Shipment is scheduled for August, 1940.

Power Units for Spectro-Chemistry

For the purpose of minimizing the error due to light source in spectro-chemical analysis, three electrical power source units have been developed by the Harry W. Dietert Company of Detroit, Michigan. The instruments are characterized thus: 3-kw ARL arc rectifier unit (shown at left in illustration) for exciting the sample to be tested with 250 volts, 4 to 14 amperes, d.c. current; ARL high voltage spark unit (shown in center in illustration) for exciting the sample with 35,000 volts, 2-kw, a.c. spark current; 5-kw high voltage arc unit (shown at right in illustration) for exciting the sample with 2500 volts, 2–5 amperes, a.c. arc current. Each unit is equipped with voltmeter, ammeter, automatic timer, safety relay, power control, and necessary switches; all mounted on an inclined switchboard panel.

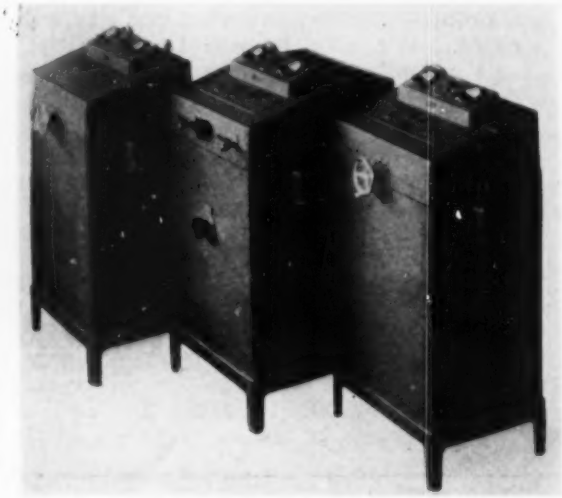

Square-Wave Generator

Type 769-A square-wave generator, which can be used to determine the frequency response, particularly under transient conditions, of amplifiers and other networks, was announced recently by the General Radio Company, 30 State Street, Cambridge, Massachusetts. A photograph of this instrument is shown in the accompanying figure. The method used is to apply square waves of appropriate frequency to the input of the network under measurement and to observe the output wave form on a cathode-ray oscillograph. This square-wave generator is particularly useful for measuring the low frequency response of television systems. The generator is actually a device for converting a sinusoidal timing signal into a square-wave signal. Squaring is accomplished by amplifying and clipping the peaks of the signal in several successive stages.

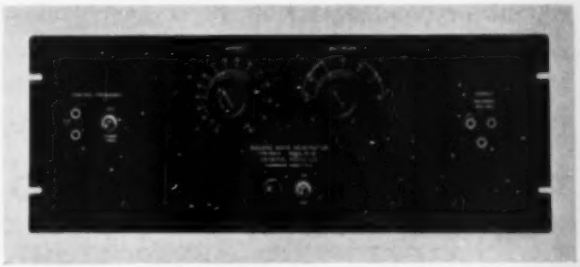

The output voltage can be obtained either unbalanced or balanced to ground. The plate-to-plate output voltage is 150 volts balanced, 75 volts unbalanced. Minimum output voltage is 10 microvolts. Output impedance is 500 ohms balanced, 250 ohms unbalanced. The impedance is independent of frequency down to d.c. Square waves with *fundamentals* from 10 to 5000 cycles per second can be produced. The output circuit will pass frequencies between 0.1 cycle and 250,000 cycles. The wave form is very close to a true rectangular shape. At low frequencies, the entire rise in voltage takes place in 0.001 cycle.

Television Transmitting Equipment

Limited strictly to broadcasters interested in television, the bulletin, DuMont Television Transmitting Equipment, recently issued by Allen B. DuMont Laboratories, Inc., of Passaic, New Jersey, deals with essential studio, transmitting and receiving equipment, including direct pick-up camera, film pick-up camera, studio lighting, special film projector, studio sound apparatus, master sweep panel with interlace control, shading and mixing controls, picture line mixer and amplifier, control room monitor for sight and sound, control test oscillograph, outdoor pick-up and sound equipment, phasmajector test pattern generator, transmitter, calibrated field strength receivers for studying coverage, antenna, and the available television receivers. A copy of this bulletin will be sent to any recognized broadcaster writing on his business letterhead, since the edition is strictly limited.

FIRST SURFACE MIRRORS

by High Vacuum Deposition

EVAPCO first surface are excellent for projection mirrors and other uses that require an opaque mirror of high reflectivity that does not tarnish or give double image.

DUOLUX semi-transparent for one exposure three color cameras, range finders, or wherever an accurate beam-splitter is needed. Made to order for all practical transmission —reflection ratios.

EVAPORATED METAL FILMS CORP.
ITHACA, N. Y.

PORTABLE POTENTIOMETERS

Rubicon portable potentiometers are available in a variety of single and double range models suitable for thermocouple, pH and instrument calibration work. Guaranteed accuracy to .1%.

These sturdy, self-contained instruments are built to give years of satisfactory service under all conditions encountered in the laboratory, shop or field. They are outstanding values in their class.

Ask for Bulletin 270.

RUBICON COMPANY
Electrical Instrument Makers
29 North Sixth Street Philadelphia, Pa.

STABILIZED A-C VOLTAGE

INPUT 95-130 volts
Instantaneous action
A magnetic unit

OUTPUT
115 volts ±½%
Stabilizes at any load within rating

No moving parts. Nothing to wear out.

RAYTHEON Voltage Stabiliser

APPLICATIONS **Broadly it insures stable operation of all precision apparatus obtaining its power from an A.C. source, for example:—**

- **Insures constant brilliancy from all types of lamps.**
- **Improves the operation of X-ray equipment.**
- **Stabilizes all electronic apparatus.**

Write for Bulletin 48-71JP.

RAYTHEON MFG. CO. WALTHAM, MASS.

The fundamentals of modern hydraulic engineering are clearly explained in

the new book

MECHANICS OF LIQUIDS

By Ralph W. Powell

This book includes full explanations of the modern theories of fluid mechanics most useful to the hydraulic engineer, as well as thorough treatment of the established principles of hydraulics. Illus. $3.50

MACMILLAN NEW YORK

ABSORPTION CELLS
With Optical Flats Fused On

Windows Flat Over Entire Area to Within 6 Wavelengths

- **Parallelism of liquid-glass interfaces is ±0.01 mm. in high-precision cells and ±0.025 mm. in standard cells.**
- **Parallelism of the faces of each window is ±10 minutes.**
- **Actual mean length marked on each cell to nearest 0.001 mm.**
- **Actual mean length between faces of windows is ±1% or ±0.005 mm. of the nominal length.**
- **Cells matched to ±0.01 mm. are obtainable.**
- **Pyrex Bodies with Pyrex or Corex "D" Windows.**
- **Fused Quartz Bodies and Windows.**

AMINCO

12 Styles
387 Standard Sizes

Write for Bulletin AP1170

AMERICAN INSTRUMENT CO.
8010 GEORGIA AVENUE · SILVER SPRING, MARYLAND

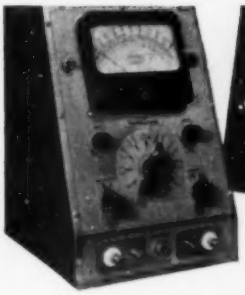

NEW PUSH-PULL ELECTRONIC VOLTMETER-OHMMETER
.05-5000 Volts DC in 9 Ranges!
.01 Ohm-1000 Megohms in 7 Ranges!

IT'S THE *Rider Volt Ohmyst!*

Here's a laboratory instrument with ranges so wide it will not only take care of today's engineering requirements—but tomorrow's as well.

It's the Rider VoltOhmyst and with it you can measure DC voltages in high resistance photo-cell circuits, television circuits, bias cells, operating voltages across tuned circuits with the signal present—with surprising speed and accuracy. This instrument covers the actual operating voltage. No circuit loading. Its input resistance of 160,000,000 ohms on all ranges between 500 volts and 5,000 volts makes the Rider VoltOhmyst a universal instrument—one that truly minimizes obsolescence. Get full details and specifications from your RCA Test Equipment Distributor—or write to the address below.

The Rider VoltOhmyst is Stock No. 163—net price $57.50.

Over 335 million RCA radio tubes have been purchased by radio users—in tubes, as in parts and test equipment, it pays to go RCA All the Way.

RCA *Test Equipment*
RCA Manufacturing Co., Inc., Camden, N. J.
A Service of the Radio Corp. of America

INDEX TO ADVERTISERS

Name	Page
American Instrument Company — Ion Type X-Ray Tube. Powder Spectrum Diffraction Cameras. Scientific Instruments and Supplies.	x
Bausch & Lomb Optical Company — Makers of Microscopes, Microtomes, Colorimeters, Refractometers, Spectrometers, Balopticons, Photomicrographic and Microprojection Apparatus and related instruments. Also makers of Orthogon Eyeglass Lenses for Better Vision.	iv
James G. Biddle Company — "Jagabi" Rheostats; Adam Hilger and Kipp & Zonen Optical Instruments; "Pointolite" Lamps; Electrical Testing and Speed-measuring Instruments.	vii
Cambridge University Press	ix
Central Scientific Company — Manufacturers of Cenco Physical Apparatus and Instruments to meet all requirements of University, College and High School Physics Laboratories. Specializing in high vacuum pumps and development of instruments and apparatus for various sciences.	Cover 4
Eastman Kodak Company — Purified Organic Chemicals for research purposes; Plates for Photography, Photomicrography, Spectroscopy, Photometry, Astronomy; Wratten Light Filters; Cameras and Films.	v
The Eppley Laboratory, Inc. — Standard Cells, thermopiles, pyrheliometers and temperature bridges.	vii
Evaporated Metal Films Corporation — First surface and semi-transparent mirrors by high vacuum deposition.	ix
Gaertner Scientific Corporation — Spectroscopes, Spectrometers, Spectrographs, Spectrophotometers, Heliostats, Measuring Microscopes, Comparators, Cathetometers, Reading Telescopes, Interferometers, Chronographs, Dividing Machines, etc.	ii
General Radio Company — Manufacturers of electronic measuring instruments; vacuum-tube voltmeters, amplifiers and oscillators; wave analyzers, noise meters and analyzers, stroboscopes; laboratory standards of capacitance, inductance and frequency; impedance bridges, decade resistors and condensers; air condensers and variable inductors; rheostats, Variacs, transformers; other laboratory accessories.	Cover 3
Harshaw Chemical Company — Optical Lithium Fluoride grown in single crystal to predetermined size. Industrial Chemicals.	vii
Journal of Scientific Instruments	ii
Leeds & Northrup Company — Manufacturers of Galvanometers, Resistors, Bridges, Condensers, Inductances, Potentiometers, Testing Sets; Temperature Measuring, Recording and Controlling Apparatus; Instruments for Measuring and Controlling Conductivity of Electrolytes and Hydrogen Ion Concentrations.	i
Macmillan Company	ix
McGraw-Hill Book Company, Inc.	v
Raytheon Mfg. Company — Voltage stabilizers and regulators. Electrical measurement and control instruments.	ix
RCA Manufacturing Company, Inc. — RCA Oscillators and Oscillographs, RCA Test Equipment, RCA Ultra-Sensitive DC Meter.	x
Rubicon Company — Galvanometers, electrometers, potentiometers, Wheatstone and Kelvin bridges, resistance boxes, hydrogen ion and conductivity apparatus.	ix
Westinghouse Electric & Manufacturing Company	iii

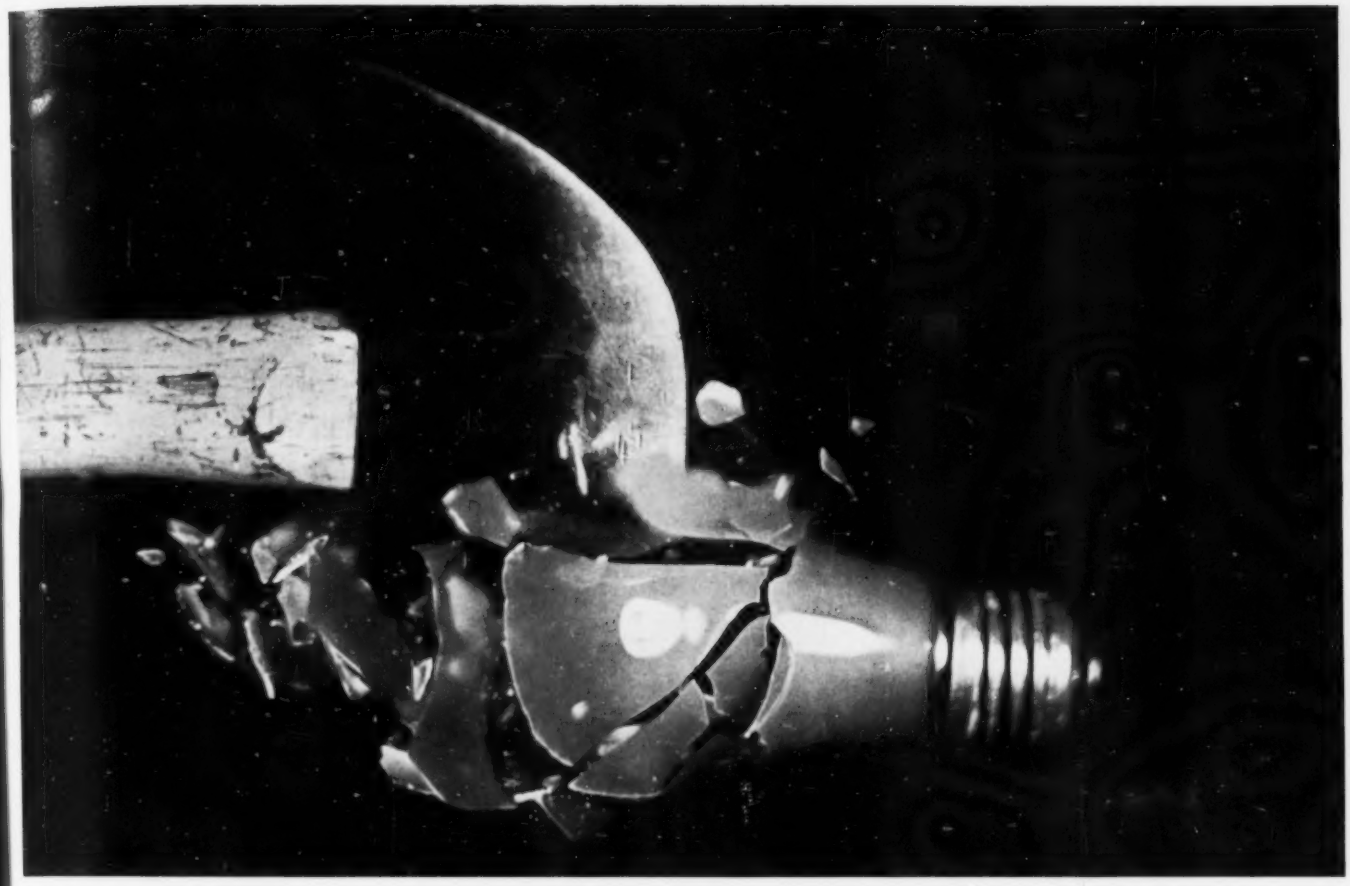

DOES IT STOP *MOTION?*

THIS unretouched single-flash photograph shows more effectively than a thousand words can tell, how the new Type 631-B STROBOTAC and the new STROBOLUX stop motion. The electric light bulb is shattered yet each particle of glass was 'stopped' before it could fly out of range of the camera.

These General Radio instruments . . . the STROBOTAC and the new STROBOLUX . . . can stop motion for you in the most complicated machine. For visual observation the STROBOTAC will freeze motion up to 100,000 rpm . . . it will show any cyclic revolving or reciprocating device, operating as fast as 100,000 rpm, in s-l-o-w motion, **as slow as a fraction of an rpm!**

TYPE 631-B STROBOTAC

The STROBOTAC has been improved in a number of ways to increase its usefulness as a speed-measuring or motion-stopping device. The rpm scale is more conveniently located on top of the case where it can be read more easily. The over-all accuracy of the STROBOTAC has been increased to ± 1%. The control switch on the front panel is simplified so that it can be set without the slightest confusion. Terminals are provided for making connection to the STROBOLUX where additional light is desired.* With all these improvements the price of the STROBOTAC remains only $95.00.

● *WRITE FOR BULLETIN 586 FOR COMPLETE INFORMATION*

GENERAL RADIO CO.
Cambridge, Mass.
Branches in New York and Los Angeles

NEW TYPE 648-A STROBOLUX

This instrument is a new development. It comprises a built-in power supply and large lamp with a 9-inch reflector, furnishing about ***100 times*** as much light as the STROBOTAC. It is for use when relatively large areas are to be illuminated or when single-flash photographs, taken over limited areas, are wanted. It can be flashed up to 6,000 times per minute by means of the STROBOTAC with which it must always be used.* The Type 648-A STROBOLUX is supplied complete with the necessary line and connecting cords. Price: $175.00.

**Your present Type 631-A STROBOTAC will be equipped, without charge, with an output jack for connecting the STROBOTAC to the STROBOLUX if the Type 631-A instrument is returned to the factory when ordering a STROBOLUX.*

CENCO HIGH VACUUM PUMP UNIT

WITH

HICKMAN DESIGN OIL DIFFUSION PUMP

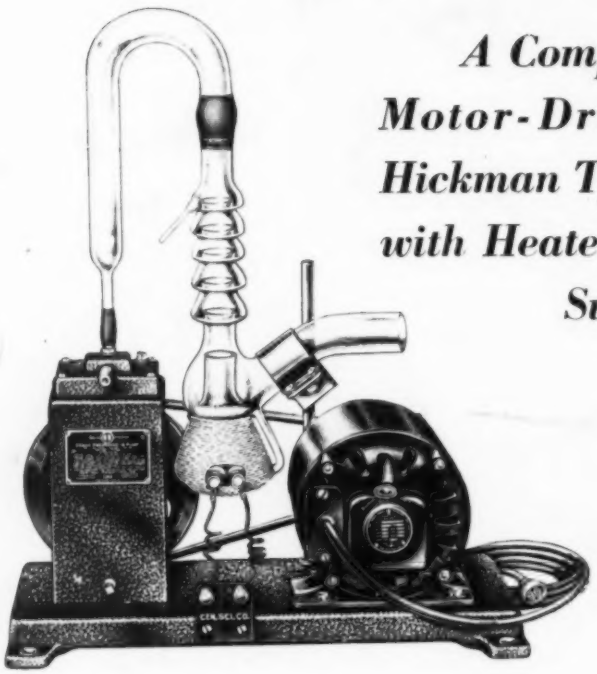

A Complete Unit including Motor-Driven Forepump and Hickman Type Oil Diffusion Pump with Heater, Mounted on a Single Substantial Base

93270A
High Vacuum Pump Unit For 115 volts—60 cycles
$100.00

FOR high-speed exhaustion of properly designed, gas-tight vacuum systems to pressures of 0.01 micron or less. The speed of pumping is in excess of 3 liters per second. No freezing trap is required to attain the ultimate low pressure, as the vapor pressure of the organic liquid or "oil" used as the pumping medium is so low that the amount of oil vapor that can diffuse out of the pump is negligible.

A sufficient quantity of Amoil is included for operation of the diffusion pump, as well as a quantity of sheet aluminum bands and Cenco Cohesive Rubber Tape for making the high vacuum connections between the pumps. From 0.8 to 1.2 amperes are required for proper operation of the diffusion pump.

For Other Hickman Type Pumps and Diffusion Pump Oils Ask for Circular 1098

CENTRAL SCIENTIFIC COMPANY

SCIENTIFIC INSTRUMENTS — TRADE MARK CENCO REG. U.S. PAT. OFF. — LABORATORY APPARATUS

New York • Boston • CHICAGO • Toronto • San Francisco

LANCASTER PRESS, INC., LANCASTER, PA.